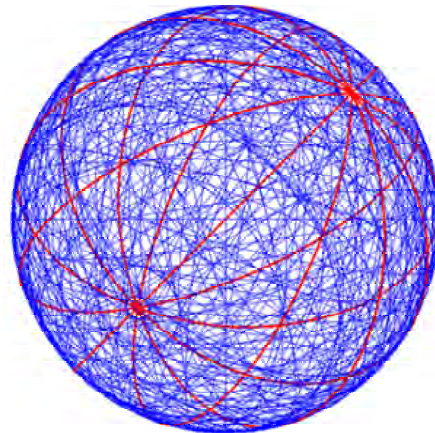


The Grand Unified Theory of Classical Quantum Mechanics

Part 1: Atomic Physics

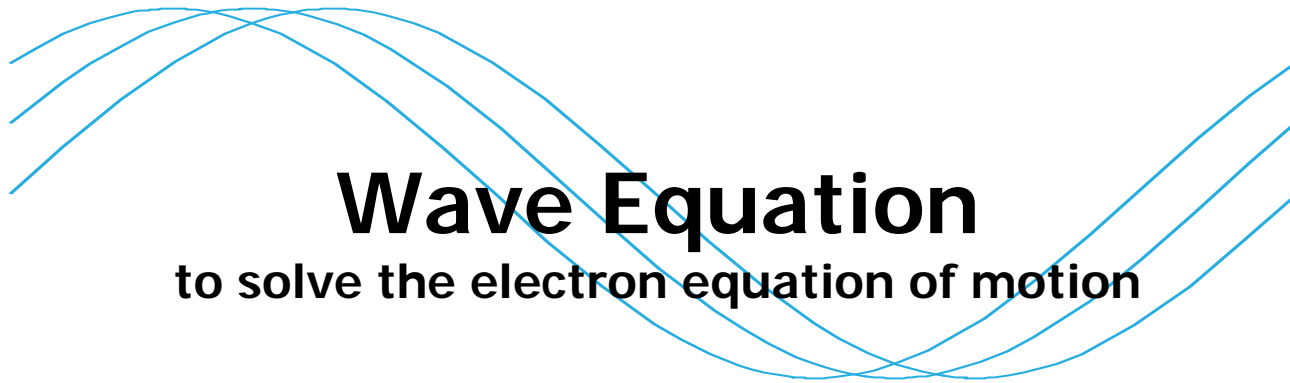


July 2005

Dr. Randell L. Mills
BlackLight Power, Inc.
493 Old Trenton Road
Cranbury, NJ 08512
609-490-1090
rmills@blacklightpower.com

Review of Theory

- Assume physical laws apply on all scales including the atomic scale
- Start with first principles
 - Conservation of mass-energy
 - Conservation of linear and angular momentum
 - **Maxwell's Equations**
 - Newton's Laws
 - Special Relativity
- **Highly predictive**– application of Maxwell's equations precisely predicts hundreds of fundamental spectral observations in exact equations with no adjustable parameters (fundamental constants only).
- In addition to first principles, the only assumptions needed to predict the Universe over 85 orders of magnitude of scale (Quarks to Cosmos):
 - Four-dimensional spacetime
 - The fundamental constants that comprise the fine structure constant
 - Fundamental particles including the photon have \hbar of angular momentum
 - The Newtonian gravitational constant G
 - The spin of the electron neutrino



Wave Equation

to solve the electron equation of motion

Although an accelerated point particle radiates, an *extended distribution* modeled as a superposition of accelerating charges does not have to radiate.

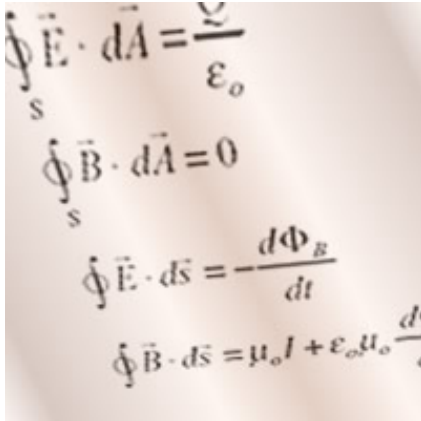
$$\left[\nabla^2 - \frac{1}{v^2} \frac{\delta^2}{\delta t^2} \right] \rho(r, \theta, \phi, t) = 0$$

H. A. Haus, Am. J. Phys., 54, 1126 (1986)

T. A. Abbott, D. J. Griffiths, Am. J. Phys., 53, 1203 (1985)

G. Goedecke, Phys. Rev. B, 135, 281 (1964)

Boundary Constraint Derived from Maxwell's Equations



Handwritten Maxwell's equations:

$$\oint_S \vec{E} \cdot d\vec{A} = \frac{Q}{\epsilon_0}$$

$$\oint_S \vec{B} \cdot d\vec{A} = 0$$

$$\oint \vec{E} \cdot d\vec{s} = -\frac{d\Phi_B}{dt}$$

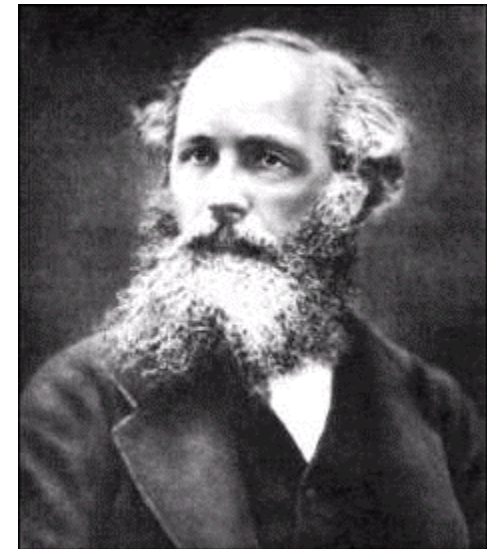
$$\oint \vec{B} \cdot d\vec{s} = \mu_0 I + \epsilon_0 \mu_0 \frac{d\Phi_E}{dt}$$

For non-radiative states, the current-density function must NOT possess spacetime Fourier components that are synchronous with waves traveling at the speed of light.

The solution for the radial function which satisfies the boundary condition is a delta function:

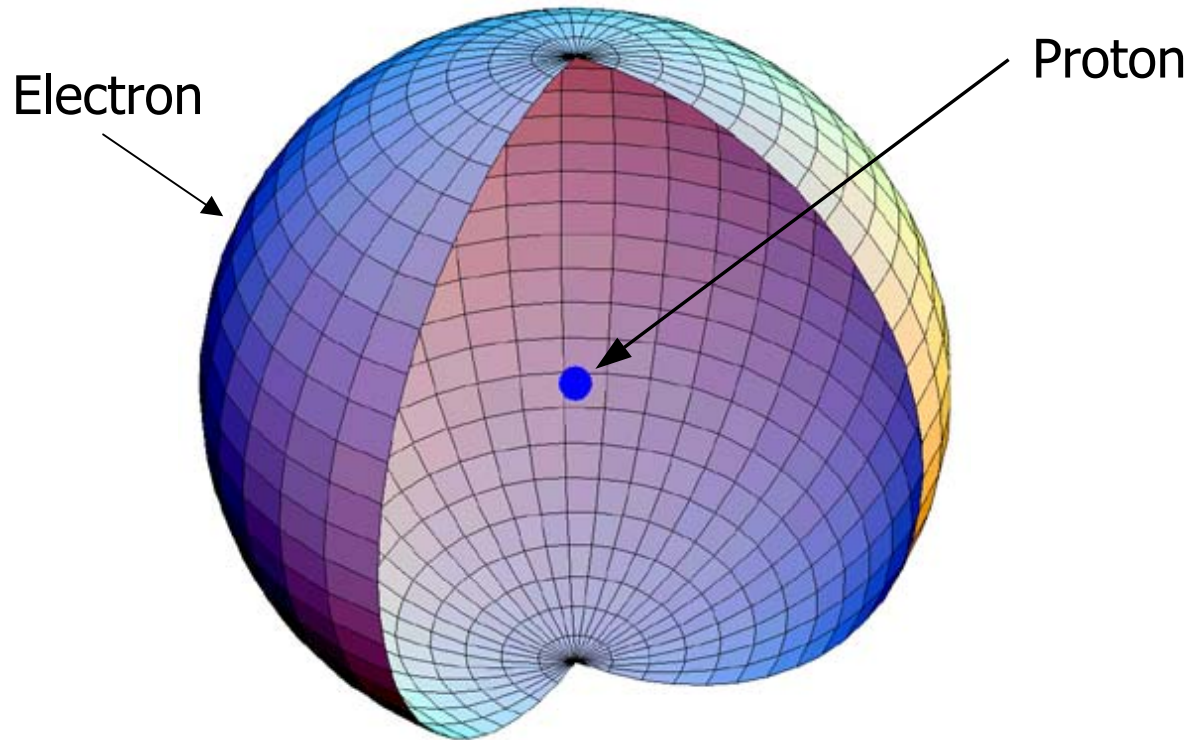
$$f(r) = \frac{1}{r^2} \delta(r - r_n) \quad \text{where } r_n = nr_1$$

The electron equation of motion comprises a constant spin function and an angular function that modulates the constant spin function on a spherical shell of zero thickness.



The Orbitsphere

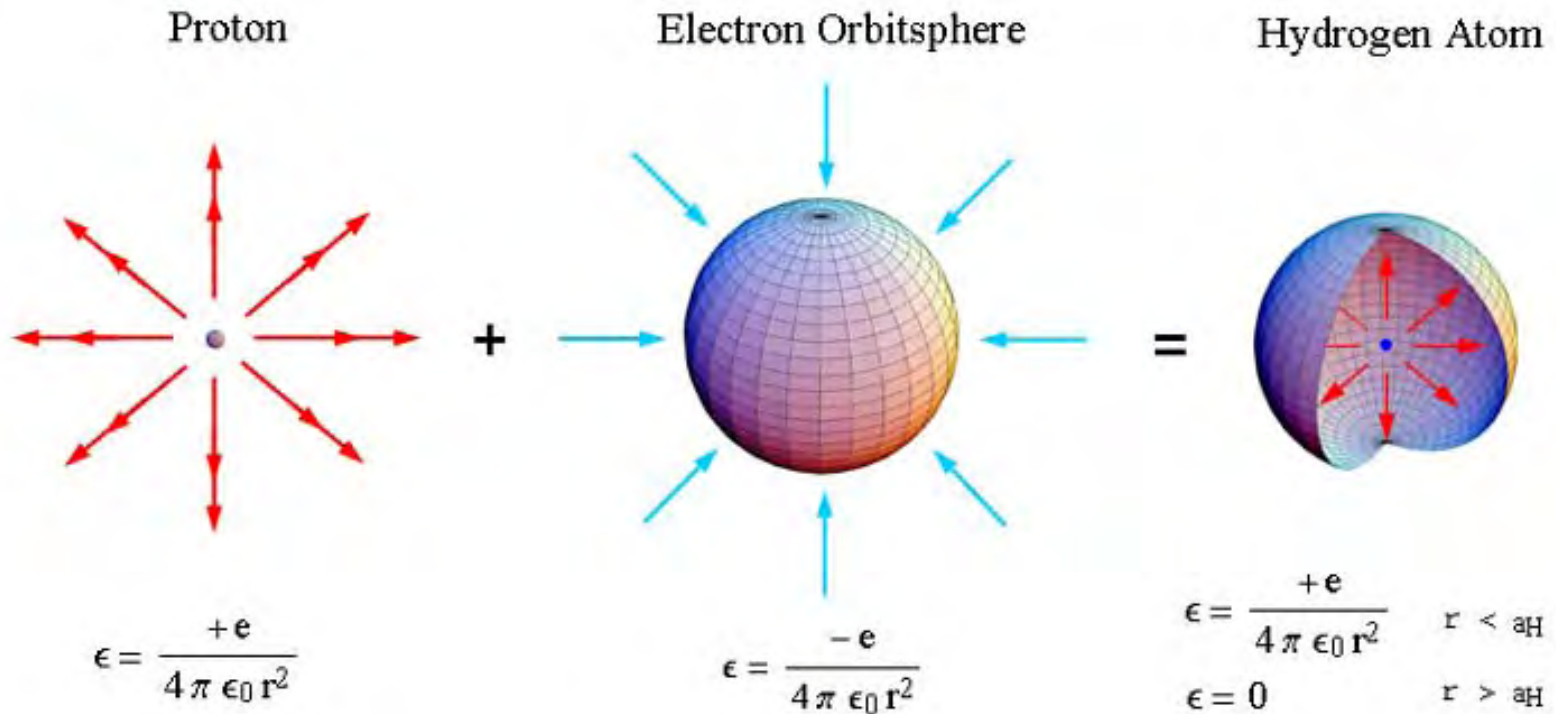
The orbitsphere or spin function is a two-dimensional spherical shell with the Bohr radius of the hydrogen atom. It is a nonradiative, minimum energy surface, and very stable due to the balanced forces that correspond to a pressure of 20 million atmospheres.



The orbitsphere has a thickness of the Schwarzschild radius:

$$r_g = \frac{2Gm_e}{c^2} = 1.3525 \times 10^{-57} \text{ m.}$$

Electric Fields of Proton, Electron, and Hydrogen Atom



The Wavelength of the Bound Electron

For time-harmonic motion on each great circle on a spherical shell

$$2\pi r = \lambda$$

The de Broglie wavelength is observed for the electron.

$$\lambda_n = \frac{h}{p_n} = \frac{h}{m_e v_n}$$

Then

$$v_n = \frac{\hbar}{m_e r_n}$$

Which is simply a statement of conservation of the angular momentum:

$$\sum |\mathbf{L}_i| = \sum |\mathbf{r} \times m_i \mathbf{v}| = m_e r_n \frac{\hbar}{m_e r_n} = \hbar$$

The de Broglie wavelength of the free electron is also due to conservation of angular momentum as shown below.

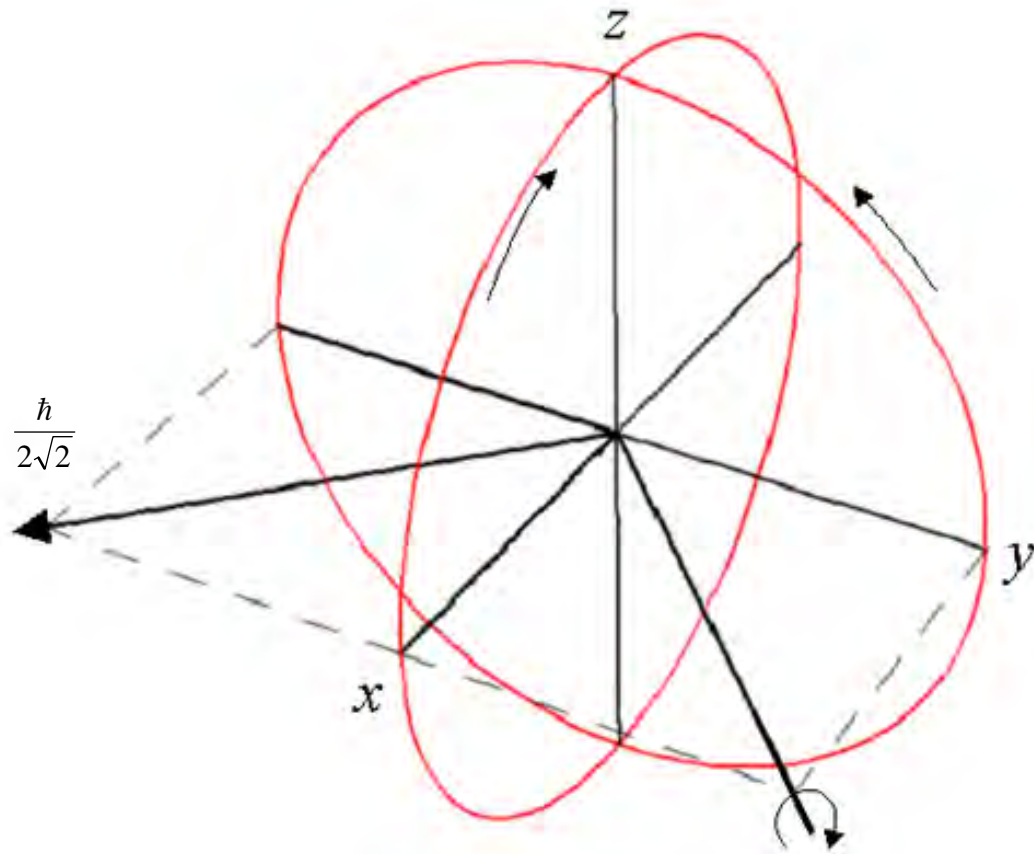
Spin Function

The uniform current density function $Y_0^0(\theta, \phi)$ that gives rise to the spin of the electron is generated from a basis set current-vector field defined as the orbitsphere current-vector field ("orbitsphere-cvf").

The orbitsphere-cvf comprises a continuum of correlated orthogonal great circle current loops.

The current pattern comprising two components is generated over the surface by two sets (*Steps One and Two*) of rotations of two orthogonal great circle current loops that serve as basis elements about each of the $(i_x, i_y, 0i_z)$ and $(-\frac{1}{\sqrt{2}}i_x, \frac{1}{\sqrt{2}}i_y, i_z)$ -axes, respectively, by π radians.

The Orthogonal Great Circle Basis Set for Step One



The current on the great circle in the $y'z'$ -plane moves counter clockwise and the current on the great circle in the $x'z'$ -plane moves clockwise. The xyz -system is the laboratory frame, and the orthogonal-current-loop basis set is rigid with respect to the $x'y'z'$ -system that rotates about the $(i_x, i_y, 0i_z)$ -axis by π radians to generate the elements of the first component of the orbit sphere-cvf. The angular momentum of the orthogonal great circle current loops in the $x'y'$ -plane that is evenly distributed over the surface is $\frac{\hbar}{2\sqrt{2}}$.

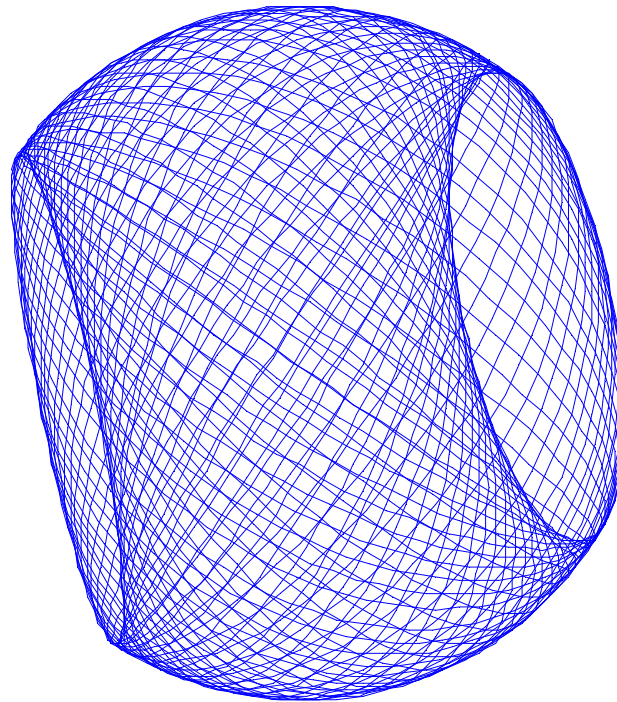
Algorithm of the Current Loops



3D View of the Resultant Semi-Sphere

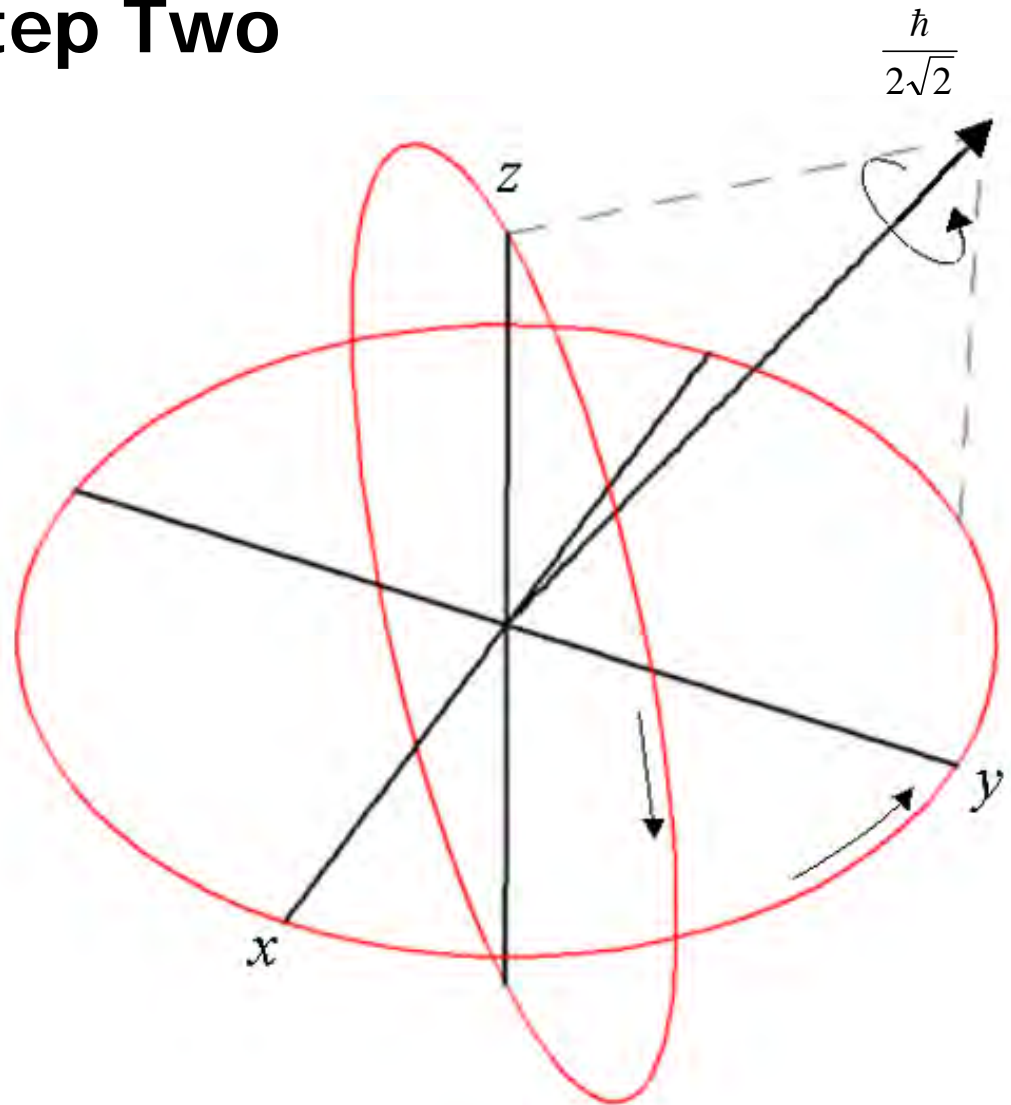


Step 1:



The Orthogonal Great Circle Basis Set for Step Two

The current on the great circle in the plane that bisects the $x'y'$ -quadrant and is parallel to the z' -axis moves clockwise, and the current on the great circle in the $x'y'$ -plane moves counterclockwise. Rotation of the great circles about the $(-\frac{1}{\sqrt{2}} i_x, \frac{1}{\sqrt{2}} i_y, i_z)$ -axis by π radians generates the elements of the second component of the orbitsphere-cvf. The angular momentum of the orthogonal great circle current loops in the plane along the $(-\frac{1}{\sqrt{2}} i_x, \frac{1}{\sqrt{2}} i_y, i_z)$ - and z -axes is $\frac{\hbar}{2\sqrt{2}}$ corresponding to each of the z and $-xy$ -components of magnitude $\frac{\hbar}{4}$.

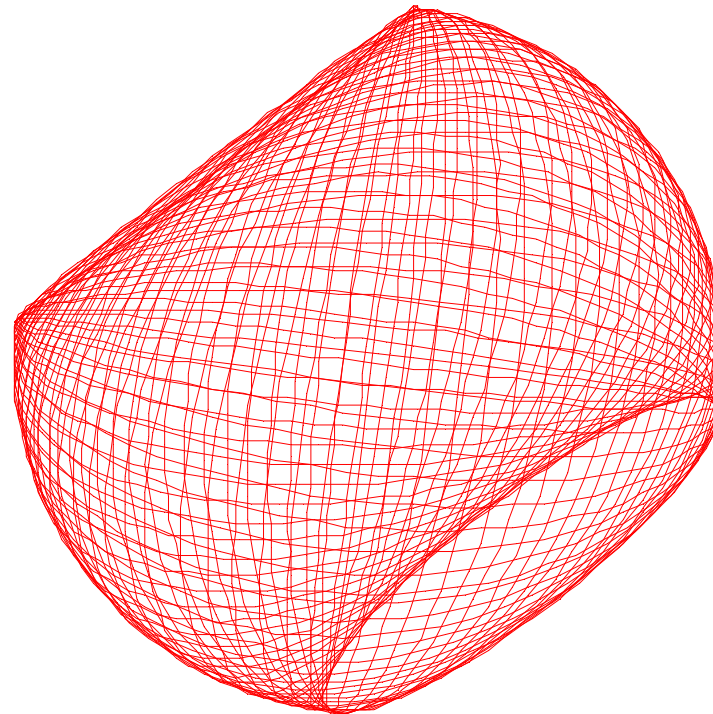


Algorithm of the Current Loops

3D View of the Resultant Semi-Sphere



Step 2:



The Rotation Matrices of the Orthogonal Great Circle Basis Set for Step One

One half of the orbitsphere-cvf, the orbitsphere-cvf component of STEP ONE, is generated by rotation of two orthogonal great circles about the $(i_x, i_y, 0i_z)$ -axis by π wherein one basis-element great circle is in the yz-plane and the other is in the xz-plane:

Step One

$$\begin{bmatrix} x' \\ y' \\ z' \end{bmatrix} = \begin{bmatrix} \frac{1}{2} + \frac{\cos \theta}{2} & \frac{1}{2} - \frac{\cos \theta}{2} & -\frac{\sin \theta}{\sqrt{2}} \\ \frac{1}{2} - \frac{\cos \theta}{2} & \frac{1}{2} + \frac{\cos \theta}{2} & \frac{\sin \theta}{\sqrt{2}} \\ \frac{\sin \theta}{\sqrt{2}} & -\frac{\sin \theta}{\sqrt{2}} & \cos \theta \end{bmatrix} \cdot \left(\begin{bmatrix} 0 \\ r_n \cos \phi \\ r_n \sin \phi \end{bmatrix} + \begin{bmatrix} r_n \cos \phi \\ 0 \\ r_n \sin \phi \end{bmatrix} \right)$$

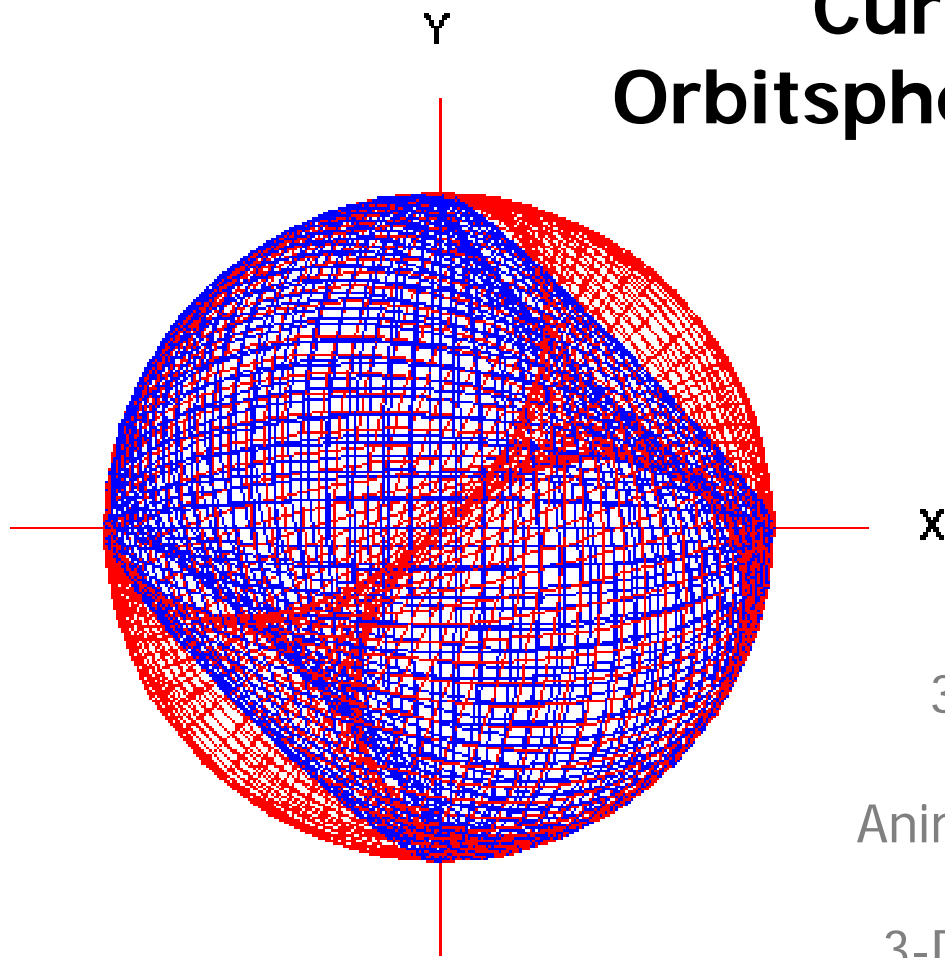
The Rotation Matrices of the Orthogonal Great Circle Basis Set for Step Two

The orbitsphere-cvf, the orbitsphere-cvf component of STEP TWO is generated by rotation of two orthogonal great circles about the $(-\frac{1}{\sqrt{2}} i_{x'}, \frac{1}{\sqrt{2}} i_{y'}, i_z)$ -axis by π wherein one basis-element great circle is in the xy-plane and the other bisects the xy-quadrant and is parallel to the z-axis:

Step Two

$$\begin{bmatrix} x' \\ y' \\ z' \end{bmatrix} = \begin{bmatrix} \frac{1}{4}(1+3\cos\theta) & \frac{1}{4}(-1+\cos\theta+2\sqrt{2}\sin\theta) & \frac{1}{4}(-\sqrt{2}+\sqrt{2}\cos\theta-2\sin\theta) \\ \frac{1}{4}(-1+\cos\theta-2\sqrt{2}\sin\theta) & \frac{1}{4}(1+3\cos\theta) & \frac{1}{4}(\sqrt{2}-\sqrt{2}\cos\theta-2\sin\theta) \\ \frac{1}{2}\left(\frac{-1+\cos\theta}{\sqrt{2}}+\sin\theta\right) & \frac{1}{4}(\sqrt{2}-\sqrt{2}\cos\theta+2\sin\theta) & \cos^2\frac{\theta}{2} \end{bmatrix} \cdot \left(\begin{bmatrix} \frac{r_n \cos\phi}{\sqrt{2}} \\ \frac{r_n \cos\phi}{\sqrt{2}} \\ r_n \sin\phi \end{bmatrix} + \begin{bmatrix} r_n \cos\phi \\ r_n \sin\phi \\ 0 \end{bmatrix} \right)$$

Current pattern of the Orbitsphere Current-Vector Field



View Along the Positive Z Axis

3-D View of Orbitsphere



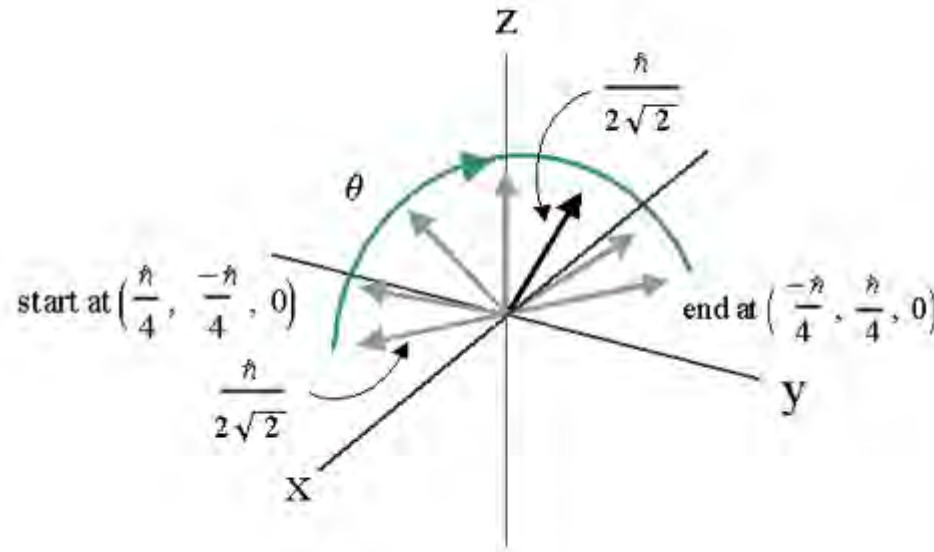
Animation of Current Points



3-D View of Current Points



Angular Momentum Projections of the Orbitsphere Current-Vector Field for Step One

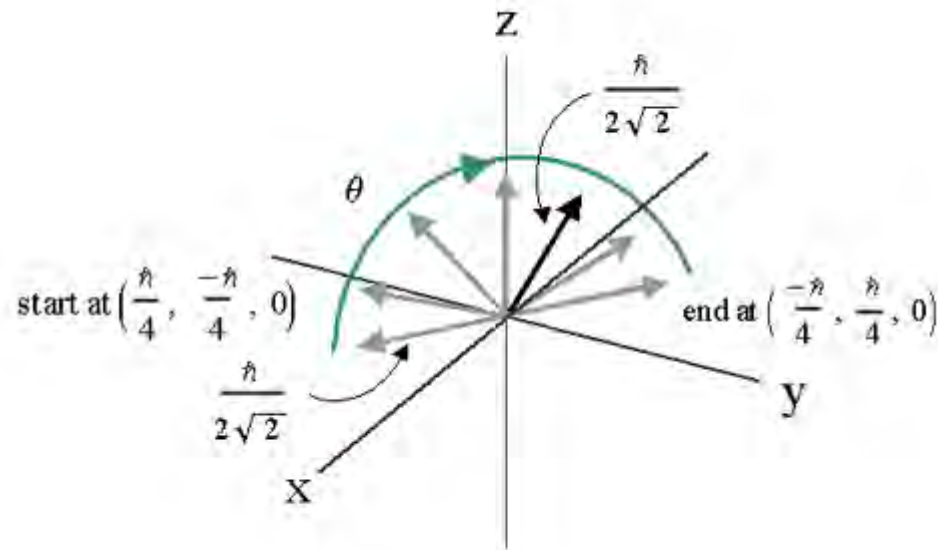


The trajectory of the resultant angular momentum vector of the orthogonal great circle current loops of magnitude $\frac{\hbar}{2\sqrt{2}}$ during Step One (gray vectors) gives $\mathbf{L}_z = \frac{\hbar}{4}$

$$\mathbf{L}_z = \sqrt{\frac{1}{\pi} \int_0^{\pi} \left[\frac{\hbar}{4} \sin \theta \right]^2 + \left[\frac{\hbar}{4} \sin \theta \right]^2} d\theta = \frac{\hbar}{2\sqrt{2}} \frac{1}{\sqrt{2}} = \frac{\hbar}{4}$$

$$\mathbf{L}_{xy} = \sqrt{\frac{2}{\pi} \int_0^{\frac{\pi}{2}} \left[\frac{\hbar}{4} \cos \theta \right]^2 + \left[\frac{\hbar}{4} \cos \theta \right]^2} d\theta - \sqrt{\frac{2}{\pi} \int_{\frac{\pi}{2}}^{\pi} \left[\frac{\hbar}{4} \cos \theta \right]^2 + \left[\frac{\hbar}{4} \cos \theta \right]^2} d\theta = \frac{\hbar}{2\sqrt{2}} \frac{1}{\sqrt{2}} - \frac{\hbar}{2\sqrt{2}} \frac{1}{\sqrt{2}} = 0$$

Angular Momentum Projections of the Orbitsphere Current-Vector Field for Step Two



The orthogonal great circle basis set rotates about the $(-\frac{1}{\sqrt{2}} i_x, \frac{1}{\sqrt{2}} i_y, i_z)$ -axis.

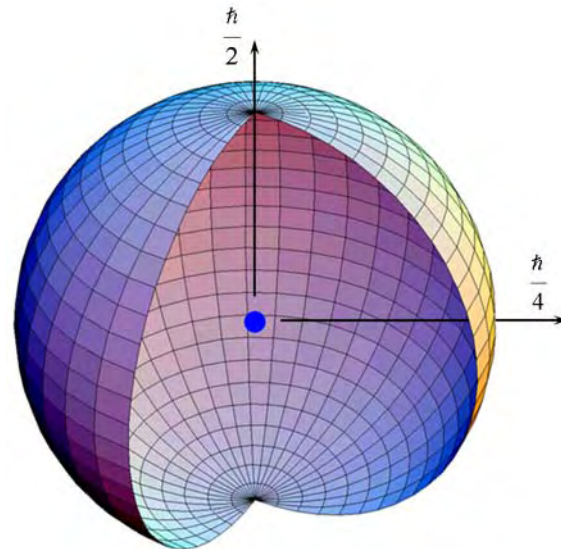
The resultant angular momentum vector of the orthogonal great circle current loops of magnitude $\frac{\hbar}{2\sqrt{2}}$ of Step Two (black vector) is stationary since it is along the $(-\frac{1}{\sqrt{2}} i_x, \frac{1}{\sqrt{2}} i_y, i_z)$ -axis.

The projections of the resultant vector for Step Two are $\mathbf{L}_{xy} = \frac{\hbar}{4}$ and $\mathbf{L}_z = \frac{\hbar}{4}$.

Exact Generation of the Uniform Current Pattern $Y_0^0(\theta, \phi)$ from Orbitsphere-CVF

The further constraint that the current density is uniform such that the charge density is uniform, corresponding to an equipotential, minimum energy surface is exactly satisfied by using the orbitsphere-cvf as a basis element to generate $Y_0^0(\theta, \phi)$.

The angular momentum is identically that given by the superposition of the primary component orbitsphere-cvfs of the orbitsphere-cvf, $\mathbf{L}_{xy} = \frac{\hbar}{4}$ and $\mathbf{L}_z = \frac{\hbar}{2}$.



Exact Generation of the Uniform Current Pattern

$Y_0^0(\theta, \phi)$ from Orbitsphere-CVF, cont'd

A convolution operator comprises an autocorrelation-type function that results in the replacement of each great circle of the primary orbitsphere-cvf with a secondary orbitsphere-cvf of matching angular momentum, orientation, and phase.

The convolution is given by rotating the matched basis-element secondary about the same axis as that which generated the primary from the basis-current loop to exactly give rise to the spherically-symmetric uniform current density, $Y_0^0(\theta, \phi)$.

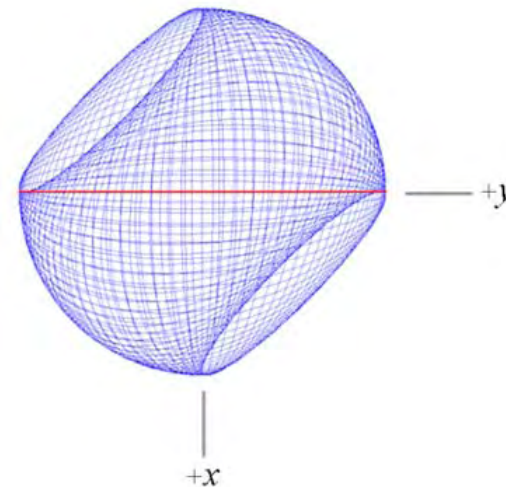
The resulting exact uniform current distribution has the same angular momentum distribution, resultant, \mathbf{L}_R , and components of $\mathbf{L}_{xy} = \frac{\hbar}{4}$ and $\mathbf{L}_z = \frac{\hbar}{2}$ as those of the orbitsphere-cvf used as a primary basis element.

STEP-ONE Matrices to Visualize the Currents of $Y_0^0(\theta, \phi)$

As an example, the current pattern of the STEP-ONE primary component orbitsphere-cvf generated by rotation of a basis element current loop in the yz-plane about the $(i_x, i_y, 0i_z)$ - axis by 2π using the matrix:

$$\begin{bmatrix} x' \\ y' \\ z' \end{bmatrix} = \begin{bmatrix} \frac{1}{2} + \frac{\cos\theta}{2} & \frac{1}{2} - \frac{\cos\theta}{2} & -\frac{\sin\theta}{\sqrt{2}} \\ \frac{1}{2} - \frac{\cos\theta}{2} & \frac{1}{2} + \frac{\cos\theta}{2} & \frac{\sin\theta}{\sqrt{2}} \\ \frac{\sin\theta}{\sqrt{2}} & -\frac{\sin\theta}{\sqrt{2}} & \cos\theta \end{bmatrix} \begin{bmatrix} 0 \\ r_n \cos\phi \\ r_n \sin\phi \end{bmatrix}$$

is shown with 6 degree increments of θ from the perspective of looking along the z-axis:



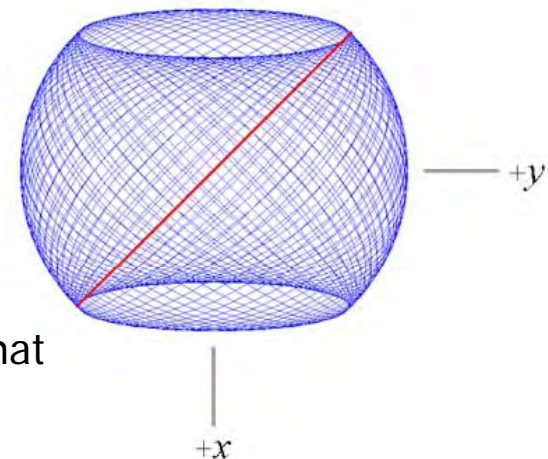
The yz-plane great circle current loop that served as a basis element that was initially in the yz-plane is shown as red. The angular momentum of this loop is along the x-axis.

Visualization cont'd

The secondary component orbitsphere-cvf that is matched for angular momentum, orientation, and phase is given the matrix:

$$\begin{bmatrix} x' \\ y' \\ z' \end{bmatrix} = \begin{bmatrix} \cos\left(\frac{\pi}{4}\right) & -\sin\left(\frac{\pi}{4}\right) & 0 \\ \sin\left(\frac{\pi}{4}\right)\cos\theta & \cos\left(\frac{\pi}{4}\right)\cos\theta & \sin\theta \\ -\sin\left(\frac{\pi}{4}\right)\sin\theta & -\cos\left(\frac{\pi}{4}\right)\sin\theta & \cos\theta \end{bmatrix} \begin{bmatrix} 0 \\ r_n \cos\phi \\ r_n \sin\phi \end{bmatrix}$$

and shown with 6 degree increments of θ from the perspective of looking along the z-axis:



The great circle current loop that served as a basis element that was initially in the yz-plane is shown as red.

The secondary component orbitsphere-cvf is aligned on the yz-plane and the resultant angular momentum vector, \mathbf{L}_R , is also along the x-axis.

Visualization cont'd

The uniform current distribution is exactly given as a infinite sum of the convolved elements comprising the secondary component orbitsphere-cvf rotated about the $(i_x, i_y, 0i_z)$ -axis by 2π using the matrix which generated the primary component orbitsphere-cvf.

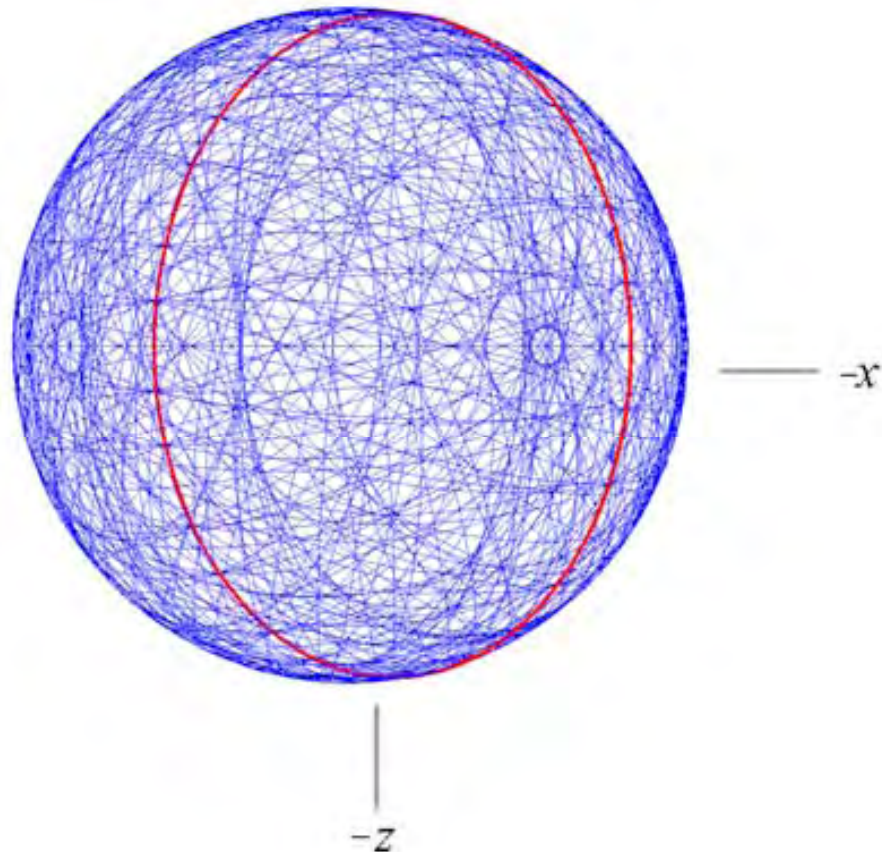
A representation that shows the current elements can be generated by showing the basis-element secondary component orbitsphere-cvf as a sum of M great circles and by showing the continuous convolution as a sum of M discrete incremental rotations of the position of the secondary component orbitsphere-cvf about the $(i_x, i_y, 0i_z)$ -axis:

$$\begin{bmatrix} x' \\ y' \\ z' \end{bmatrix} = \sum_{m=1}^{m=M} \begin{bmatrix} \frac{1}{2} + \frac{\cos\left(\frac{m2\pi}{M}\right)}{2} & \frac{1}{2} - \frac{\cos\left(\frac{m2\pi}{M}\right)}{2} & -\frac{\sin\left(\frac{m2\pi}{M}\right)}{\sqrt{2}} \\ \frac{1}{2} - \frac{\cos\left(\frac{m2\pi}{M}\right)}{2} & \frac{1}{2} + \frac{\cos\left(\frac{m2\pi}{M}\right)}{2} & \frac{\sin\left(\frac{m2\pi}{M}\right)}{\sqrt{2}} \\ \frac{\sin\left(\frac{m2\pi}{M}\right)}{\sqrt{2}} & -\frac{\sin\left(\frac{m2\pi}{M}\right)}{\sqrt{2}} & \cos\left(\frac{m2\pi}{M}\right) \end{bmatrix} \cdot \sum_{n=1}^{n=N} \begin{bmatrix} \cos\left(\frac{\pi}{4}\right) & -\sin\left(\frac{\pi}{4}\right) & 0 \\ \sin\left(\frac{\pi}{4}\right)\cos\left(\frac{n2\pi}{N}\right) & \cos\left(\frac{\pi}{4}\right)\cos\left(\frac{n2\pi}{N}\right) & \sin\left(\frac{n2\pi}{N}\right) \\ -\sin\left(\frac{\pi}{4}\right)\sin\left(\frac{n2\pi}{N}\right) & -\cos\left(\frac{\pi}{4}\right)\sin\left(\frac{n2\pi}{N}\right) & \cos\left(\frac{n2\pi}{N}\right) \end{bmatrix} \begin{bmatrix} 0 \\ r_n \cos \phi \\ r_n \sin \phi \end{bmatrix}$$

Visualization cont'd

A representation of the uniform current pattern of the $Y_0^0(\theta, \phi)$ orbitsphere shown with 30 degree increments ($N = M = 12$) of the angle to generate the secondary component orbitsphere-cvf and 30 degree increments of the rotation of this basis element about the $(i_x, i_y, 0i_z)$ -axis shown from the perspective that is transverse to the z-axis is:

3-D View of
Uniform Function



The great circle current loop that served as a basis element that was initially in the plane along the $(i_x, -i_y, 0i_z)$ - and z-axes of each secondary component orbitsphere-cvf is shown as red.

Stern-Gerlach Experiment

The Stern-Gerlach experiment implies a magnetic moment of one Bohr magneton and an associated angular momentum quantum number of 1/2. Historically, this quantum number is called the spin quantum number, s ($s = \frac{1}{2}$; $m_s = \pm \frac{1}{2}$).

The superposition of the vector projection of the orbitalsphere angular momentum on the z-axis is $\frac{\hbar}{2}$ with an orthogonal component of $\frac{\hbar}{4}$.

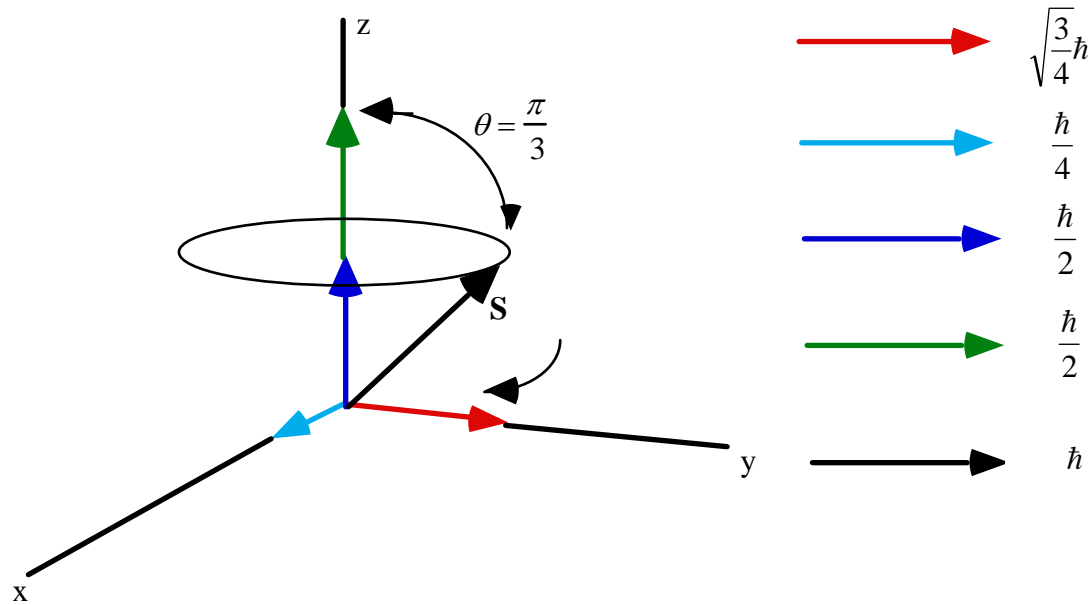
Excitation of a resonant Larmor precession gives rise to \hbar on an axis \mathbf{S} that precesses about the z-axis called the spin axis at the Larmor frequency at an angle of $\theta = \frac{\pi}{3}$.

The projections of the precessing components are:

$$\mathbf{S}_{\perp} = \hbar \sin \frac{\pi}{3} = \pm \sqrt{\frac{3}{4}} \hbar \mathbf{i}_{Y_R}$$

$$\mathbf{S}_{\parallel} = \pm \hbar \cos \frac{\pi}{3} = \pm \frac{\hbar}{2} \mathbf{i}_{Z_R}$$

Stern-Gerlach Experiment con't



Animation of
Larmor
Precession



The intrinsic angular momentum is on the z-axis is $\frac{\hbar}{2}$, but the excitation of the precessing \mathbf{S} component gives \hbar —twice the angular momentum on the z-axis due to the contribution from the precessing vector \mathbf{S} .

The superposition of the $\frac{\hbar}{2}$ z-axis component of the orbitsphere angular momentum and the $\frac{\hbar}{2}$ z-axis component of \mathbf{S} gives \hbar corresponding to the observed Zeeman splitting due to an electron magnetic moment of a Bohr magneton, $\mu_B = \frac{e\hbar}{2m_e}$.

Electron g Factor

Conservation of angular momentum of the orbit sphere permits a discrete change of its "kinetic angular momentum" ($\mathbf{r} \times m\mathbf{v}$) by the applied magnetic field of $\frac{\hbar}{2}$, and concomitantly the "potential angular momentum" ($\mathbf{r} \times e\mathbf{A}$) must change by $-\frac{\hbar}{2}$.

$$\begin{aligned}\Delta\mathbf{L} &= \frac{\hbar}{2} - \mathbf{r} \times e\mathbf{A} \\ &= \left[\frac{\hbar}{2} - \frac{e\phi}{2\pi} \right] \hat{z}\end{aligned}$$

In order that the change of angular momentum, $\Delta\mathbf{L}$, equals zero, ϕ must be $\Phi_0 = \frac{h}{2e}$, the magnetic flux quantum.

The magnetic moment of the electron is parallel or antiparallel to the applied field only.

Electron g Factor cont'd

Power flow during the spin-flip transition is governed by the Poynting power theorem,

$$\nabla \cdot (\mathbf{E} \times \mathbf{H}) = -\frac{\partial}{\partial t} \left[\frac{1}{2} \mu_0 \mathbf{H} \cdot \mathbf{H} \right] - \frac{\partial}{\partial t} \left[\frac{1}{2} \varepsilon_0 \mathbf{E} \cdot \mathbf{E} \right] - \mathbf{J} \cdot \mathbf{E}$$

The total energy of the flip transition is the sum of the energy of reorientation of the magnetic moment, the magnetic energy, the electric energy, and the dissipated energy of a fluxon trading the orbitsphere, respectively.

$$\Delta E_{mag}^{spin} = 2 \left(1 + \frac{\alpha}{2\pi} + \frac{2}{3} \alpha^2 \left(\frac{\alpha}{2\pi} \right) - \frac{4}{3} \left(\frac{\alpha}{2\pi} \right)^2 \right) \mu_B \mathbf{B}$$

$$\Delta E_{mag}^{spin} = g \mu_B \mathbf{B}$$

Where the stored magnetic energy corresponding to the $\frac{\partial}{\partial t} \left[\frac{1}{2} \mu_0 \mathbf{H} \cdot \mathbf{H} \right]$ term increases, the stored electric energy corresponding to the $\frac{\partial}{\partial t} \left[\frac{1}{2} \varepsilon_0 \mathbf{E} \cdot \mathbf{E} \right]$ term increases, and the $\mathbf{J} \cdot \mathbf{E}$ term is dissipative.

The spin-flip transition can be considered as involving a magnetic moment of g times that of a Bohr magneton. The calculated value of the $\frac{g}{2}$ factor is **1.001 159 652 137**. The experimental value of $\frac{g}{2}$ is **1.001 159 652 188(4)**.

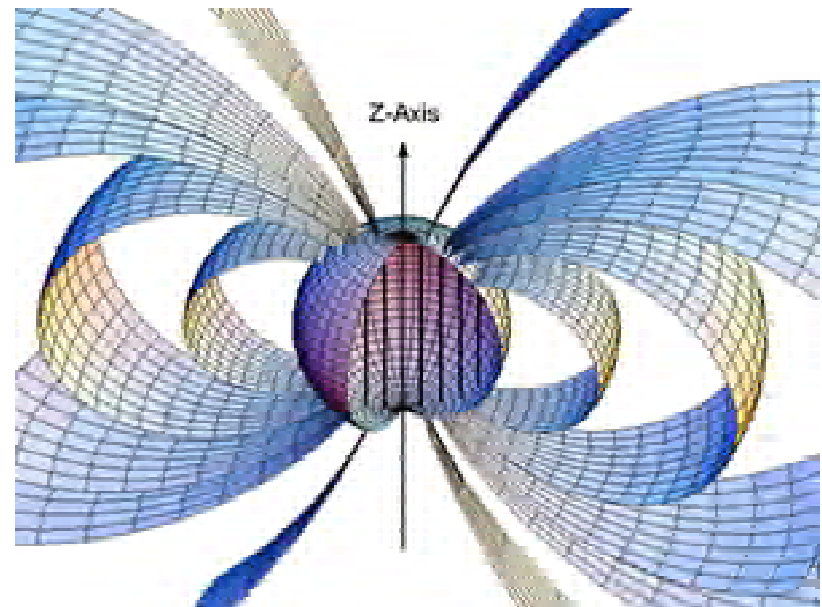
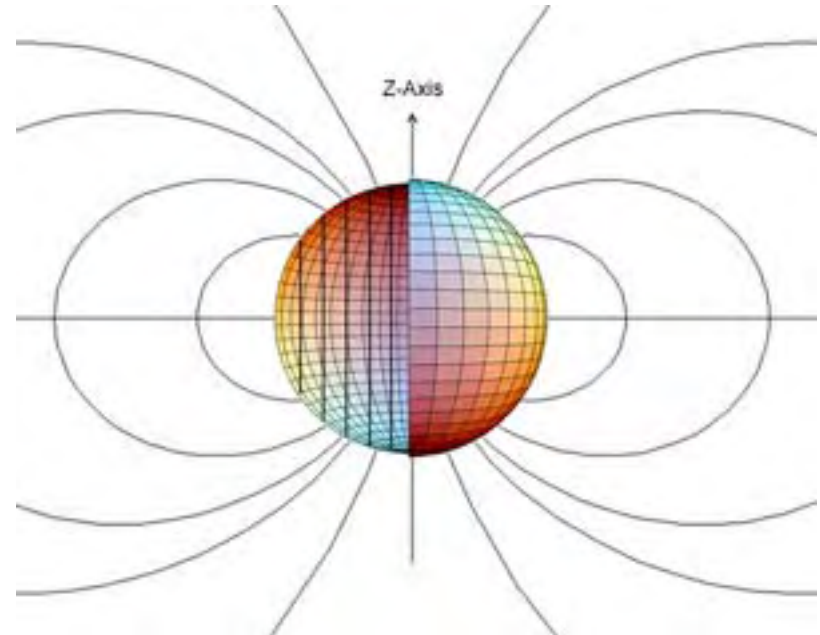
Magnetic Field of the Electron

$$\mathbf{H} = \frac{e\hbar}{m_e r_n^3} (\mathbf{i}_r \cos \theta - \mathbf{i}_\theta \sin \theta)$$

for $r < r_n$

$$\mathbf{H} = \frac{e\hbar}{2m_e r^3} (\mathbf{i}_r 2 \cos \theta + \mathbf{i}_\theta \sin \theta)$$

for $r > r_n$



Derivation of the Magnetic Energy

The energy stored in the magnetic field of the electron is

$$E_{mag} = \frac{1}{2} \mu_o \int_0^{2\pi} \int_0^{\pi} \int_0^{\infty} H^2 r^2 \sin \theta dr d\theta d\Phi$$

$$E_{mag \text{ total}} = \frac{\pi \mu_o e^2 \hbar^2}{m_e^2 r_1^3}$$

Angular Functions

Based on the radial solution, the angular charge and current-density functions of the electron, $A(\theta, \phi, t)$, must be a solution of the wave equation in two dimensions (plus time),

$$\left[\nabla^2 - \frac{1}{v^2} \frac{\delta^2}{\delta t^2} \right] A(\theta, \phi, t) = 0$$

where $\rho(r, \theta, \phi, t) = f(r)A(\theta, \phi, t) = \frac{1}{r^2} \delta(r - r_n)A(\theta, \phi, t)$

and $A(\theta, \phi, t) = Y(\theta, \phi)k(t)$

$$\left[\frac{1}{r^2 \sin \theta} \frac{\delta}{\delta \theta} \left(\sin \theta \frac{\delta}{\delta \theta} \right)_{r, \phi} + \frac{1}{r^2 \sin^2 \theta} \left(\frac{\delta^2}{\delta \phi^2} \right)_{r, \theta} - \frac{1}{v^2} \frac{\delta^2}{\delta t^2} \right] A(\theta, \phi, t) = 0$$

where v is the linear velocity of the electron

Charge-Density Functions

The charge-density functions including the time-function factor are

$$\ell = 0$$

$$\rho(r, \theta, \phi, t) = \frac{e}{8\pi r^2} [\delta(r - r_n)] [Y_0^0(\theta, \phi) + Y_\ell^m(\theta, \phi)]$$

$$\ell \neq 0$$

$$\rho(r, \theta, \phi, t) = \frac{e}{4\pi r^2} [\delta(r - r_n)] [Y_0^0(\theta, \phi) + \text{Re}\{Y_\ell^m(\theta, \phi)e^{i\omega_n t}\}]$$

where

$$\text{Re}\{Y_\ell^m(\theta, \phi)e^{i\omega_n t}\} = P_\ell^m(\cos \theta) \cos(m\phi + \omega_n t)$$

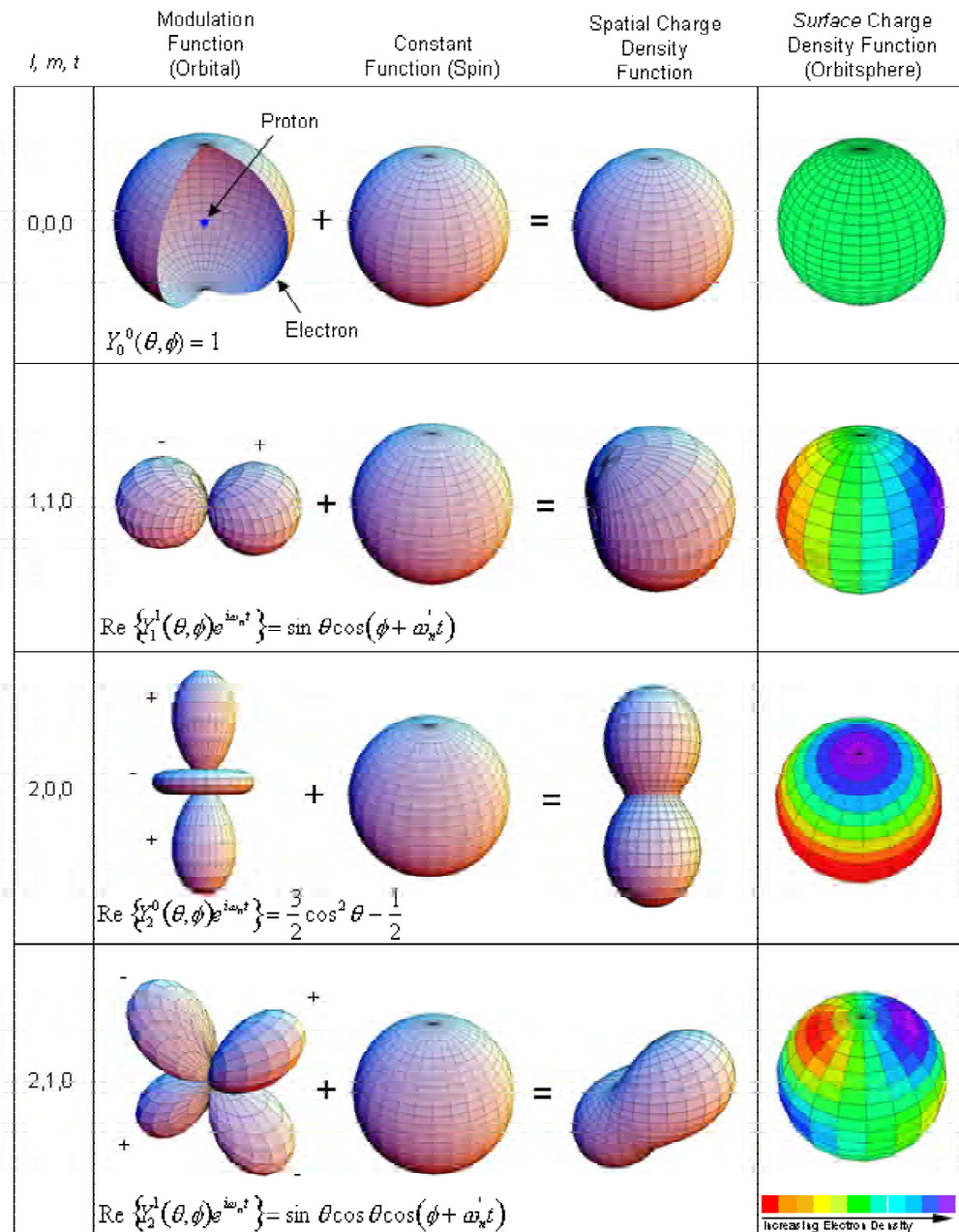
and $\omega_n = 0$ for $m = 0$

Spin and Orbital Parameters

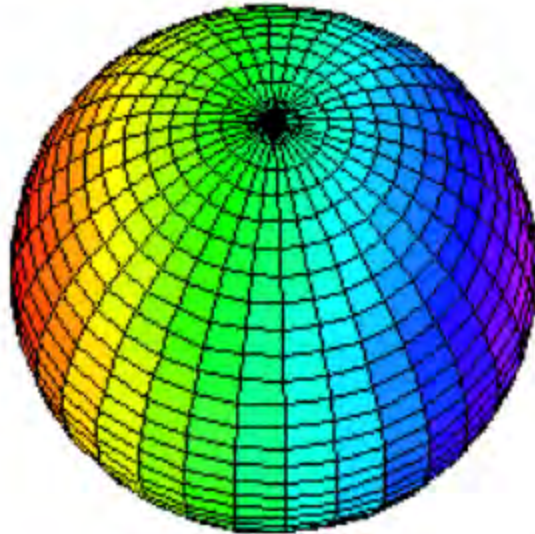
- The constant spin function is modulated by a time and spherical harmonic function.
- The modulation or traveling charge density wave corresponds to an orbital angular momentum in addition to a spin angular momentum.
- These states are typically referred to as p, d, f, etc. states or orbitals and correspond to an ℓ quantum number not equal to zero.

Orbital and Spin Functions

The orbital function modulates the constant (spin) function. (shown for $t=0$; three-dimensional view)

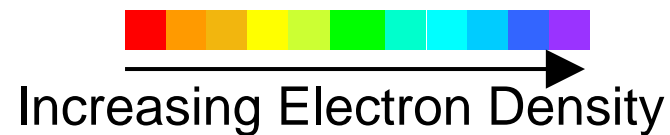


Charge Density Wave Moves on the Surface About the Z-Axis

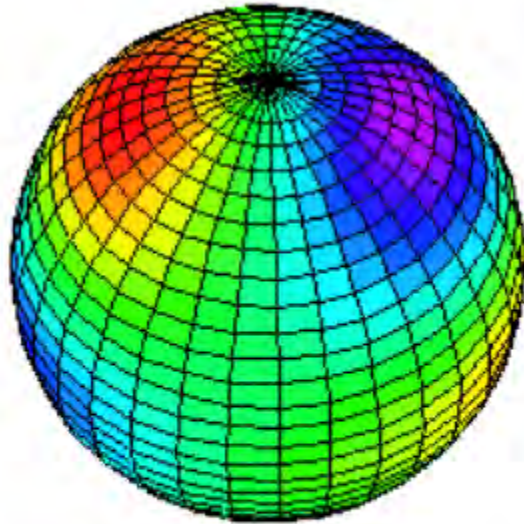


Px or Py Surface Charge Density
Wave (Orbital)

© Blacklight Power Inc.

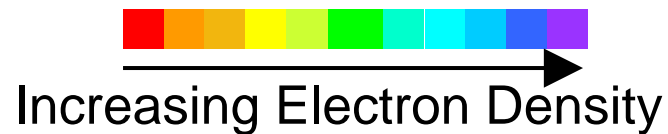


Charge Density Wave Moves on the Surface About the Z-Axis



D_{xz} or D_{yz} Surface Charge Density
Wave (Orbital)

© Blacklight Power Inc.



Moment of Inertia and Spin and Rotational Energies

$$\ell = 0$$

$$I_z = I_{spin} = \frac{m_e r_n^2}{2}$$

$$L_z = I\omega_z = \pm \frac{\hbar}{2}$$

$$E_{rotational} = E_{rotational, spin} = \frac{1}{2} \left[I_{spin} \left(\frac{\hbar}{m_e r_n^2} \right)^2 \right] = \frac{1}{2} \left[\frac{m_e r_n^2}{2} \left(\frac{\hbar}{m_e r_n^2} \right)^2 \right] = \frac{1}{4} \left[\frac{\hbar^2}{2I_{spin}} \right]$$

Moment of Inertia and Spin and Rotational Energies cont'd

$$\ell \neq 0$$

$$I_{\text{orbital}} = m_e r_n^2 \left[\frac{\ell(\ell+1)}{\ell^2 + 2\ell + 1} \right]^{\frac{1}{2}} = m_e r_n^2 \left[\frac{\ell}{\ell+1} \right]^{\frac{1}{2}}$$

$$L_z = m\hbar$$

$$E_{\text{rotational, orbital}} = \frac{\hbar^2}{2I} \left[\frac{\ell(\ell+1)}{\ell^2 + 2\ell + 1} \right]$$

$$T = \frac{\hbar^2}{2m_e r_n^2}$$

$$\langle E_{\text{rotational, orbital}} \rangle = 0$$

Special Relativistic Correction to the Electron Radius

The relationship between the electron wavelength and its radius is given by

$$2\pi r = \lambda \quad \text{where } \lambda \text{ is the de Broglie wavelength.}$$

The distance along each great circle in the direction of instantaneous motion undergoes length contraction and time dilation. Using a phase matching condition, the wavelengths of the electron and laboratory inertial frames are equated, and the corrected radius is given by

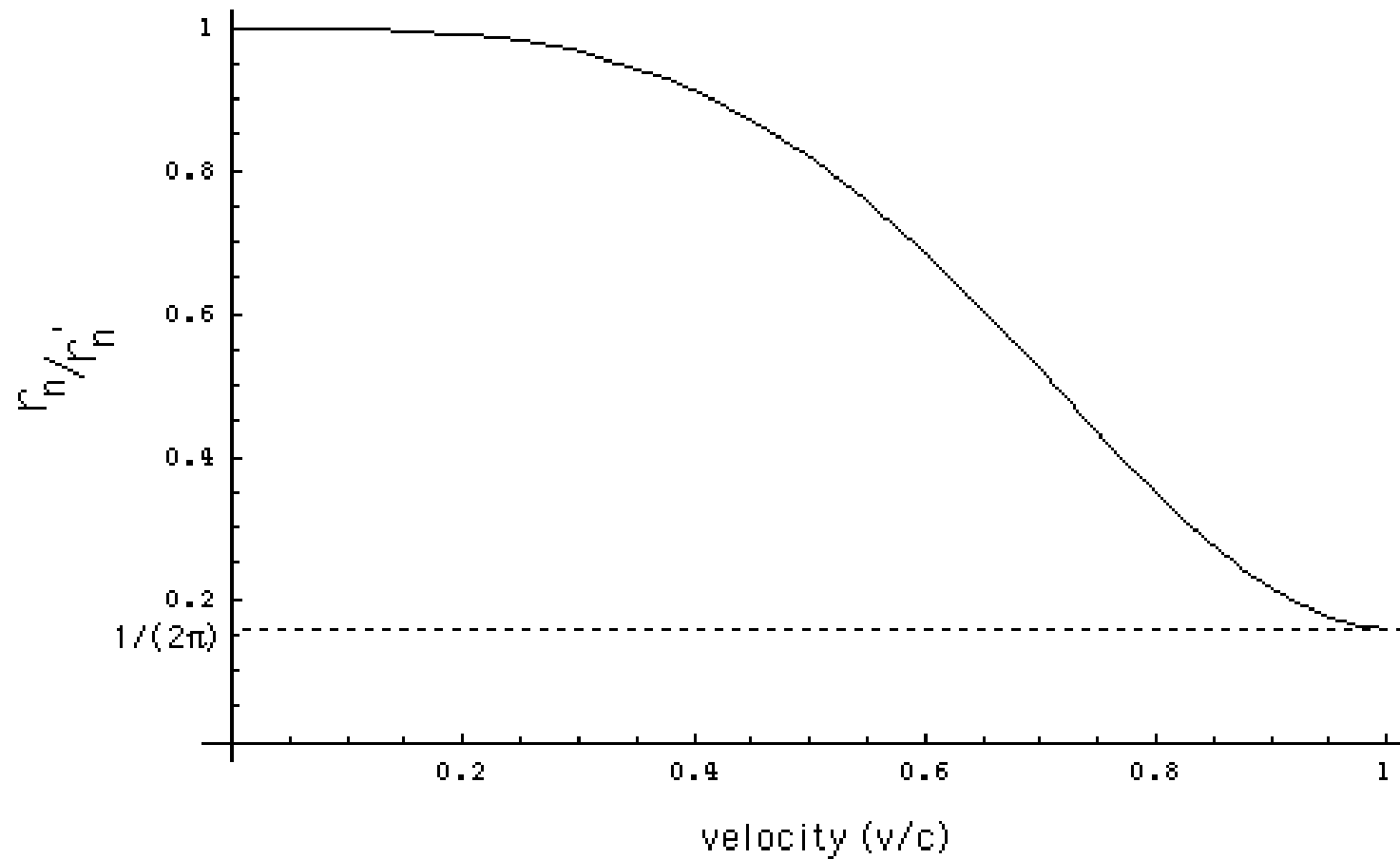
$$r_n = r'_n \left[\sqrt{1 - \left(\frac{v}{c}\right)^2} \sin \left[\frac{\pi}{2} \left(1 - \left(\frac{v}{c}\right)^2\right)^{3/2} \right] + \frac{1}{2\pi} \cos \left[\frac{\pi}{2} \left(1 - \left(\frac{v}{c}\right)^2\right)^{3/2} \right] \right]$$

where the electron velocity is given by

$$v_n = \frac{\hbar}{m_e r_n}$$

$\frac{e}{m_e}$ of the electron, the electron angular momentum of \hbar , and μ_B are invariant, but the mass and charge densities increase in the laboratory frame due to the relativistically contracted electron radius. As $v \rightarrow c$, $r/r' \rightarrow \frac{1}{2\pi}$ and $r = \lambda$.

The Normalized Radius as a Function of the Velocity Due to Relativistic Contraction



Nonradiation Condition (Acceleration Without Radiation)

$$\begin{aligned}
 K(s, \Theta, \Phi, \omega) = & 4\pi\omega_n \frac{\sin(2s_n r_n)}{2s_n r_n} \otimes 2\pi \sum_{\nu=1}^{\infty} \frac{(-1)^{\nu-1} (\pi \sin \Theta)^{2(\nu-1)}}{(\nu-1)!(\nu-1)!} \frac{\Gamma\left(\frac{1}{2}\right)\Gamma\left(\nu+\frac{1}{2}\right)}{(\pi \cos \Theta)^{2\nu+1} 2^{\nu+1}} \frac{2\nu!}{(\nu-1)!} s^{-2\nu} \\
 & \otimes 2\pi \sum_{\nu=1}^{\infty} \frac{(-1)^{\nu-1} (\pi \sin \Phi)^{2(\nu-1)}}{(\nu-1)!(\nu-1)!} \frac{\Gamma\left(\frac{1}{2}\right)\Gamma\left(\nu+\frac{1}{2}\right)}{(\pi \cos \Phi)^{2\nu+1} 2^{\nu+1}} \frac{2\nu!}{(\nu-1)!} s^{-2\nu} \frac{1}{4\pi} [\delta(\omega - \omega_n) + \delta(\omega + \omega_n)]
 \end{aligned}$$

$$\mathbf{s}_n \bullet \mathbf{v}_n = \mathbf{s}_n \bullet \mathbf{c} = \omega_n$$

$$r_n = \lambda_n$$

Spacetime harmonics of $\frac{\omega_n}{c} = k$ or $\frac{\omega_n}{c} \sqrt{\frac{\epsilon}{\epsilon_0}} = k$ for which

the Fourier transform of the current-density function is nonzero do not exist. Radiation due to charge motion does not occur in any medium when this boundary condition is met.

Nonradiation Based on the Electron Electromagnetic Fields and the Poynting Power Vector

The general multipole field solution to Maxwell's equations in a source-free region of empty space with the assumption of a time dependence $e^{i\omega_n t}$ is

$$\begin{aligned} \mathbf{B} &= \sum_{\ell,m} \left[a_E(\ell,m) f_\ell(kr) \mathbf{X}_{\ell,m} - \frac{i}{k} a_M(\ell,m) \nabla \times g_\ell(kr) \mathbf{X}_{\ell,m} \right] \\ \mathbf{E} &= \sum_{\ell,m} \left[\frac{i}{k} a_E(\ell,m) \nabla \times f_\ell(kr) \mathbf{X}_{\ell,m} + a_M(\ell,m) g_\ell(kr) \mathbf{X}_{\ell,m} \right] \end{aligned} \quad (1)$$

Nonradiation Based on the Electron Electromagnetic Fields and the Poynting Power Vector con'd

For the electron source current comprising a multipole of order (ℓ, m) the far fields are given by

$$\mathbf{B} = -\frac{i}{k} a_M(\ell, m) \nabla \times g_\ell(kr) \mathbf{X}_{\ell, m}$$

$$\mathbf{E} = a_M(\ell, m) g_\ell(kr) \mathbf{X}_{\ell, m}$$
(2)

and the time-averaged power radiated per solid angle $\frac{dP(\ell, m)}{d\Omega}$ is

$$\frac{dP(\ell, m)}{d\Omega} = \frac{c}{8\pi k^2} |a_M(\ell, m)|^2 |\mathbf{X}_{\ell, m}|^2$$
(3)

where is $a_M(\ell, m)$

$$a_M(\ell, m) = \frac{-ek^2}{c\sqrt{\ell(\ell+1)}} \frac{\omega_n}{2\pi} Nj_\ell(kr_n) \Theta \sin(mks)$$
(4)

In the case that k is the lightlike k^0 , then $k = \omega_n / c$, in Eq. (4), and Eqs. (2-3) vanishes for

$$s = vT_n = R = r_n = \lambda_n$$
(5)

There is no radiation.

Force Balance Equation

$$\frac{m_e v_1^2}{4\pi r_1^2 r_1} = \frac{e Ze}{4\pi r_1^2 4\pi\epsilon_0 r_1^2} - \frac{1}{4\pi r_1^2} \frac{\hbar^2}{mr_1^3}$$

$$r_1 = \frac{a_H}{Z}$$

Energy Calculations

- Potential Energy

$$V = \frac{-Ze^2}{4\pi\epsilon_0 r_1} = \frac{-Z^2 e^2}{4\pi\epsilon_0 a_H} = -Z^2 \times 4.3675 \times 10^{-18} \text{ J} = -Z^2 \times 27.2 \text{ eV}$$

- Kinetic Energy

$$T = \frac{Z^2 e^2}{8\pi\epsilon_0 a_H} = Z^2 \times 13.59 \text{ eV} \quad T = E_{ele} = -\frac{1}{2} \epsilon_0 \int_{\infty}^{r_1} \mathbf{E}^2 dv$$

where $\mathbf{E} = -\frac{Ze}{4\pi\epsilon_0 r^2}$

- Electric Energy

$$E_{ele} = -\frac{Z^2 e^2}{8\pi\epsilon_0 a_H} = -Z^2 \times 2.1786 \times 10^{-18} \text{ J} = -Z^2 \times 13.598 \text{ eV}$$

Some Calculated Parameters for the Hydrogen Atom (n=1)

radius	$r_1 = a_H$	$5.2918 \times 10^{-11} \text{ m}$
potential energy	$V = \frac{-e^2}{4\pi\epsilon_0 a_H}$	-27.196 eV
kinetic energy	$T = \frac{e^2}{8\pi\epsilon_0 a_H}$	13.598 eV
angular velocity (spin)	$\omega_1 = \frac{\hbar}{m_e r_1^2}$	$4.13 \times 10^{16} \text{ rads}^{-1}$
linear velocity	$v_1 = r_1 \omega_1$	$2.19 \times 10^6 \text{ ms}^{-1}$
wavelength	$\lambda_1 = 2\pi r_1$	$3.325 \times 10^{-10} \text{ m}$
spin quantum number	$s = \frac{1}{2}$	$\frac{1}{2}$
moment of inertia	$I = \frac{m_e r_1^2}{2}$	$1.277 \times 10^{-51} \text{ kgm}^2$
angular kinetic energy	$E_{angular} = \frac{1}{2} I \omega_1^2$	6.795 eV

Some Calculated Parameters for the Hydrogen Atom (n=1) cont'd

magnitude of the angular momentum	\hbar	$1.0545 \times 10^{-34} \text{ Js}$
projection of the angular momentum onto the transverse-axis	$\frac{\hbar}{4}$	$2.636 \times 10^{-35} \text{ Js}$
projection of the angular momentum onto the z -axis	$S_z = \frac{\hbar}{2}$	$5.273 \times 10^{-35} \text{ Js}$
mass density	$\frac{m_e}{4 \pi r_1^2}$	$2.589 \times 10^{-11} \text{ kgm}^{-2}$
charge -density	$\frac{e}{4 \pi r_1^2}$	4.553 Cm^{-2}

Calculated Energies (Relativistic) and Calculated Ionization Energies for Some One-electron Atoms

Atom	Calculated r_1 (a_0)	Calculated Kinetic Energy (eV)	Calculated Ionization Energy (eV)	Experimental Ionization Energy (eV)
H	1.000	13.59	13.59849	13.59844
He^+	0.500	54.35	54.40986	54.41778
Li^{2+}	0.333	122.28	122.43743	122.45429
Be^{3+}	0.250	217.40	217.68689	217.71865
B^{4+}	0.200	339.68	340.16647	340.2258
C^{5+}	0.167	489.14	489.88727	489.99334
N^{6+}	0.143	665.77	666.86361	667.046
O^{7+}	0.125	869.58	871.11351	871.4101

Excited States

- The orbitsphere is a dynamic spherical resonator cavity which traps photons of discrete frequencies.
- The relationship between an allowed radius and the "photon standing wave" wavelength is $2\pi r = n\lambda$
where n is an integer.
- The relationship between an allowed radius and the electron wavelength is $2\pi r = n\lambda$
where $n=1,2,3,4,\dots$
- The radius of an orbitsphere increases with the absorption of electromagnetic energy.
- The solutions to Maxwell's equations for modes that can be excited in the orbitsphere resonator cavity give rise to four quantum numbers, and the energies of the modes are the experimentally known hydrogen spectrum.

Excited States cont'd

The relationship between the electric field equation and the "trapped photon" source charge-density function is given by Maxwell's equation in two dimensions

$$\mathbf{n} \cdot (\mathbf{E}_1 - \mathbf{E}_2) = \frac{\sigma}{\epsilon_0}$$

The photon standing electromagnetic wave is phase matched to with the electron

$$\mathbf{E}_{r_{\text{photon } n,\ell,m}} = \frac{e(na_H)^\ell}{4\pi\epsilon_0} \frac{1}{r^{(\ell+2)}} \left[-Y_0^0(\theta, \phi) + \frac{1}{n} \left[Y_0^0(\theta, \phi) + \text{Re}\{Y_\ell^m(\theta, \phi)e^{i\omega_n t}\} \right] \right] \delta(r - r_n)$$

$$\omega_n = 0 \text{ for } m = 0 \quad n = 1, 2, 3, 4, \dots \quad \ell = 1, 2, \dots, n - 1 \quad m = -\ell, -\ell + 1, \dots, 0, \dots, +\ell$$

$$\mathbf{E}_{r_{\text{total}}} = \frac{e}{4\pi\epsilon_0 r^2} + \frac{e(na_H)^\ell}{4\pi\epsilon_0} \frac{1}{r^{(\ell+2)}} \left[-Y_0^0(\theta, \phi) + \frac{1}{n} \left[Y_0^0(\theta, \phi) + \text{Re}\{Y_\ell^m(\theta, \phi)e^{i\omega_n t}\} \right] \right] \delta(r - r_n)$$

$$\omega_n = 0 \text{ for } m = 0$$

For $r=na_H$ and $m=0$, the total radial electric field is

$$\mathbf{E}_{r_{\text{total}}} = \frac{1}{n} \frac{e}{4\pi\epsilon_0 (na_H)^2}$$

Photon Absorption

- The energy of the photon which excites a mode in the electron spherical resonator cavity from radius a_H to radius na_H is

$$E_{\text{photon}} = \frac{e^2}{8\pi\epsilon_0 a_H} \left[1 - \frac{1}{n^2} \right] = h\nu = \hbar\omega$$

- The change in angular velocity of the orbitsphere for an excitation from $n=1$ to $n=n$ is

$$\Delta\omega = \frac{\hbar}{m_e (a_H)^2} - \frac{\hbar}{m_e (na_H)^2} = \frac{\hbar}{m_e (a_H)^2} \left[1 - \frac{1}{n^2} \right]$$

- The kinetic energy change of the transition is

$$\frac{1}{2} m_e (\Delta v)^2 = \frac{e^2}{8\pi\epsilon_0 a_H} \left[1 - \frac{1}{n^2} \right] = \hbar\omega$$

- The change in angular velocity of the electron orbitsphere is identical to the angular velocity of the photon necessary for the excitation, ω_{photon}
- The **correspondence principle holds**

Orbital and Spin Splitting

The ratio of the square of the angular momentum, M^2 , to the square of the energy, U^2 , for a pure (1, m) multipole

$$\frac{M^2}{U^2} = \frac{m^2}{\omega^2}$$

The magnetic moment is defined as $\mu = \frac{\text{charge x angular momentum}}{2 \times \text{mass}}$

The radiation of a multipole of order (1, m) carries $m\hbar$ units of the z component of angular momentum per photon of energy $\hbar\omega$. Thus, the z component of the angular momentum of the corresponding excited state electron orbit sphere is $L_z = m\hbar$.

Therefore,

$$\mu_z = \frac{em\hbar}{2m_e} = m\mu_B$$

where μ_B is the Bohr magneton.

The orbital splitting energy is

$$E_{mag}^{orb} = m\mu_B \mathbf{B}$$

Orbital and Spin Splitting cont'd

The spin and orbital splitting energies superimpose; thus, the principal excited state energy levels of the hydrogen atom are split by the energy $E_{mag}^{spin/orb}$

$$E_{mag}^{spin/orb} = m \frac{e\hbar}{2m_e} \mathbf{B} + m_s g \frac{e\hbar}{m_e} \mathbf{B}$$

where

$$n = 2, 3, 4, \dots$$

$$\ell = 1, 2, \dots, n-1$$

$$m = -\ell, -\ell+1, \dots, 0, \dots, +\ell$$

$$m_s = \pm \frac{1}{2}$$

Selection Rules for the Electric Dipole Transition

$$\Delta m = 0, \pm 1$$

$$\Delta m_s = 0$$

Resonant Line Shape

$$\frac{1}{\tau} = \frac{\text{power}}{\text{energy}} = \frac{1}{m_e c^2} \frac{\eta}{24\pi} \left(\frac{e\hbar}{m_e a_0^2} \right)^2 \left[\frac{1}{n_i - n_f} \left(\frac{1}{n_f} - \frac{1}{n_i} \right) \right]^2$$

$$= 2.678 \times 10^9 \mathfrak{R} s^{-1}$$

where \mathfrak{R} is defined as $\mathfrak{R} = \left[\frac{1}{n_i - n_f} \left(\frac{1}{n_f} - \frac{1}{n_i} \right) \right]^2$

$$\mathbf{E}(\omega) \propto \int_0^{\infty} e^{-\alpha t} e^{-i\omega t} dt = \frac{1}{\alpha - i\omega}$$

The relationship between the rise-time and the bandwidth for exponential decay is

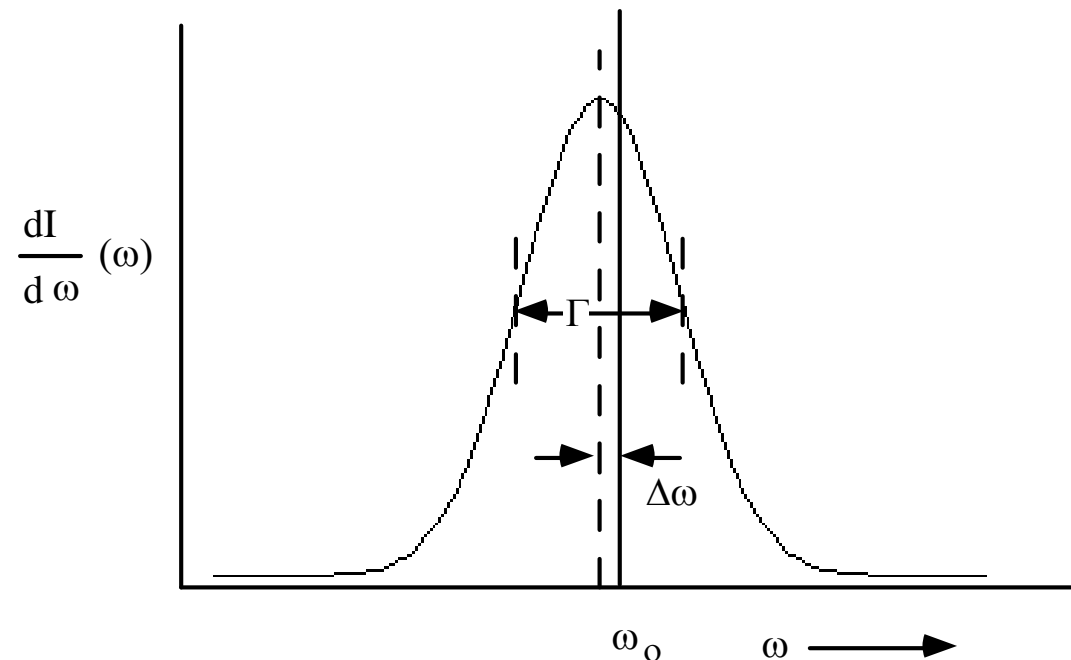
$$\tau\Gamma = \frac{1}{\pi}$$

The energy radiated per unit frequency interval is

$$\frac{dI(\omega)}{d\omega} = I_0 \frac{\Gamma}{2\pi} \frac{1}{(\omega - \omega_0 - \Delta\omega)^2 + (\Gamma/2)^2}$$

Broadening of the Spectral Line and the Radiative Reaction

Broadening of the spectral line due to the rise-time and shifting of the spectral line due to the radiative reaction. The resonant line shape has width Γ . The level shift is $\Delta\omega$.



Lamb Shift

The Lamb Shift of the ${}^2P_{1/2}$ state of the hydrogen atom is due to conservation of energy and linear momentum of the emitted photon, electron, and atom.

Electron Component

$$\Delta f = \frac{\Delta\omega}{2\pi} = \frac{E_{h\nu}}{h} = \frac{(E_{h\nu})^2}{2h\mu_e c^2} = 1052.48 \text{ MHz}$$

where $E_{h\nu}$ is

$$E_{h\nu} = 13.5983 \text{ eV} \left(1 - \frac{1}{n^2}\right) \frac{3}{4\pi} \sqrt{\frac{3}{4}} - h\Delta f$$

$$h\Delta f \lll 10 \text{ eV}; \quad n = 2$$

$$\therefore E_{h\nu} = 13.5983 \text{ eV} \left(1 - \frac{1}{2^2}\right) \frac{3}{4\pi} \sqrt{\frac{3}{4}}$$

Lamb Shift cont'd

Atom Component

$$\Delta f = \frac{\Delta\omega}{2\pi} = \frac{E_{h\nu}}{h} = \frac{(E_{h\nu})^2}{2hm_Hc^2} = \frac{\left(13.5983 \text{ eV} \left(1 - \frac{1}{2^2}\right) \left(1 + \frac{1}{2} - \sqrt{\frac{3}{4}}\right)\right)^2}{2hm_Hc^2} = 5.3839 \text{ MHz}$$

Sum of the Components

$$\Delta f = 1052.48 \text{ MHz} + 5.3839 \text{ MHz} = 1057.87 \text{ MHz}$$

The experimental Lamb Shift is $\Delta f = 1057.862 \text{ MHz}$

The other core results of QED can be replicated using closed form equations containing fundamental constants only without involving renormalization and virtual particles. The results derived from Maxwell's equations are in remarkable agreement with the experimental values and the accuracy is only limited by the accuracy of the fundamental constants.

Fine Structure Spin-Orbital Coupling

The fine structure energy is the Lamb-shifted relativistic interaction energy between the spin and orbital magnetic moments due to the corresponding angular momenta.

The energy, E_{FS} and frequency, Δf_{FS} , for the ${}^2P_{3/2} \rightarrow {}^2P_{1/2}$ transition called the fine structure splitting is given by the sum:

$$E_{FS} = \frac{\alpha^5 (2\pi)^2}{8} m_e c^2 \sqrt{\frac{3}{4}} + \left(13.5983 \text{ eV} \left(1 - \frac{1}{2^2} \right) \right)^2 \left[\frac{\left(\frac{3}{4\pi} \left(1 - \sqrt{\frac{3}{4}} \right) \right)^2}{2h\mu_e c^2} + \frac{\left(1 + \left(1 - \sqrt{\frac{3}{4}} \right) \right)^2}{2hm_H c^2} \right]$$

$$= 4.5190 \times 10^{-5} \text{ eV} + 1.75407 \times 10^{-7} \text{ eV}$$

$$= 4.53659 \times 10^{-5} \text{ eV}$$

$$\Delta f_{FS} = 10,927.0 \text{ MHz} + 42.4132 \text{ MHz} = 10,969.4 \text{ MHz}$$

The energy of $4.53659 \times 10^{-5} \text{ eV}$ corresponds to a frequency of 10,969.4 MHz, or a wavelength of 2.73298 cm.

The experimental value of the ${}^2P_{3/2} - {}^2P_{1/2}$ transition frequency is 10,969.1 MHz.

Hyperfine Structure

The hyperfine structure of the hydrogen atom is calculated from the force balance contribution between the electron and the proton.

The energy corresponds to the Stern-Gerlach and stored electric and magnetic energy changes.

The total energy of the transition from antiparallel to parallel alignment, $\Delta E_{total}^{S/N}$, is given as the sum:

$$\begin{aligned}\Delta E_{total}^{S/N} &= -\mu_0 \mu_B \mu_P \sqrt{\frac{3}{4}} \left(\frac{1}{r_+^3} + \frac{1}{r_-^3} \right) + \frac{-e^2}{8\pi\epsilon_0} \left[\frac{1}{r_+} - \frac{1}{r_-} \right] + \left(-1 - \left(\frac{2}{3} \right)^2 - \frac{\alpha}{4} \right) 4\pi\mu_0 \mu_B^2 \left(\frac{1}{r_+^3} - \frac{1}{r_-^3} \right) \\ &= -1.918365 \times 10^{-24} \text{ J} + 9.597048 \times 10^{-25} \text{ J} + 1.748861 \times 10^{-26} \text{ J} \\ &= -9.411714 \times 10^{-25} \text{ J}\end{aligned}$$

where

$$r = a_H \pm \frac{2\pi\alpha \mu_P}{ec} \sqrt{\frac{3}{4}}$$

The energy is expressed in terms of wavelength using the Planck relationship:

$$\lambda = \frac{hc}{\Delta E_{total}^{S/N}} = 21.10610 \text{ cm}$$

The experimental value from the hydrogen maser is 21.10611 cm.

Muonium Hyperfine Structure Interval

The hyperfine structure of muonium is calculated from the force balance contribution between the electron and the muon.

The energy corresponds to the Stern-Gerlach and stored electric and magnetic energy changes.

The energy of the ground state ($1^2S_{1/2}$) hyperfine structure interval of muonium, $\Delta E(\Delta \nu_{Mu})$

is given as the sum:

$$\begin{aligned} \Delta E(\Delta \nu_{Mu}) &= -\mu_0 \mu_B \mu_\mu \sqrt{\frac{3}{4}} \left(\frac{1}{r_{2+}^3} + \frac{1}{r_{2-}^3} \right) + \frac{-e^2}{8\pi\epsilon_0} \left[\frac{1}{r_{2+}} - \frac{1}{r_{2-}} \right] \\ &\quad + 4\pi\mu_0 \left(-1 - \left(\frac{2}{3} \cos \frac{\pi}{3} \right)^2 - \alpha \right) \left(\mu_B^2 \left(\frac{1}{r_{2+}^3} - \frac{1}{r_{2-}^3} \right) + \mu_{B,\mu}^2 \left(\frac{1}{r_{1+}^3} - \frac{1}{r_{1-}^3} \right) \right) \\ &= -6.02890320 \times 10^{-24} J + 3.02903048 \times 10^{-24} J + 4.23209178 \times 10^{-26} J + 1.36122030 \times 10^{-28} J \\ &= -2.95741568 \times 10^{-24} J \end{aligned}$$

where $r_2 = a_\mu \pm \frac{2\pi\alpha \mu_\mu}{ec} \sqrt{\frac{3}{4}}$ and $r_1 = \frac{a_\mu \pm \frac{2\pi\alpha \mu_\mu}{ec} \sqrt{\frac{3}{4}}}{\left(\frac{m_\mu}{m_e} \pm \frac{m_\mu e\alpha c}{2\hbar^2} \mu_0 \mu_\mu \sqrt{\frac{3}{4}} \right)^{1/3}}$

Muonium Hyperfine Structure Interval cont'd

Using Planck's equation, the interval frequency, $\Delta\nu_{Mu}$, and wavelength, $\Delta\lambda_{Mu}$, are

$$\Delta\nu_{Mu} = 4.46330328 \text{ GHz}$$

$$\Delta\lambda_{Mu} = 6.71682919 \text{ cm}$$

The experimental hyperfine structure interval of muonium is

$$\Delta E(\Delta\nu_{Mu}) = -2.957415336 \times 10^{-24} \text{ J}$$

$$\Delta\nu_{Mu} = 4.463302765(53) \text{ GHz (12ppm)}$$

$$\Delta\lambda_{Mu} = 6.71682998 \text{ cm}$$

Positronium Hyperfine Structure

The leptons are at the same radius, and the positronium hyperfine interval is given by the sum of the Stern-Gerlach, $\Delta E_{\text{spin-spin}}$, and fine structure, $\Delta E_{s/o} (^3S_1 \rightarrow ^1S_0)$, energies.

The hyperfine structure interval of positronium ($^3S_1 \rightarrow ^1S_0$) is given by the sum:

$$\begin{aligned} \Delta E_{\text{Ps hyperfine}} &= \Delta E_{\text{spin-spin}} + \Delta E_{s/o} (^3S_1 \rightarrow ^1S_0) \\ &= \frac{g\mu_o e^2 \hbar^2}{8m_e^2 (2a_0)^3} + \frac{3g\alpha^5 (2\pi)^2}{8} m_e c^2 \sqrt{\frac{3}{4}} \\ &= \frac{g\alpha^5 (2\pi)^2}{8} m_e c^2 \left(\frac{1}{8\pi\alpha} + \frac{3\sqrt{3}}{2} \right) \\ &= 8.41155110 \times 10^{-4} \text{ eV} \end{aligned}$$

Using Planck's equation, the interval in frequency, $\Delta\nu$, is

$$\Delta\nu = 203.39041 \text{ GHz}$$

The experimental ground-state hyperfine structure interval is

$$\Delta E_{\text{Ps hyperfine}} (\text{experimental}) = 8.41143 \times 10^{-4} \text{ eV}$$

$$\Delta\nu (\text{experimental}) = 203.38910(74) \text{ GHz (3.6ppm)}$$

Excited States of Helium

The orbitsphere is a resonator cavity which traps single photons of discrete frequencies.

In the ground state of the helium atom, both electrons are at $r_1 = r_2 = 0.567a_0$.

When a photon is absorbed, one of the initially indistinguishable electrons called electron 1 moves to a smaller radius, and the other called electron 2 moves to a greater radius.

The radii of electron 2 are determined from the force balance of the electric, magnetic, and centrifugal forces that corresponds to the minimum of energy of the system.

The excited-state energies are then given by the electric energies at these radii.

Excited States of Helium cont'd

Singlet Excited States with $\ell = 0$ ($1s^2 \rightarrow 1s^1(ns)^1$)

Force Balance Equation

$$\frac{m_e v^2}{r_2} = \frac{\hbar^2}{m_e r_2^3} = \frac{1}{n} \frac{e^2}{4\pi\epsilon_0 r_2^2} + \frac{2}{3} \frac{1}{n} \frac{\hbar^2}{2m_e r_2^3} \sqrt{s(s+1)}$$

Radius of electron 2

$$r_2 = \left[n - \frac{\sqrt{3}}{3} \right] a_{He} \quad n = 2, 3, 4, \dots$$

The excited-state energy is the energy stored in the electric field, E_{ele} , which is the energy of electron 2 relative to the ionized electron at rest having zero energy:

$$E_{ele} = -\frac{1}{n} \frac{e^2}{8\pi\epsilon_0 r_2}$$

Excited States of Helium cont'd

Triplet Excited States with $\ell = 0$ ($1s^2 \rightarrow 1s^1(ns)^1$)

Force Balance Equation

$$\frac{m_e v^2}{r_2} = \frac{\hbar^2}{m_e r_2^3} = \frac{1}{n} \frac{e^2}{4\pi\epsilon_0 r_2^2} + 2 \frac{2}{3} \frac{1}{n} \frac{\hbar^2}{2m_e r_2^3} \sqrt{s(s+1)}$$

Radius of electron 2

$$r_2 = \left[n - \frac{2\sqrt{\frac{3}{4}}}{3} \right] a_{He} \quad n = 2, 3, 4, \dots$$

Excited States of Helium cont'd

Singlet Excited States with $\ell \neq 0$

Force Balance Equation

$$\frac{m_e v^2}{r_2} = \frac{\hbar^2}{m_e r_2^3} = \frac{1}{n} \frac{e^2}{4\pi\epsilon_0 r_2^2} - \frac{1}{n} \frac{\frac{3}{2}}{(2\ell+1)!!} \left(\frac{\ell+1}{\ell}\right)^{1/2} \frac{1}{\ell+2} \frac{1}{2} \frac{\hbar^2}{m_e r^3} \left(\sqrt{s(s+1)} - \sqrt{\frac{\ell}{\ell+1}} \right)$$

Radius of electron 2

$$r_2 = \left[n + \frac{\frac{3}{4}}{(2\ell+1)!!} \frac{1}{\ell+2} \left(\frac{\ell+1}{\ell}\right)^{1/2} \left(\sqrt{\frac{3}{4}} - \sqrt{\frac{\ell}{\ell+1}} \right) \right] a_{He} \quad n = 2, 3, 4, \dots$$

Excited States of Helium cont'd

Triplet Excited States with $\ell \neq 0$

Force Balance Equation

$$\frac{m_e v^2}{r_2} = \frac{\hbar^2}{m_e r_2^3} = \frac{1}{n} \frac{e^2}{4\pi\epsilon_0 r_2^2} + \frac{1}{n} \frac{\frac{3}{2}}{(2\ell+1)!!} \left(\frac{\ell+1}{\ell}\right)^{1/2} \frac{1}{\ell+2} \frac{1}{2} \frac{\hbar^2}{m_e r_2^3} \left(2\sqrt{s(s+1)} - \sqrt{\frac{\ell}{\ell+1}}\right)$$

Radius of electron 2

$$r_2 = \left[n - \frac{\frac{3}{4}}{(2\ell+1)!!} \frac{1}{\ell+2} \left(\frac{\ell+1}{\ell}\right)^{1/2} \left(2\sqrt{\frac{3}{4}} - \sqrt{\frac{\ell}{\ell+1}}\right) \right] a_{He} \quad n = 2, 3, 4, \dots$$

Excited States of Helium cont'd

For over 100 states, the r-squared value is 0.999994, and the typical average relative difference is about 5 significant figures which is within the error of the experimental data.

Calculated and experimental energies of states of helium.

n	ℓ	r_1 (a_{He}) ^a	r_2 (a_{He}) ^b	Term Symbol	E_{ele} CQM He I Energy Levels ^c (eV)	NIST He I Energy Levels ^d (eV)	Difference CQM-NIST (eV)	Relative Difference ^e (CQM-NIST)
1	0	0.56699	0.566987	1s ² 1S	-24.58750	-24.58741	-0.000092	0.0000038
2	0	0.506514	1.42265	1s2s 3S	-4.78116	-4.76777	-0.0133929	0.0028090
2	0	0.501820	1.71132	1s2s 1S	-3.97465	-3.97161	-0.0030416	0.0007658
2	1	0.500571	1.87921	1s2p 3P ₂ ⁰	-3.61957	-3.6233	0.0037349	-0.0010308
2	1	0.500571	1.87921	1s2p 3P ₁ ⁰	-3.61957	-3.62329	0.0037249	-0.0010280
2	1	0.500571	1.87921	1s2p 3P ₀ ⁰	-3.61957	-3.62317	0.0036049	-0.0009949
2	1	0.499929	2.01873	1s2p 1P ⁰	-3.36941	-3.36936	-0.0000477	0.0000141

Excited States of Helium cont'd

n	ℓ	r_1 (a_{He}) ^a	r_2 (a_{He}) ^b	Term Symbol	E_{ele} CQM He I Energy Levels ^c (eV)	NIST He I Energy Levels ^d (eV)	Difference CQM-NIST (eV)	Relative Difference ^e (CQM-NIST)
3	0	0.500850	2.42265	1s3s ³ S	-1.87176	-1.86892	-0.0028377	0.0015184
3	0	0.500302	2.71132	1s3s ¹ S	-1.67247	-1.66707	-0.0054014	0.0032401
3	1	0.500105	2.87921	1s3p ³ P ₂ ⁰	-1.57495	-1.58031	0.0053590	-0.0033911
3	1	0.500105	2.87921	1s3p ³ P ₁ ⁰	-1.57495	-1.58031	0.0053590	-0.0033911
3	1	0.500105	2.87921	1s3p ³ P ₀ ⁰	-1.57495	-1.58027	0.0053190	-0.0033659
3	2	0.500011	2.98598	1s3d ³ D ₃	-1.51863	-1.51373	-0.0049031	0.0032391
3	2	0.500011	2.98598	1s3d ³ D ₂	-1.51863	-1.51373	-0.0049031	0.0032391
3	2	0.500011	2.98598	1s3d ³ D ₁	-1.51863	-1.51373	-0.0049031	0.0032391
3	2	0.499999	3.00076	1s3d ¹ D	-1.51116	-1.51331	0.0021542	-0.0014235
3	1	0.499986	3.01873	1s3p ¹ P ⁰	-1.50216	-1.50036	-0.0017999	0.0011997
4	0	0.500225	3.42265	1s4s ³ S	-0.99366	-0.99342	-0.0002429	0.0002445
4	0	0.500088	3.71132	1s4s ¹ S	-0.91637	-0.91381	-0.0025636	0.0028054
4	1	0.500032	3.87921	1s4p ³ P ₂ ⁰	-0.87671	-0.87949	0.0027752	-0.0031555
4	1	0.500032	3.87921	1s4p ³ P ₁ ⁰	-0.87671	-0.87949	0.0027752	-0.0031555
4	1	0.500032	3.87921	1s4p ³ P ₀ ⁰	-0.87671	-0.87948	0.0027652	-0.0031442
4	2	0.500003	3.98598	1s4d ³ D ₃	-0.85323	-0.85129	-0.0019398	0.0022787
4	2	0.500003	3.98598	1s4d ³ D ₂	-0.85323	-0.85129	-0.0019398	0.0022787
4	2	0.500003	3.98598	1s4d ³ D ₁	-0.85323	-0.85129	-0.0019398	0.0022787

Excited States of Helium cont'd

n	ℓ	r_1 (a_{He}) ^a	r_2 (a_{He}) ^b	Term Symbol	E_{ele} CQM He I Energy Levels ^c (eV)	NIST He I Energy Levels ^d (eV)	Difference CQM-NIST (eV)	Relative Difference ^e (CQM-NIST)
4	2	0.500000	4.00076	1s4d ¹ D	-0.85008	-0.85105	0.0009711	-0.0011411
4	3	0.500000	3.99857	1s4f ³ F ₃ ⁰	-0.85054	-0.85038	-0.0001638	0.0001926
4	3	0.500000	3.99857	1s4f ³ F ₄ ⁰	-0.85054	-0.85038	-0.0001638	0.0001926
4	3	0.500000	3.99857	1s4f ³ F ₂ ⁰	-0.85054	-0.85038	-0.0001638	0.0001926
4	3	0.500000	4.00000	1s4f ¹ F ⁰	-0.85024	-0.85037	0.0001300	-0.0001529
4	1	0.499995	4.01873	1s4p ¹ P ⁰	-0.84628	-0.84531	-0.0009676	0.0011446
5	0	0.500083	4.42265	1s5s ³ S	-0.61519	-0.61541	0.0002204	-0.0003582
5	0	0.500035	4.71132	1s5s ¹ S	-0.57750	-0.57617	-0.0013253	0.0023002
5	1	0.500013	4.87921	1s5p ³ P ₂ ⁰	-0.55762	-0.55916	0.0015352	-0.0027456
5	1	0.500013	4.87921	1s5p ³ P ₁ ⁰	-0.55762	-0.55916	0.0015352	-0.0027456
5	1	0.500013	4.87921	1s5p ³ P ₀ ⁰	-0.55762	-0.55915	0.0015252	-0.0027277
5	2	0.500001	4.98598	1s5d ³ D ₃	-0.54568	-0.54472	-0.0009633	0.0017685
5	2	0.500001	4.98598	1s5d ³ D ₂	-0.54568	-0.54472	-0.0009633	0.0017685
5	2	0.500001	4.98598	1s5d ³ D ₁	-0.54568	-0.54472	-0.0009633	0.0017685
5	2	0.500000	5.00076	1s5d ¹ D	-0.54407	-0.54458	0.0005089	-0.0009345
5	3	0.500000	4.99857	1s5f ³ F ₃ ⁰	-0.54431	-0.54423	-0.0000791	0.0001454
5	3	0.500000	4.99857	1s5f ³ F ₄ ⁰	-0.54431	-0.54423	-0.0000791	0.0001454
5	3	0.500000	4.99857	1s5f ³ F ₂ ⁰	-0.54431	-0.54423	-0.0000791	0.0001454
5	3	0.500000	5.00000	1s5f ¹ F ⁰	-0.54415	-0.54423	0.0000764	-0.0001404

Excited States of Helium cont'd

n	ℓ	r_1 (a_{He}) ^a	r_2 (a_{He}) ^b	Term Symbol	E_{ele} CQM He I Energy Levels ^c (eV)	NIST He I Energy Levels ^d (eV)	Difference CQM-NIST (eV)	Relative Difference ^e (CQM-NIST)
5	4	0.500000	4.99988	1s5g ³ G ₄	-0.54417	-0.54417	0.0000029	-0.0000054
5	4	0.500000	4.99988	1s5g ³ G ₅	-0.54417	-0.54417	0.0000029	-0.0000054
5	4	0.500000	4.99988	1s5g ³ G ₃	-0.54417	-0.54417	0.0000029	-0.0000054
5	4	0.500000	5.00000	1s5g ¹ G	-0.54415	-0.54417	0.0000159	-0.0000293
5	1	0.499998	5.01873	1s5p ¹ P ⁰	-0.54212	-0.54158	-0.0005429	0.0010025
6	0	0.500038	5.42265	1s6s ³ S	-0.41812	-0.41838	0.0002621	-0.0006266
6	0	0.500016	5.71132	1s6s ¹ S	-0.39698	-0.39622	-0.0007644	0.0019291
6	1	0.500006	5.87921	1s6p ³ P ⁰ ₂	-0.38565	-0.38657	0.0009218	-0.0023845
6	1	0.500006	5.87921	1s6p ³ P ⁰ ₁	-0.38565	-0.38657	0.0009218	-0.0023845
6	1	0.500006	5.87921	1s6p ³ P ⁰ ₀	-0.38565	-0.38657	0.0009218	-0.0023845
6	2	0.500001	5.98598	1s6d ³ D ₃	-0.37877	-0.37822	-0.0005493	0.0014523
6	2	0.500001	5.98598	1s6d ³ D ₂	-0.37877	-0.37822	-0.0005493	0.0014523
6	2	0.500001	5.98598	1s6d ³ D ₁	-0.37877	-0.37822	-0.0005493	0.0014523
6	2	0.500000	6.00076	1s6d ¹ D	-0.37784	-0.37813	0.0002933	-0.0007757
6	3	0.500000	5.99857	1s6f ³ F ⁰ ₃	-0.37797	-0.37793	-0.0000444	0.0001176
6	3	0.500000	5.99857	1s6f ³ F ⁰ ₄	-0.37797	-0.37793	-0.0000444	0.0001176
6	3	0.500000	5.99857	1s6f ³ F ⁰ ₂	-0.37797	-0.37793	-0.0000444	0.0001176
6	3	0.500000	6.00000	1s6f ¹ F ⁰	-0.37788	-0.37793	0.0000456	-0.0001205

Excited States of Helium cont'd

n	ℓ	r_1 (a_{He}) ^a	r_2 (a_{He}) ^b	Term Symbol	E_{ele} CQM He I Energy Levels ^c (eV)	NIST He I Energy Levels ^d (eV)	Difference CQM-NIST (eV)	Relative Difference ^e (CQM-NIST)
6	4	0.500000	5.99988	1s6g ³ G ₄	-0.37789	-0.37789	-0.0000023	0.0000060
6	4	0.500000	5.99988	1s6g ³ G ₅	-0.37789	-0.37789	-0.0000023	0.0000060
6	4	0.500000	5.99988	1s6g ³ G ₃	-0.37789	-0.37789	-0.0000023	0.0000060
6	4	0.500000	6.00000	1s6g ¹ G	-0.37788	-0.37789	0.0000053	-0.0000140
6	5	0.500000	5.99999	1s6h ³ H ₄ ⁰	-0.37789	-0.37788	-0.0000050	0.0000133
6	5	0.500000	5.99999	1s6h ³ H ₅ ⁰	-0.37789	-0.37788	-0.0000050	0.0000133
6	5	0.500000	5.99999	1s6h ³ H ₆ ⁰	-0.37789	-0.37788	-0.0000050	0.0000133
6	5	0.500000	6.00000	1s6h ¹ H ⁰	-0.37788	-0.37788	-0.0000045	0.0000119
6	1	0.499999	6.01873	1s6p ¹ P ⁰	-0.37671	-0.37638	-0.0003286	0.0008730
7	0	0.500019	6.42265	1s7s ³ S	-0.30259	-0.30282	0.0002337	-0.0007718
7	0	0.500009	6.71132	1s7s ¹ S	-0.28957	-0.2891	-0.0004711	0.0016295
7	1	0.500003	6.87921	1s7p ³ P ₂ ⁰	-0.28250	-0.28309	0.0005858	-0.0020692
7	1	0.500003	6.87921	1s7p ³ P ₁ ⁰	-0.28250	-0.28309	0.0005858	-0.0020692
7	1	0.500003	6.87921	1s7p ³ P ₀ ⁰	-0.28250	-0.28309	0.0005858	-0.0020692
7	2	0.500000	6.98598	1s7d ³ D ₃	-0.27819	-0.27784	-0.0003464	0.0012468
7	2	0.500000	6.98598	1s7d ³ D ₂	-0.27819	-0.27784	-0.0003464	0.0012468
7	2	0.500000	6.98598	1s7d ³ D ₁	-0.27819	-0.27784	-0.0003464	0.0012468
7	2	0.500000	7.00076	1s7d ¹ D	-0.27760	-0.27779	0.0001907	-0.0006864

Excited States of Helium cont'd

n	ℓ	r_1 (a_{He}) ^a	r_2 (a_{He}) ^b	Term Symbol	E_{ele} CQM He I Energy Levels ^c (eV)	NIST He I Energy Levels ^d (eV)	Difference CQM-NIST (eV)	Relative Difference ^e (CQM-NIST)
7	3	0.500000	6.99857	1s7f $^3F_3^0$	-0.27769	-0.27766	-0.0000261	0.0000939
7	3	0.500000	6.99857	1s7f $^3F_4^0$	-0.27769	-0.27766	-0.0000261	0.0000939
7	3	0.500000	6.99857	1s7f $^3F_2^0$	-0.27769	-0.27766	-0.0000261	0.0000939
7	3	0.500000	7.00000	1s7f $^1F^0$	-0.27763	-0.27766	0.0000306	-0.0001102
7	4	0.500000	6.99988	1s7g 3G_4	-0.27763	-0.27763	-0.0000043	0.0000155
7	4	0.500000	6.99988	1s7g 3G_5	-0.27763	-0.27763	-0.0000043	0.0000155
7	4	0.500000	6.99988	1s7g 3G_3	-0.27763	-0.27763	-0.0000043	0.0000155
7	4	0.500000	7.00000	1s7g 1G	-0.27763	-0.27763	0.0000004	-0.0000016
7	5	0.500000	6.99999	1s7h $^3H_5^0$	-0.27763	-0.27763	0.0000002	-0.0000009
7	5	0.500000	6.99999	1s7h $^3H_6^0$	-0.27763	-0.27763	0.0000002	-0.0000009
7	5	0.500000	6.99999	1s7h $^3H_4^0$	-0.27763	-0.27763	0.0000002	-0.0000009
7	5	0.500000	7.00000	1s7h $^1H^0$	-0.27763	-0.27763	0.0000006	-0.0000021
7	6	0.500000	7.00000	1s7i 3I_5	-0.27763	-0.27762	-0.0000094	0.0000339
7	6	0.500000	7.00000	1s7i 3I_6	-0.27763	-0.27762	-0.0000094	0.0000339
7	6	0.500000	6.78349	1s7i 3I_7	-0.27763	-0.27762	-0.0000094	0.0000339
7	6	0.500000	7.00000	1s7i 1I	-0.27763	-0.27762	-0.0000094	0.0000338
7	1	0.500000	7.01873	1s7p $^1P^0$	-0.27689	-0.27667	-0.0002186	0.0007900

Excited States of Helium cont'd

n	ℓ	r_1 (a_{He}) ^a	r_2 (a_{He}) ^b	Term Symbol	E_{ele} CQM He I Energy Levels ^c (eV)	NIST He I Energy Levels ^d (eV)	Difference CQM-NIST (eV)	Relative Difference ^e (CQM-NIST)
8	0	0.500011	7.42265	1s8s ³ S	-0.22909	-0.22928	0.0001866	-0.0008139
8	0	0.500005	7.71132	1s8s ¹ S	-0.22052	-0.2202	-0.0003172	0.0014407
9	0	0.500007	8.42265	1s9s ³ S	-0.17946	-0.17961	0.0001489	-0.0008291
9	0	0.500003	8.71132	1s9s ¹ S	-0.17351	-0.1733	-0.0002141	0.0012355
10	0	0.500004	9.42265	1s10s ³ S	-0.14437	-0.1445	0.0001262	-0.0008732
10	0	0.500002	9.71132	1s10s ¹ S	-0.14008	-0.13992	-0.0001622	0.0011594
11	0	0.500003	10.42265	1s11s ³ S	-0.11866	-0.11876	0.0001037	-0.0008734
11	0	0.500001	10.71132	1s11s ¹ S	-0.11546	-0.11534	-0.0001184	0.0010268
						Avg.	-0.000112	0.0000386

Instability of Excited States

The relationship between the electric field equation and the "trapped photon" source charge-density function is given by Maxwell's equation in two dimensions

$$\mathbf{n} \cdot (\mathbf{E}_1 - \mathbf{E}_2) = \frac{\sigma}{\epsilon_0}$$

$$n = 2, 3, 4, \dots,$$

$$\sigma_{photon} = \frac{e}{4\pi(r_n)^2} \left[Y_0^0(\theta, \phi) - \frac{1}{n} \left[Y_0^0(\theta, \phi) + \text{Re} \left\{ Y_\ell^m(\theta, \phi) e^{i\omega_n t} \right\} \right] \right] \delta(r - r_n)$$

$$\sigma_{electron} = \frac{-e}{4\pi(r_n)^2} \left[Y_0^0(\theta, \phi) + \text{Re} \left\{ Y_\ell^m(\theta, \phi) e^{i\omega_n t} \right\} \right] \delta(r - r_n)$$

$$\sigma_{photon} + \sigma_{electron} = \frac{e}{4\pi(r_n)^2}$$

$$\left[Y_0^0(\theta, \phi) \dot{\delta}(r - r_n) - \frac{1}{n} Y_0^0(\theta, \phi) \delta(r - r_n) - \left(1 + \frac{1}{n} \right) \left[\text{Re} \left\{ Y_\ell^m(\theta, \phi) e^{i\omega_n t} \right\} \right] \delta(r - r_n) \right]$$

Excited states are radiative since spacetime harmonics of $\frac{\omega_n}{c} = k$ or $\frac{\omega_n}{c} \sqrt{\frac{\epsilon}{\epsilon_0}} = k$ do exist for which the spacetime Fourier transform of the current density function is nonzero.

Stability of “Ground” and Hydrino States

$$\sigma_{photon} = \frac{e}{4\pi(r_n)^2} \left[Y_0^0(\theta, \phi) - \frac{1}{n} \left[Y_0^0(\theta, \phi) + \text{Re} \left\{ Y_\ell^m(\theta, \phi) e^{i\omega_n t} \right\} \right] \right] \delta(r - r_n) \quad n = 1, \frac{1}{2}, \frac{1}{3}, \frac{1}{4}, \dots,$$

$$\sigma_{electron} = \frac{-e}{4\pi(r_n)^2} \left[Y_0^0(\theta, \phi) + \text{Re} \left\{ Y_\ell^m(\theta, \phi) e^{i\omega_n t} \right\} \right] \delta(r - r_n) \quad n = 1, \frac{1}{2}, \frac{1}{3}, \frac{1}{4}, \dots,$$

$$\sigma_{photon} + \sigma_{electron} = \frac{-e}{4\pi(r_n)^2} \left[\frac{1}{n} Y_0^0(\theta, \phi) + \left(1 + \frac{1}{n} \right) \text{Re} \left\{ Y_\ell^m(\theta, \phi) e^{i\omega_n t} \right\} \right] \delta(r - r_n)$$

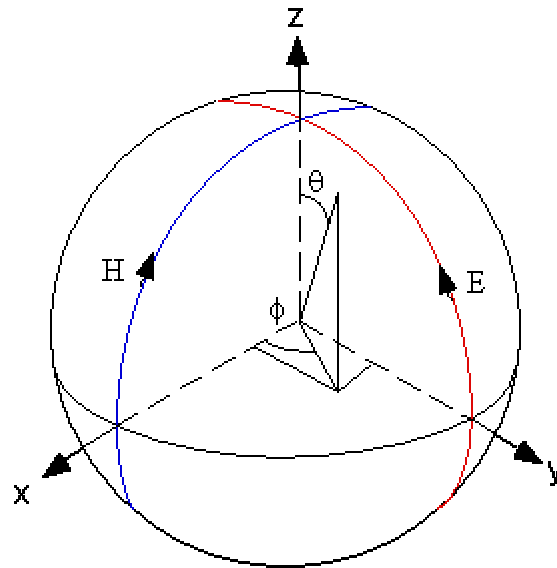
These states are nonradiative since spacetime harmonics of $\frac{\omega_n}{c} = k$ or $\frac{\omega_n}{c} \sqrt{\frac{\epsilon}{\epsilon_0}} = k$ for which the Fourier transform of the current-density function is nonzero do not exist.

Photon Equations

The angular-momentum density, \mathbf{m} , of the emitted photon is

$$\mathbf{m} = \int \frac{1}{8\pi c} \text{Re}[\mathbf{r} \times (\mathbf{E} \times \mathbf{B}^*)] dx^4 = \hbar$$

The Cartesian coordinate system $x'y'z'$ wherein the first great circle magnetic field line lies in the $x'z'$ -plane, and the second great circle electric field line lies in the $y'z'$ -plane.



The Field-Line Pattern of the Right-Handed Circularly Polarized Photon is Generated by a Rotation of the Orthogonal Great Circle Electric and Magnetic Field Lines

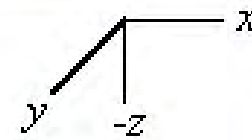
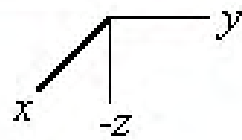
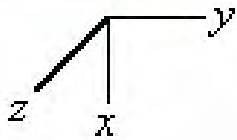
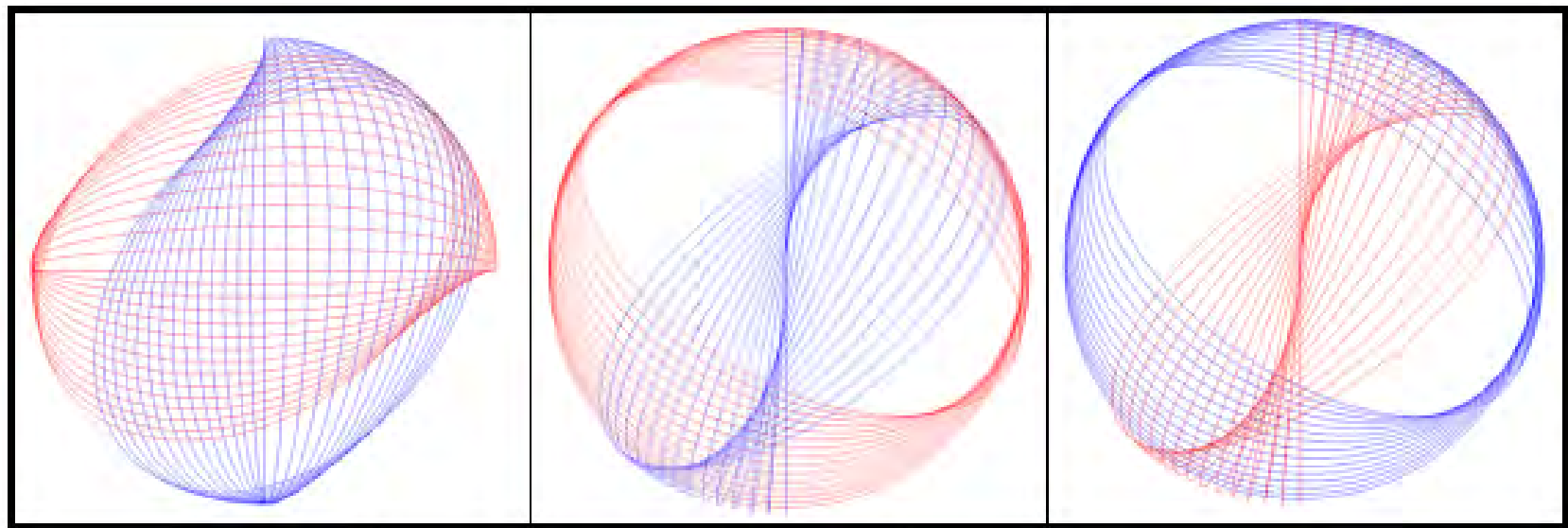
The right-handed-circularly-polarized photon electric and magnetic vector field (RHCP photon-e&mvf) is generated by the rotation of the basis elements comprising the great circle magnetic field line in the xz-plane and the great circle electric field line in the yz-plane about the $(i_x, i_y, 0i_z)$ -axis by $\frac{\pi}{2}$:

E FIELD and H FIELD:

$$\begin{bmatrix} x' \\ y' \\ z' \end{bmatrix} = \begin{bmatrix} \frac{1}{2} + \frac{\cos \theta}{2} & \frac{1}{2} - \frac{\cos \theta}{2} & -\frac{\sin \theta}{\sqrt{2}} \\ \frac{1}{2} - \frac{\cos \theta}{2} & \frac{1}{2} + \frac{\cos \theta}{2} & \frac{\sin \theta}{\sqrt{2}} \\ \frac{\sin \theta}{\sqrt{2}} & -\frac{\sin \theta}{\sqrt{2}} & \cos \theta \end{bmatrix} \cdot \left(\begin{bmatrix} 0 \\ r_n \cos \phi \\ r_n \sin \phi \end{bmatrix}_{\text{Red}} + \begin{bmatrix} r_n \cos \phi \\ 0 \\ r_n \sin \phi \end{bmatrix}_{\text{Blue}} \right)$$

The Field-Line Pattern of a Right-Handed Circularly-Polarized Photon

Electric field lines red --- Magnetic field lines blue



The Field-Line Pattern of the Left-Handed Circularly Polarized Photon is Generated by a Rotation of the Orthogonal Great Circle Electric and Magnetic Field Lines

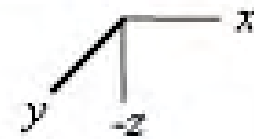
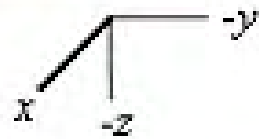
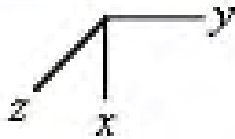
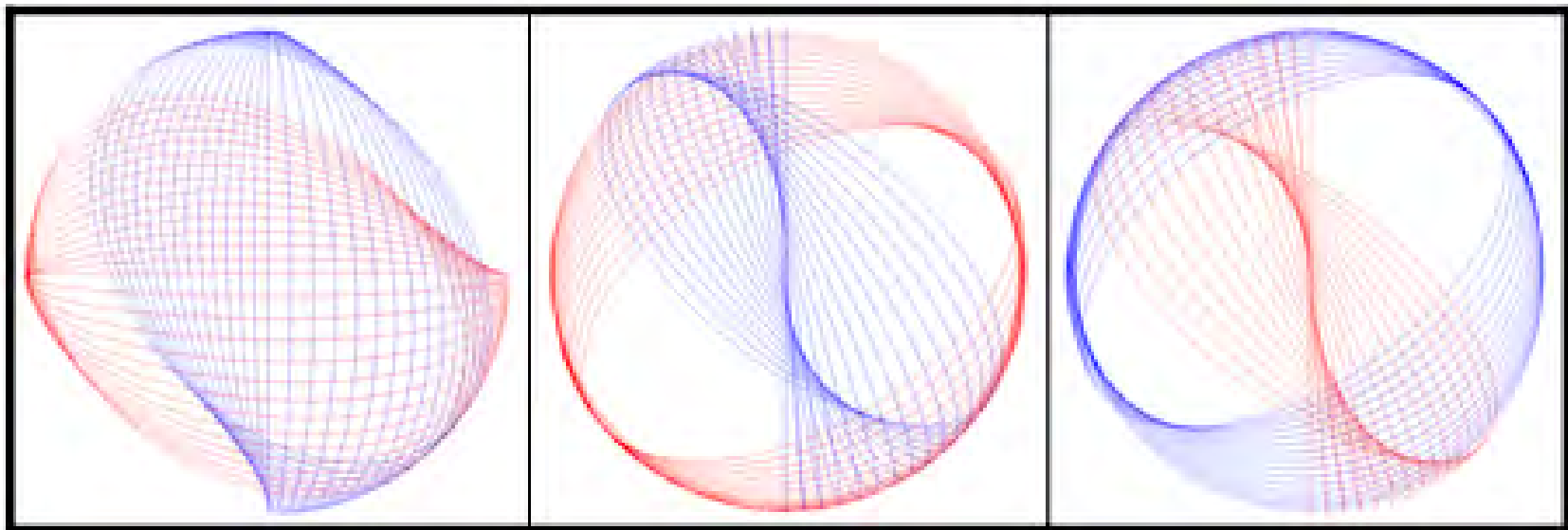
The left-handed-circularly-polarized photon electric and magnetic vector field (LHCP photon-e&mvf) is generated by the rotation of the basis elements comprising the great circle magnetic field line in the xz-plane and the great circle electric field line in the yz-plane about the $(i_x, -i_y, 0i_z)$ -axis by $\frac{\pi}{2}$:

E FIELD and H FIELD:

$$\begin{bmatrix} x' \\ y' \\ z' \end{bmatrix} = \begin{bmatrix} \frac{1}{2} + \frac{\cos \theta}{2} & -\frac{1}{2} + \frac{\cos \theta}{2} & \frac{\sin \theta}{\sqrt{2}} \\ -\frac{1}{2} + \frac{\cos \theta}{2} & \frac{1}{2} + \frac{\cos \theta}{2} & \frac{\sin \theta}{\sqrt{2}} \\ -\frac{\sin \theta}{\sqrt{2}} & -\frac{\sin \theta}{\sqrt{2}} & \cos \theta \end{bmatrix} \cdot \left(\begin{bmatrix} 0 \\ r_n \cos \phi \\ r_n \sin \phi \end{bmatrix}_{\text{Red}} + \begin{bmatrix} r_n \cos \phi \\ 0 \\ r_n \sin \phi \end{bmatrix}_{\text{Blue}} \right)$$

The Field-Line Pattern of a Left-Handed Circularly Polarized Photon

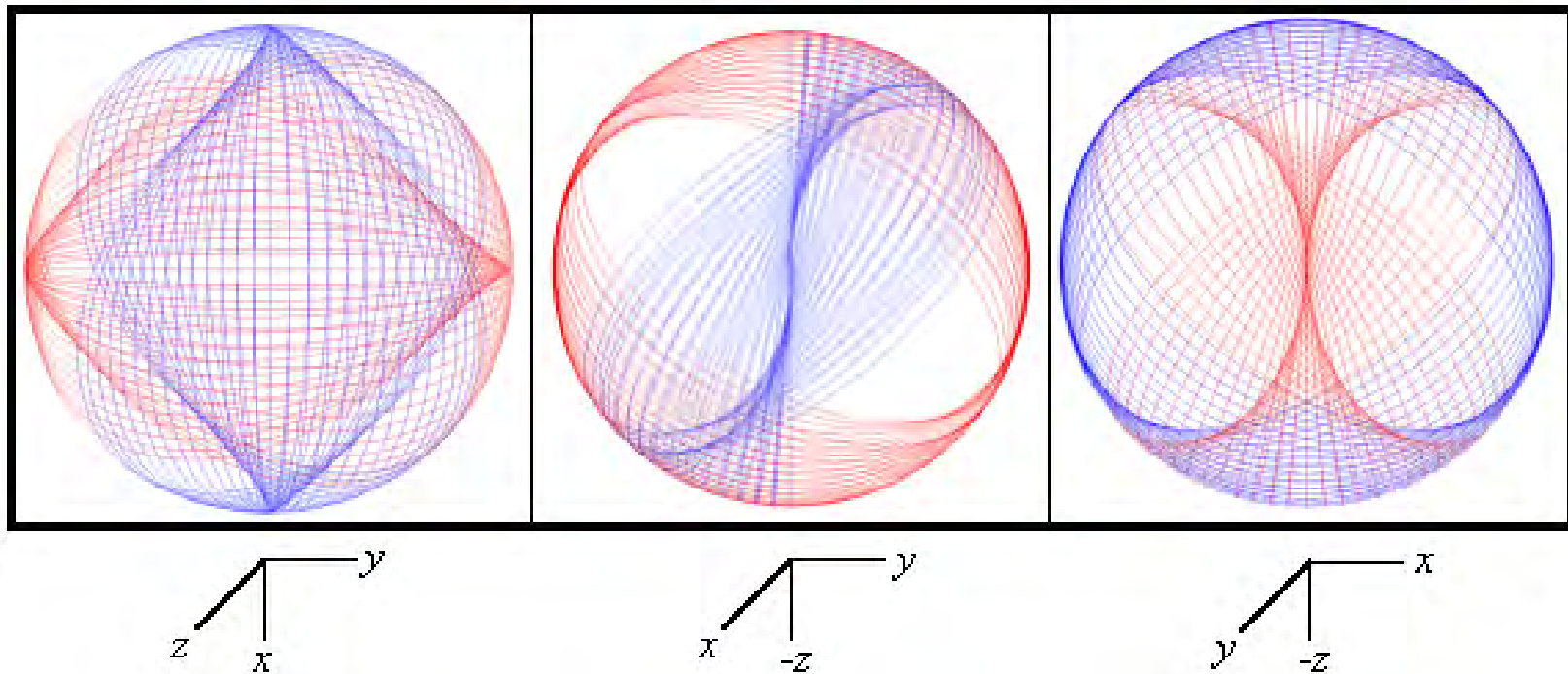
Electric field lines red --- Magnetic field lines blue



The Field-Line Pattern of a Linearly Polarized Photon

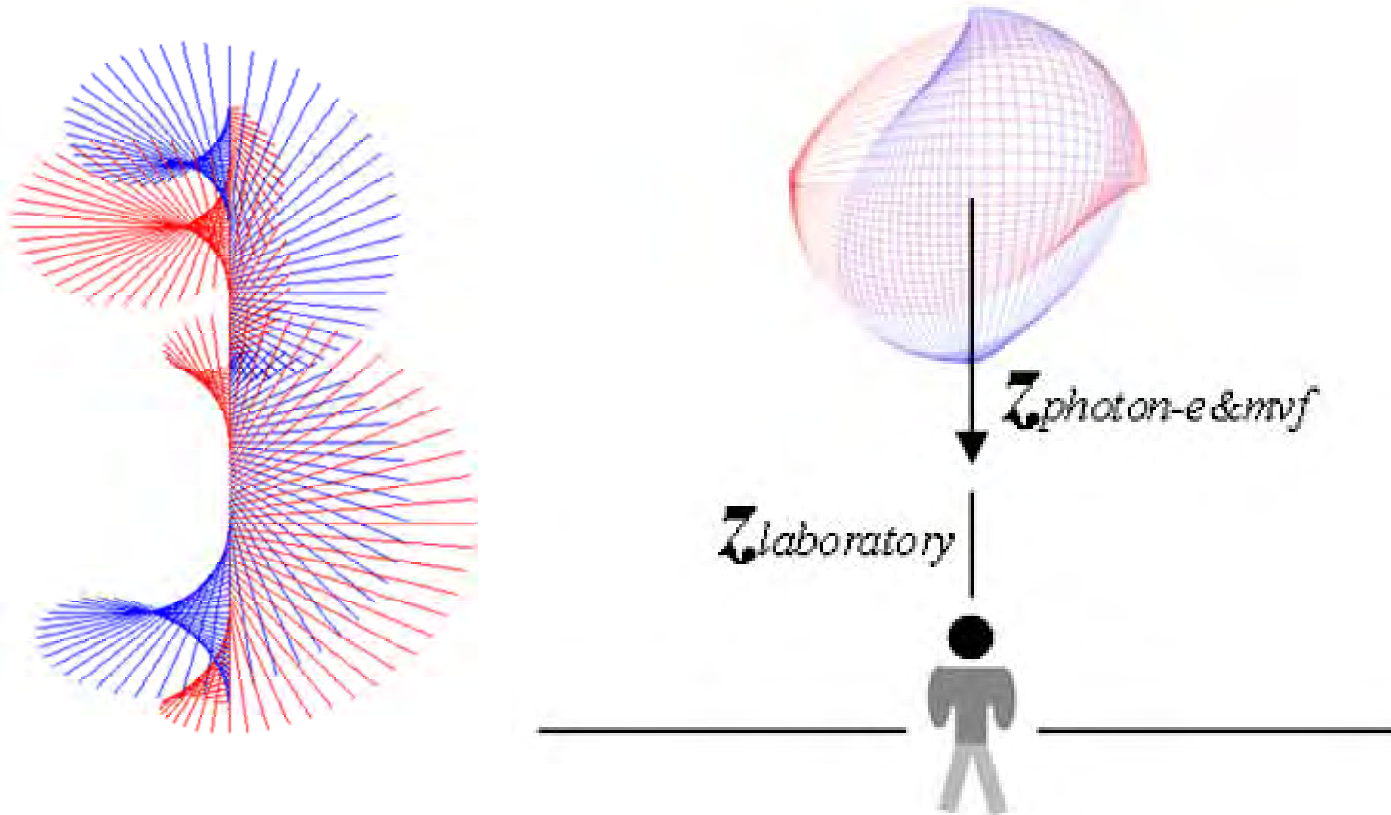
The linearly polarized (LP) photon-e&mvf is generated by the superposition of the RHCP photon-e&mvf and the LHCP photon-e&mvf:

Electric field lines red --- Magnetic field lines blue

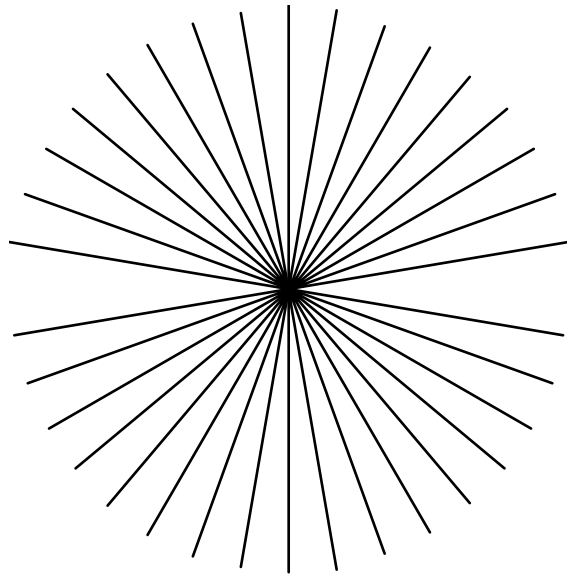


The Field of the Photon Observed from the Laboratory Frame

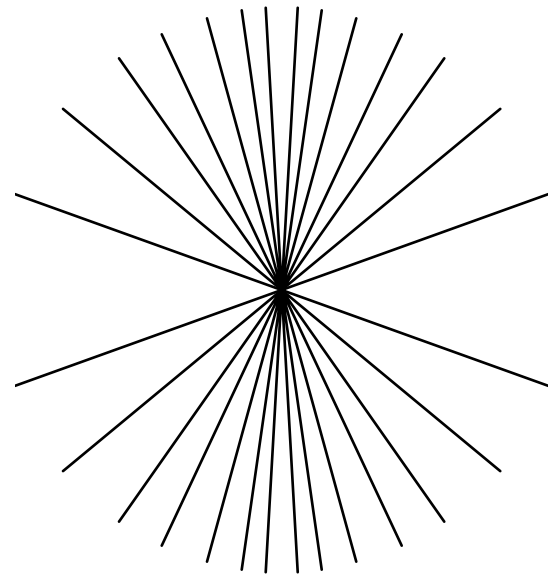
Consider an observer at the origin of his frame with the photon- $e&mvf$ stationary in its own frame propagating at light-speed c relative to the observer along its z -axis ($z_{\text{photon-}e\&mvf}$) that is collinear to the z -axis of the observer, $z_{\text{laboratory}}$



**Electric Field of a
Moving Point
Charge $v=1/3c$**



**Electric Field of a
Moving Point
Charge $v=4/5c$**



The Photon Equation in the Lab Frame of a Right-Handed Circularly-Polarized Photon Orbitsphere

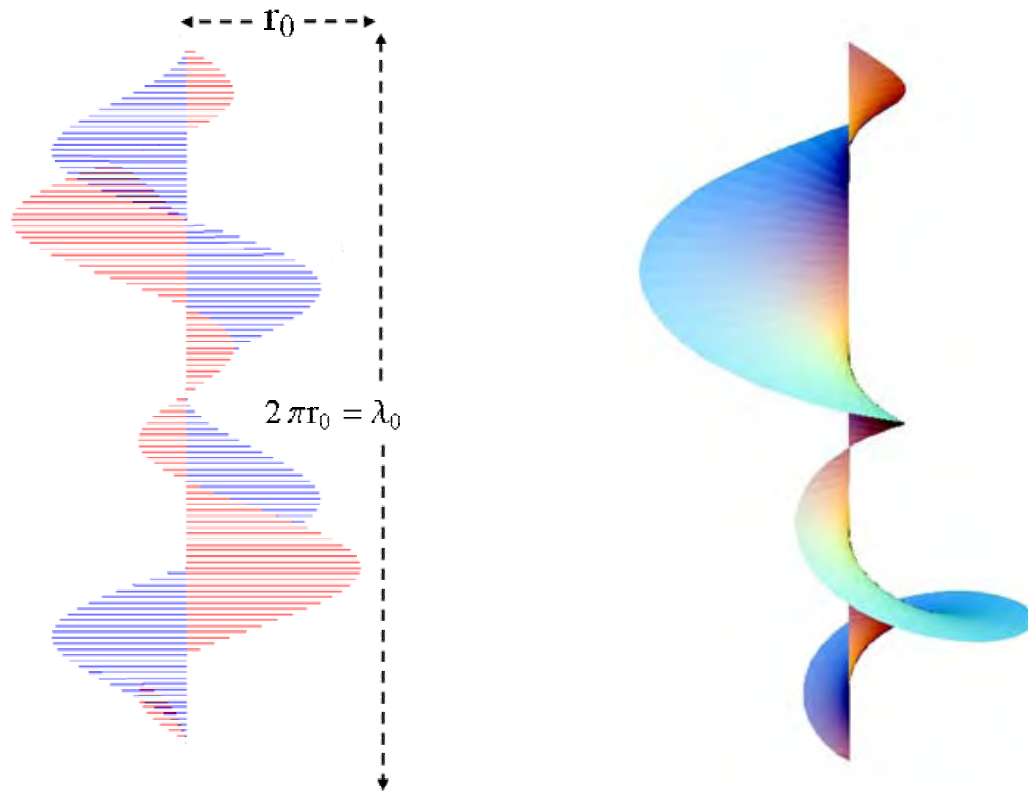
$$\mathbf{E} = \mathbf{E}_0 [\mathbf{x} + i\mathbf{y}] e^{-jk_z z} e^{-j\omega t}$$

$$\mathbf{H} = \left(\frac{\mathbf{E}_0}{\eta} \right) [\mathbf{y} - i\mathbf{x}] e^{-jk_z z} e^{-j\omega t} = \mathbf{E}_0 \sqrt{\frac{\epsilon}{\mu}} [\mathbf{y} - i\mathbf{x}] e^{-jk_z z} e^{-j\omega t}$$

with a wavelength of $\lambda = 2\pi \frac{c}{\omega}$

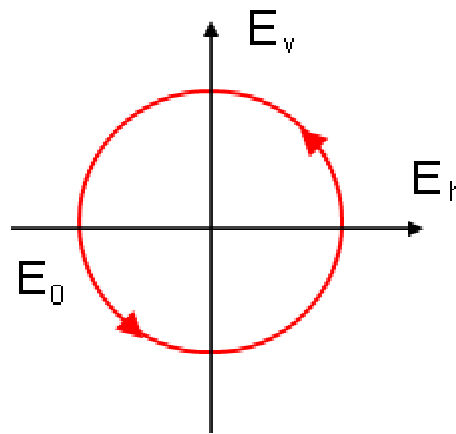
The relationship between the photon e&mvf radius and wavelength is $2\pi r_0 = \lambda_0$

The Electric Field Lines of a Right-Handed Circularly-Polarized Photon E&MVF



Right: Surface plot of the electric field lines (red) of a right-handed circularly polarized photon e&mvf as seen along the axis of propagation in the lab inertial reference frame as it passes a fixed point. Left: Side view of vector plot of electric and magnetic field lines.

The Electric Field Rotation



The electric field rotation of a right-handed circularly polarized photon $e\&mvf$ as seen transverse to the axis of propagation in the lab inertial reference frame as it passes a fixed point.

Elliptically Polarized Photons

Magnitude of the magnetic and electric field lines vary as a function of angular position (θ, ϕ) on the spherical e&mvf.

$$\mathbf{E}_{\phi, \theta} = \frac{e}{4\pi\epsilon_0 r_n^2} \left(-1 + \frac{1}{n} \left[Y_0^0(\theta, \phi) + \text{Re} \left\{ Y_\ell^m(\theta, \phi) e^{i\omega_n t} \right\} \right] \right) \delta \left(r - \frac{\lambda}{2\pi} \right) ;$$

$$\omega_n = 0 \quad \text{for} \quad m = 0$$

A photon is emitted when an electron is bound. Relations between the free-space photon wavelength, radius, and velocity and the corresponding parameters of a free electron as it is bound are:

- r_n , the radius of the photon e&mvf, is equal to $r_n \frac{c}{v_n} = na_H \frac{c}{v_n}$, the electron orbitsphere radius times the ratio of the speed of light c and v_n , the velocity of the orbitsphere.

- λ , the photon wavelength, is equal to $\lambda_n \frac{c}{v_n}$, where λ_n is the orbitsphere de Broglie wavelength.

- $\omega = \frac{2\pi c}{\lambda}$, the photon angular velocity, is equal to ω_n , the orbitsphere angular velocity.

Spherical Wave

Photons superimpose, and the amplitude due to N photons is

$$\mathbf{E}_{total} = \sum_{n=1}^N \frac{e^{-ik_r |\mathbf{r}-\mathbf{r}'|}}{4\pi |\mathbf{r}-\mathbf{r}'|} f(\theta, \varphi)$$

In the far field, the emitted wave is a spherical wave

$$\mathbf{E}_{total} = E_o \frac{e^{-ikr}}{r}$$

- The Green Function is given as the solution of the wave equation. Thus, the superposition of photons gives the classical result.
- As r goes to infinity, the spherical wave becomes a plane wave.
- The double slit interference pattern is predicted.
- From the equation of a photon, the wave-particle duality arises naturally.
- The energy is always given by Planck's equation; yet, an interference pattern is observed when photons add over time or space.

Equations of the Free Electron

Mass Density Function of a Free Electron is a two dimensional disk having the mass density distribution in the $xy(\rho)$ -plane

$$\rho_m(\rho, \phi, z) = \frac{m_e}{\frac{2}{3}\pi\rho_0^3} \sqrt{\rho_0^2 - \rho^2} \delta(z)$$

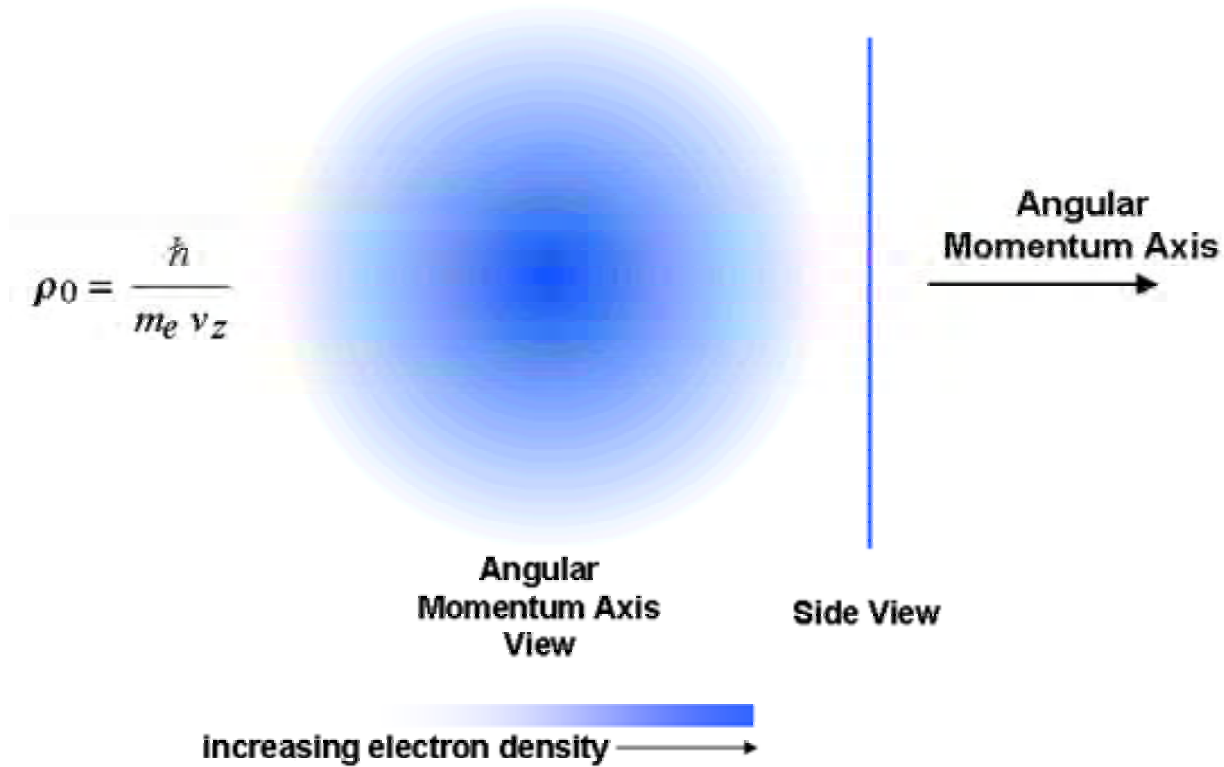
Charge Density Distribution, $\rho_e(\rho, \phi, z)$, in the xy -plane

$$\rho_e(\rho, \phi, z) = \frac{e}{\frac{2}{3}\pi\rho_0^3} \sqrt{\rho_0^2 - \rho^2} \delta(z)$$

The wave-particle duality arises naturally.

Consistent with scattering experiments.

The Free Electron



The angular-momentum-axis view of the magnitude of the mass (charge) density function in the xy-plane of a polarized free electron; side-view of a free electron along the axis of propagation—z-axis.



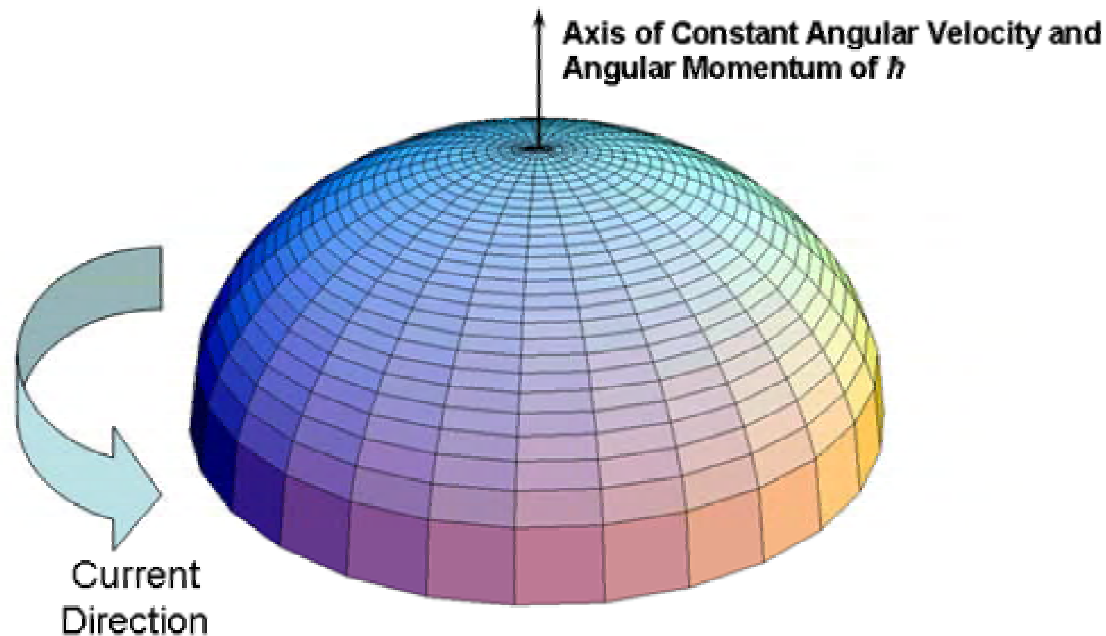
3-D View



Charge Density Function (the size of the electron in the xy-plane centered about the origin as a function of its velocity is shown with the charge density plotted in on the z-axis)

Current-Density Function

$$\mathbf{J}(\rho, \phi, z, t) = \left[\frac{e}{\frac{2}{3}\pi\rho_0^3} \sqrt{\rho_0^2 - \rho^2} \frac{5}{2} \frac{\hbar}{m_e \rho_0^2} \mathbf{i}_\phi \right] + \frac{e\hbar}{m_e \rho_0} \delta\left(z - \frac{\hbar}{m_e \rho_0} t\right) \mathbf{i}_z$$



The magnitude plotted along the z-axis of the current-density function, J , of the free electron traveling at 10^5 ms^{-1} relative to the observer.

The radius of the xy-plane-lamina disc is $1.16 \times 10^{-9} \text{ m}$.

The maximum current density at $\rho = 0$ is $1.23 \times 10^{13} \text{ Am}^{-2}$.

Angular Momentum

$$\mathbf{L}_z = \int_0^{2\pi} \int_0^{\rho_0} \frac{m_e}{\frac{2}{3}\pi\rho_0^3} \sqrt{\rho_0^2 - \rho^2} \frac{5}{2} \frac{\hbar}{m_e \rho_0^2} \rho^2 \rho d\rho d\phi$$

$$\mathbf{L}_z = \hbar$$

Nonradiation Condition

$$\frac{e}{\frac{4}{3}\pi\rho_0^3} \frac{\hbar}{m_e} \text{sinc}(2\pi\mathbf{s}\vec{\rho}_o) + 2\pi e \frac{\hbar}{m_e\rho_0} \delta(\omega - \mathbf{k}_z \bullet \mathbf{v}_z)$$
$$\mathbf{J}_\perp \propto \text{sinc}(\mathbf{s}\vec{\rho}_o) = \frac{\sin 2\pi\mathbf{s}\vec{\rho}_o}{2\pi\mathbf{s}\vec{\rho}_o}$$

$$2\pi\vec{\rho}_o = \lambda_o$$

Consider the radial wave vector of the sinc function, when the radial projection of the velocity is c

$$\mathbf{s} \bullet \mathbf{v} = \mathbf{s} \bullet \mathbf{c} = \omega_o$$

The relativistically corrected wavelength is

$$\vec{\rho}_o = \lambda_o$$

$$\lambda_o = \frac{h}{m_e v_z} = 2\pi\rho_o$$

Classical Physics of the de Broglie Relation

The linear velocity of the free electron can be considered to be due to absorption of photons that excite surface currents corresponding to a decreased de Broglie wavelength where the free electron is equivalent to a continuum excited state with conservation of the parameters of the bound electron.

The relationship between the electron wavelength and the linear velocity is

$$\frac{\lambda}{2\pi} = \rho_o = \frac{\hbar}{m_e v_z} = k^{-1} = \frac{v_z}{\omega_z}$$

In this case, the angular frequency ω_z is given by

$$\omega_z = \frac{\hbar}{m_e \rho_0^2}$$

which conserves the photon's angular momentum of \hbar with that of the electron.

Classical Physics of the de Broglie Relation cont'd

The total energy, E_T , is given by the sum of the change in the free-electron translational kinetic energy, T , the rotational energy, E_{rot} , corresponding to the current of the loops, and the potential energy, E_{mag} due to the radiation reaction force \mathbf{F}_{mag} , the magnetic attractive force between the current loops due to the relative rotational or current motion:

$$\begin{aligned} E_T &= T + E_{rot} + E_{mag} \\ &= \frac{1}{2} \frac{\hbar^2}{m_e \rho_0^2} + \frac{5}{4} \frac{\hbar^2}{m_e \rho_0^2} - \frac{5}{4} \frac{\hbar^2}{m_e \rho_0^2} \\ &= \frac{1}{2} \frac{\hbar^2}{m_e \rho_0^2} \end{aligned}$$

Thus, the total energy, E_T , of the excitation of a free-electron transitional state by a photon having \hbar of angular momentum and an energy given by Planck's equation of $\hbar\omega$ is

$$E_T = T = \frac{1}{2} m_e v_z^2 = \frac{1}{2} \frac{h^2}{m_e \lambda^2} = \frac{1}{2} \hbar \omega_z$$

where λ is the de Broglie wavelength.

Classical Physics of the de Broglie Relation cont'd

The angular momentum of the free electron of \hbar is unchanged.

The energies in the currents in the plane lamina are balanced so that the total energy is unchanged.

The radius ρ_0 decreases to match the de Broglie wavelength and frequency at an increased velocity.

At this velocity, the kinetic energy matches the energy provided by the photon wherein the de Broglie frequency matches the photon frequency and both the electron-kinetic energy and the photon energy are given by Planck's equation.

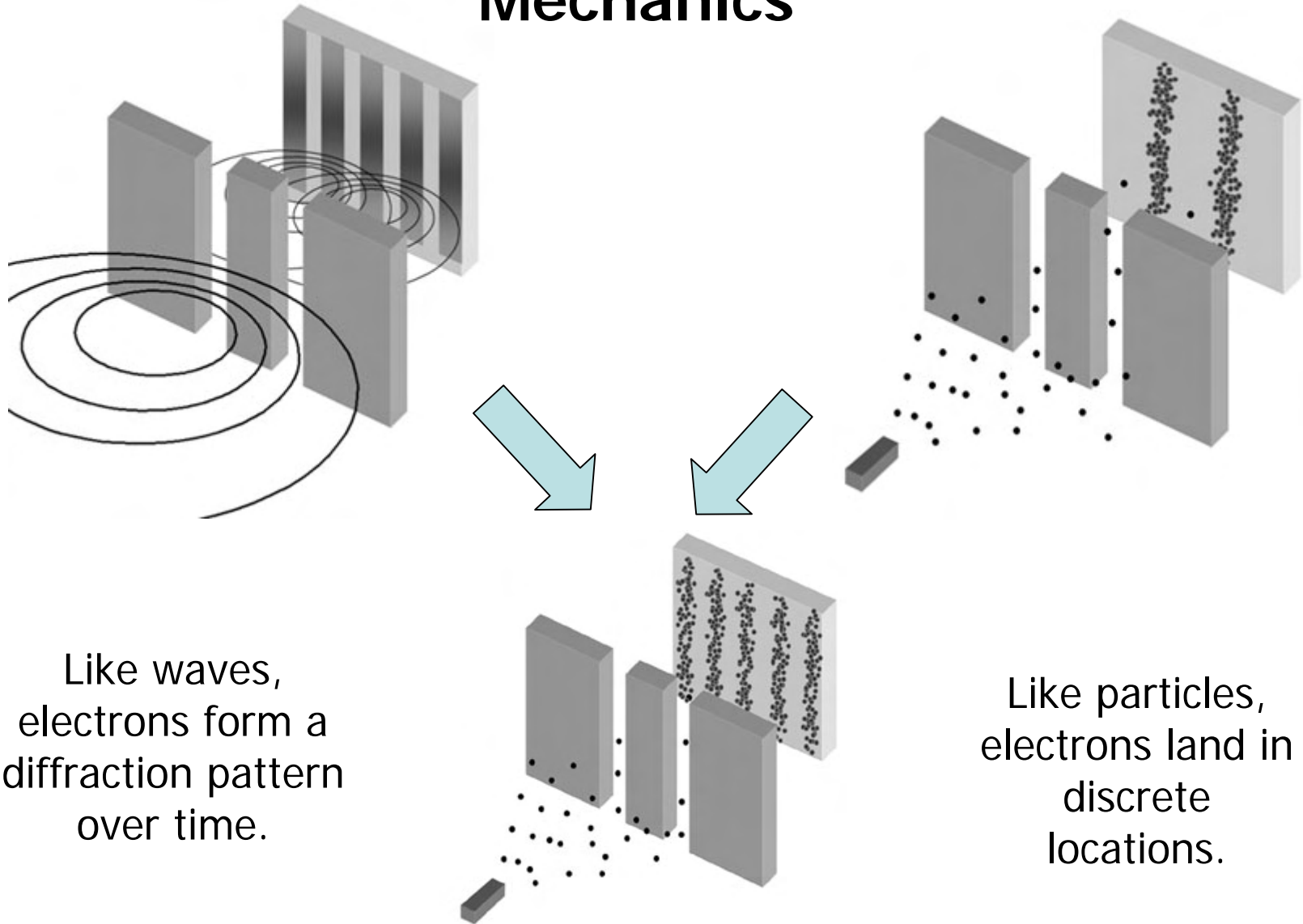
Classical Physics of the de Broglie Relation cont'd

The correspondence principle is the basis of the de Broglie wavelength relationship.

The de Broglie relationship is not an independent fundamental property of matter in conflict with physical laws as formalized in the wave-particle-duality-related postulates of quantum mechanics and the corresponding Schrödinger wave equation.

The Stern-Gerlach experimental results and the double-slit interference pattern of electrons are also predicted classically.

The Central Mystery of Quantum Mechanics



Like waves,
electrons form a
diffraction pattern
over time.

Like particles,
electrons land in
discrete
locations.

Classical Electron Diffraction

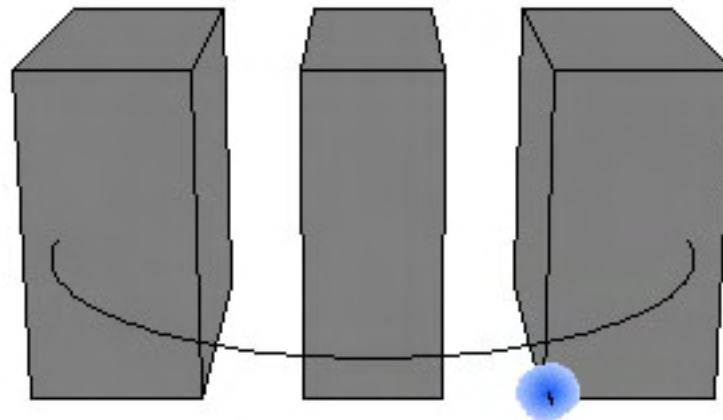
- The electron interacts with both slits via charge-induced photons.
- The angular momentum vector of the electron precesses about that of the absorbed photon.
- The photon-momentum distribution is imprinted onto that of the electrons such that transverse momentum distribution in the far-field is a result of this interaction.
- Rather than uncertainty in position and momentum according to the Uncertainty Principle:

$$\Delta x \Delta p \geq \frac{\hbar}{2}$$

- Δp is the *physical momentum change of the incident electron*. and Δx is the *physical distance change from the incident direction* such that the distribution in the far field is the Fourier transform of the slit pattern.



Animation of the
Double Slit Exp



Stern-Gerlach Experiment

The Stern Gerlach experiment demonstrates that the magnetic moment of the electron can only be parallel or antiparallel to an applied magnetic field.

This implies a spin quantum number of $1/2$ corresponding to an angular momentum on the z-axis of $\frac{\hbar}{2}$. However, the Zeeman splitting energy corresponds to a magnetic moment of a Bohr magneton μ_B and implies an electron angular momentum on the z-axis of \hbar —twice that expected.

Stern-Gerlach Experiment cont'd

The application of a magnetic field causes a resonant excitation of the Larmor precession wherein the corresponding photon has \hbar of angular momentum on the x'-axis.

The corresponding torque causes the electron to precess about the x- and z-axes giving rise to Larmor precession about the $(i_x, 0i_y, i_z)$ - or $(-i_x, 0i_y, i_z)$ -axis at steady state depending on the initial direction of the free-electron magnetic moment relative to the applied magnetic-field direction, parallel or antiparallel.

The \hbar of angular momentum on the z'-axis and the \hbar of angular momentum on the x'-axis gives a resultant stationary projection of $\sqrt{2\hbar}$ into the $(i_x, 0i_y, i_z)$ axis or $(-i_x, 0i_y, i_z)$ -axis.

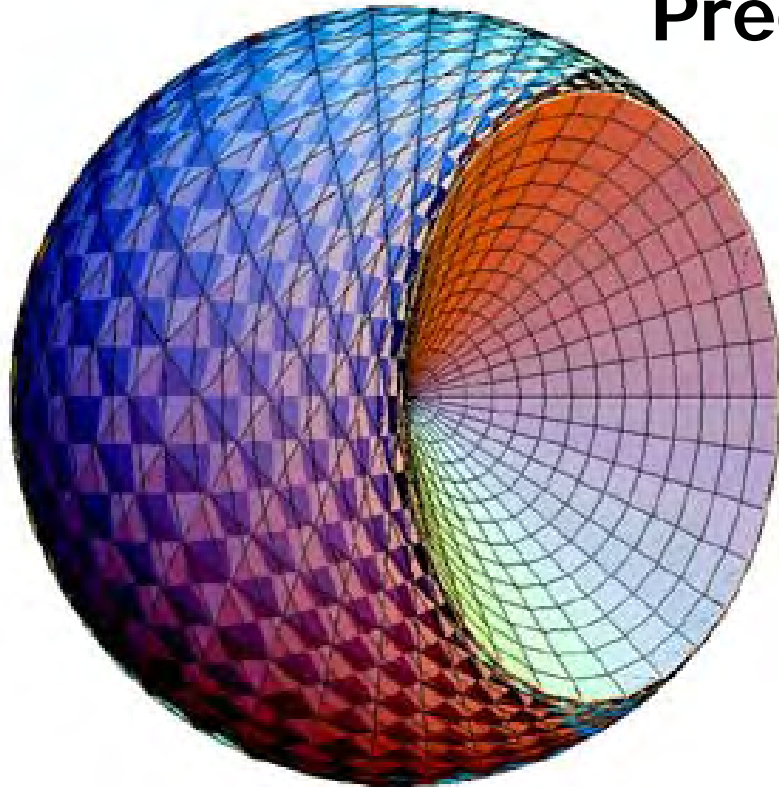
Stern-Gerlach Experiment cont'd

The static projection of the resultant angular momentum onto the z-axis is \hbar with a contribution of $\frac{\hbar}{2}$ from each of the intrinsic electron current and the photon.

The precessing electron can further interact with a resonant photon directed along the x-axis that rotates the z-axis-directed static projection of the resultant of \hbar such that it flips to the opposite direction.

The RF photon gives rise to Zeeman splitting—energy levels corresponding to flipping of the parallel or antiparallel alignment of the electron magnetic moment of a Bohr magneton with the magnetic field.

Free Electron Momentum-Density Function Over One Period of Larmor Precession



Rotation of the plane-lamina disc comprised of concentric circles about the $(i_x, 0i_y, i_z)$ - or $(-i_x, 0i_y, i_z)$ -axes by 2π during a Larmor-precession period generates the equivalent of the momentum-density pattern of a component orbitosphere-cvf (o-cvf) called the primary o-cvf for each of the concentric circular current loops in the xy -plane (ρ -plane).

The continuous progression of larger current loops along ρ generates a continuum of o-cvfs for $0 \leq \rho \leq \rho_0$ over a period that comprise two conical surfaces joined at the origin and facing in the opposite directions along the $(i_x, 0i_y, i_z)$ - or $(-i_x, 0i_y, i_z)$ -axis, the axis of rotation.

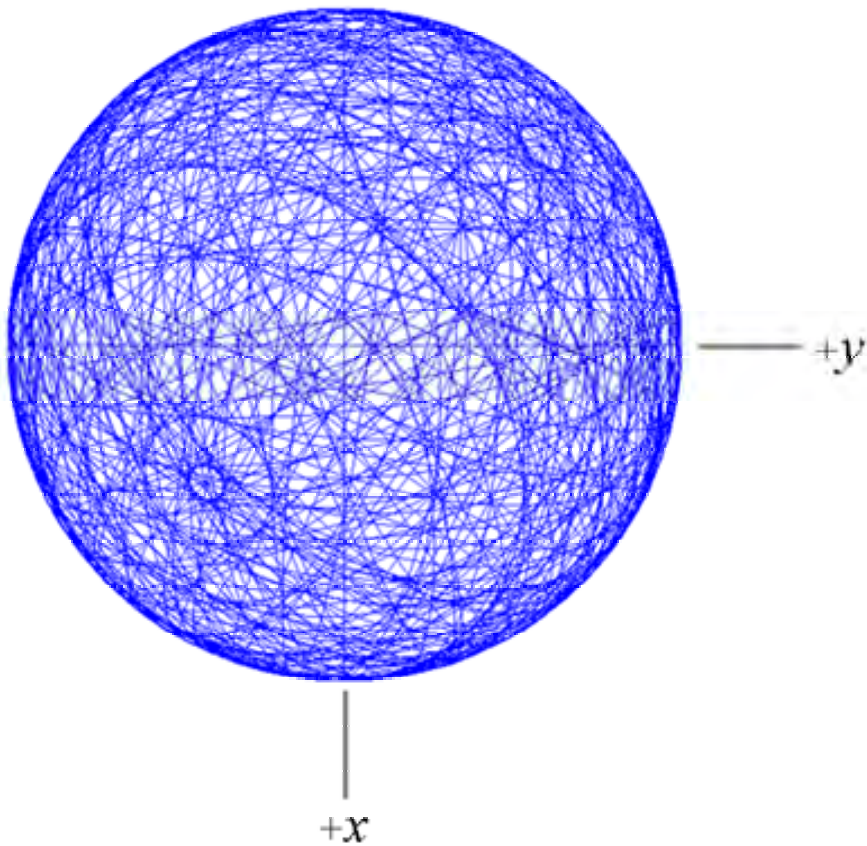


Free Electron Wobble



Convolution

The Uniform Current Pattern as a Function of Radius ρ of the Free Electron During a Stern-Gerlach Transition



Component Wobble to Form Uniform



3-D View of Uniform Function

A uniform spherical momentum density is formed over time by each circular current basis element at position ρ by combined Larmor and spin-flip rotations.

The resulting spatial momentum density over a period interacts with the external applied magnetic field in a manner that is equivalent to that of orbitosphere function, $Y_0^0(\theta, \phi)$, having a uniform momentum density on a spherical shell of radius ρ_0 , a total sum of the magnitude of the angular momentum from the contributions from all of the infinitesimal points on the orbitosphere of \hbar and $\mathbf{L}_z = \frac{\hbar}{2}$.

$Y_0^0(\theta, \phi)$ cont'd

Since the projection of the intrinsic free electron angular momentum and that of the resonant photon that excites the Larmor precession onto the z-axis are both $\frac{\hbar}{2}$, the Larmor-excited free electron behaves equivalently to the bound electron.

Flux must be linked in the same manner in units of the magnetic flux quantum,
 $\Phi_0 = \frac{h}{2e}$.

Consequently, the g factor for the free electron is the same as that of the bound electron, and the energy of the transition between these states is that of the resonant photon given by

$$\Delta E_{mag}^{spin} = g\mu_B B$$

Two Electron Atoms

Central Force Balance Equation with Nonradiation Condition

$$\frac{m_e}{4\pi r_2^2} \frac{v_2^2}{r_2} = \frac{e}{4\pi r_2^2} \frac{(Z-1)e}{4\pi\epsilon_0 r_2^2} + \frac{1}{4\pi r_2^2} \frac{\hbar^2}{Zm_e r_2^3} \sqrt{s(s+1)}$$

$$r_2 = r_1 = a_0 \left(\frac{1}{Z-1} - \frac{\sqrt{s(s+1)}}{Z(Z-1)} \right); s = \frac{1}{2}$$

Two Electron Atoms cont'd

Ionization Energies Calculated Using the Poynting Power Theorem

For helium, which has no electric field beyond r_1

$$\textit{Ionization Energy}(\textit{He}) = -E(\textit{electric}) + E(\textit{magnetic})$$

where

$$E(\textit{electric}) = -\frac{(Z-1)e^2}{8\pi\epsilon_0 r_1}$$

$$E(\textit{magnetic}) = \frac{2\pi\mu_0 e^2 \hbar^2}{m_e^2 r_1^3}$$

Where

For $3 \leq Z$

$$\textit{Ionization Energy} = -\textit{Electric Energy} - \frac{1}{Z} \textit{Magnetic Energy}$$

The Calculated Energies for Some Two-Electron Atoms

Atom	r_1 (a_0)	Electric Energy (eV)	Magnetic Energy (eV)	Calculated Ionization Energy(eV)	Experimental Ionization Energy (eV)
<i>He</i>	0.567	-23.96	0.63	24.59	24.59
<i>Li</i> ⁺	0.356	-76.41	2.54	75.56	75.64
<i>Be</i> ²⁺	0.261	-156.08	6.42	154.48	153.89
<i>B</i> ³⁺	0.207	-262.94	12.96	260.35	259.37
<i>C</i> ⁴⁺	0.171	-396.98	22.83	393.18	392.08
<i>N</i> ⁵⁺	0.146	-558.20	36.74	552.95	552.06
<i>O</i> ⁶⁺	0.127	-746.59	55.35	739.67	739.32
<i>F</i> ⁷⁺	0.113	-962.17	79.37	953.35	953.89

Elastic Electron Scattering from Helium Atoms

Aperture distribution function, $a(\rho, \phi, z)$, for the scattering of an incident electron plane wave $\pi(z)$

by the He atom

$$\frac{2}{4\pi(0.567a_o)^2} [\delta(r - 0.567a_o)]$$

is

$$a(\rho, \phi, z) = \pi(z) \otimes \frac{2}{4\pi(0.567a_o)^2} [\delta(r - 0.567a_o)]$$

$$a(\rho, \phi, z) = \frac{2}{4\pi(0.567a_o)^2} \sqrt{(0.567a_o)^2 - z^2} \delta(\rho - \sqrt{(0.567a_o)^2 - z^2})$$

Far Field Scattering (Circular Symmetry)

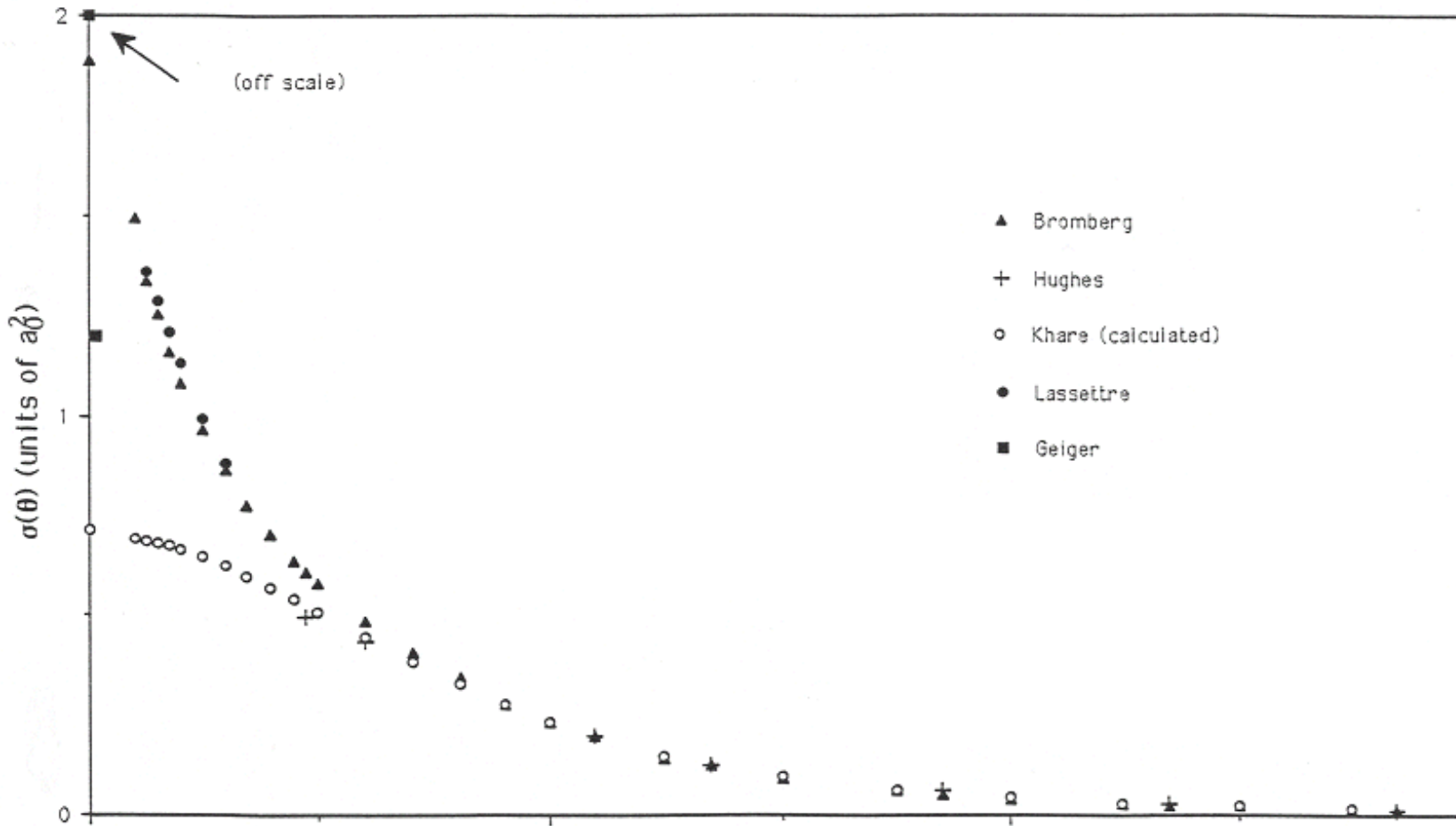
$$F(s) = \frac{2}{4\pi(0.567a_o)^2} 2\pi \int_0^\infty \int_{-\infty}^\infty \sqrt{(0.567a_o)^2 - z^2} \delta(\rho - \sqrt{(0.567a_o)^2 - z^2}) J_0(s\rho) e^{-iwz} \rho d\rho dz$$

$$I_1^{ed} = F(s)^2$$

$$= I_e \left\{ \left[\frac{2\pi}{(z_o w)^2 + (z_o s)^2} \right]^{\frac{1}{2}} \right. \\ \left. \left\{ 2 \left[\frac{z_o s}{(z_o w)^2 + (z_o s)^2} \right] J_{3/2} \left[((z_o w)^2 + (z_o s)^2)^{1/2} \right] - \left[\frac{z_o s}{(z_o w)^2 + (z_o s)^2} \right]^2 J_{5/2} \left[((z_o w)^2 + (z_o s)^2)^{1/2} \right] \right\} \right\}^2$$

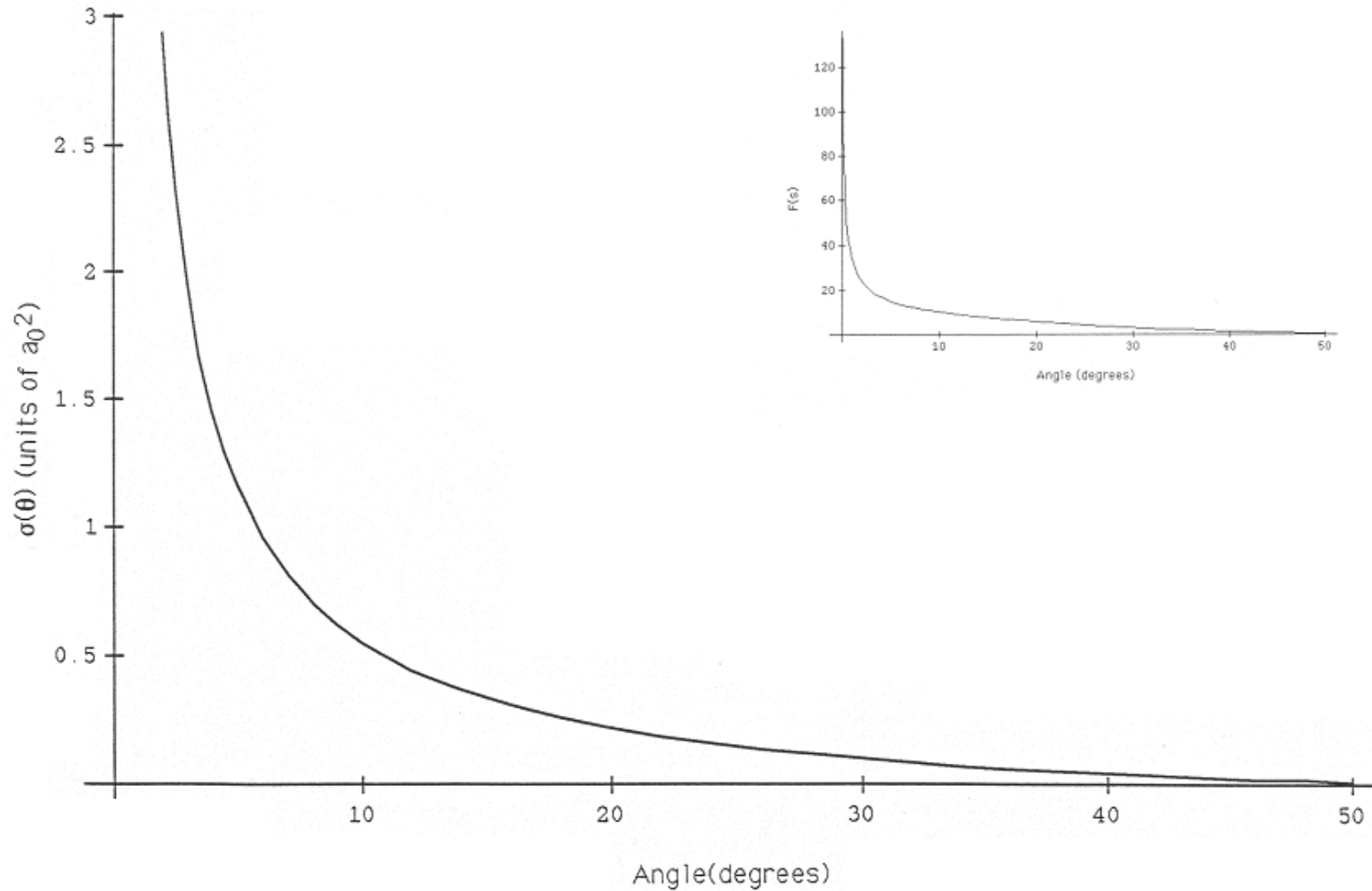
$$s = \frac{4\pi}{\lambda} \sin \frac{\theta}{2}; \quad w = 0 \text{ (units of } \text{\AA}^{-1}\text{)}$$

Experimental Results and Born Approximation



The experimental results of Bromberg, the extrapolated experimental data of Hughes, the small angle data of Geiger, and the semiexperimental results of Lassetre for the elastic differential cross section for the elastic scattering of electrons by helium atoms and the elastic differential cross section as a function of angle numerically calculated by Khare using the first Born approximation and first-order exchange approximation.

The Closed Form Function



The closed form function for the elastic differential cross section for the elastic scattering of electrons by helium atoms. The scattering amplitude function, $F(s)$, is shown as an insert.

One- Through Twenty-Electron Atoms

The physical approach based on Maxwell's equations was applied to multielectron atoms that were solved exactly.

The classical predictions of the ionization energies were solved for the physical electrons comprising concentric orbitspheres ("bubble-like" charge-density functions) that are electrostatic and magnetostatic corresponding to a constant charge distribution and a constant current corresponding to spin angular momentum.

Alternatively, the charge is a superposition of a constant and a dynamical component.

In the latter case, charge density waves on the surface are time and spherically harmonic and correspond additionally to electron orbital angular momentum that superimposes the spin angular momentum.

One- Through Twenty-Electron Atoms cont'd

Thus, the electrons of multielectron atoms all exist as orbitspheres of discrete radii which are given by r_n of the radial Dirac delta function, $\delta(r - r_n)$.

These electron orbitspheres may be spin paired or unpaired depending on the force balance which applies to each electron.

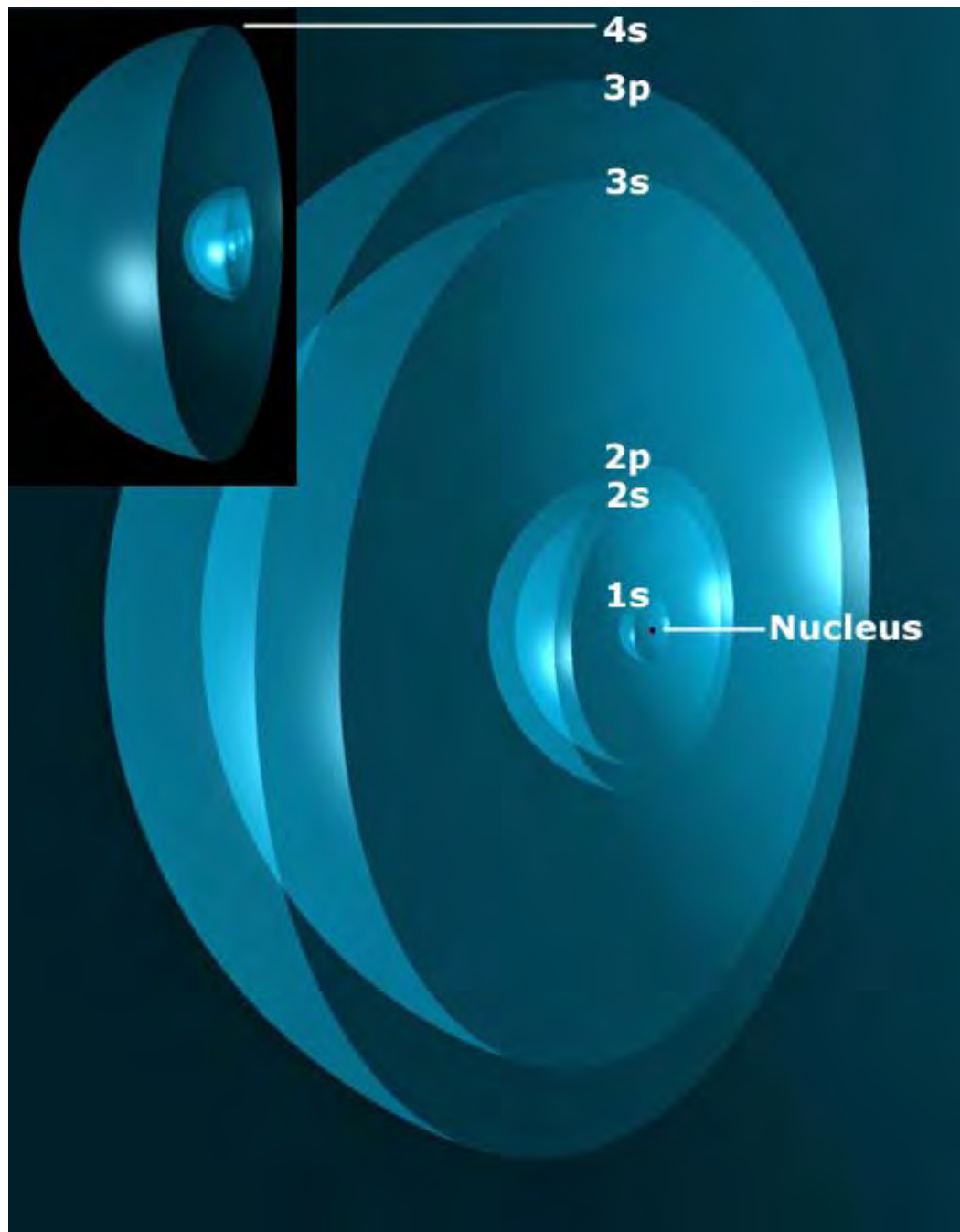
Ultimately, the electron configuration must be a minimum of energy. Minimum energy configurations are given by solutions to Laplace's equation.

Electrons of an atom with the same principal and ℓ quantum numbers align parallel until each of the m_ℓ levels are occupied, and then pairing occurs until each of the m_ℓ levels contain paired electrons.

The electron configuration for one through twenty-electron atoms that achieves an energy minimum is: $1s < 2s < 2p < 3s < 3p < 4s$.

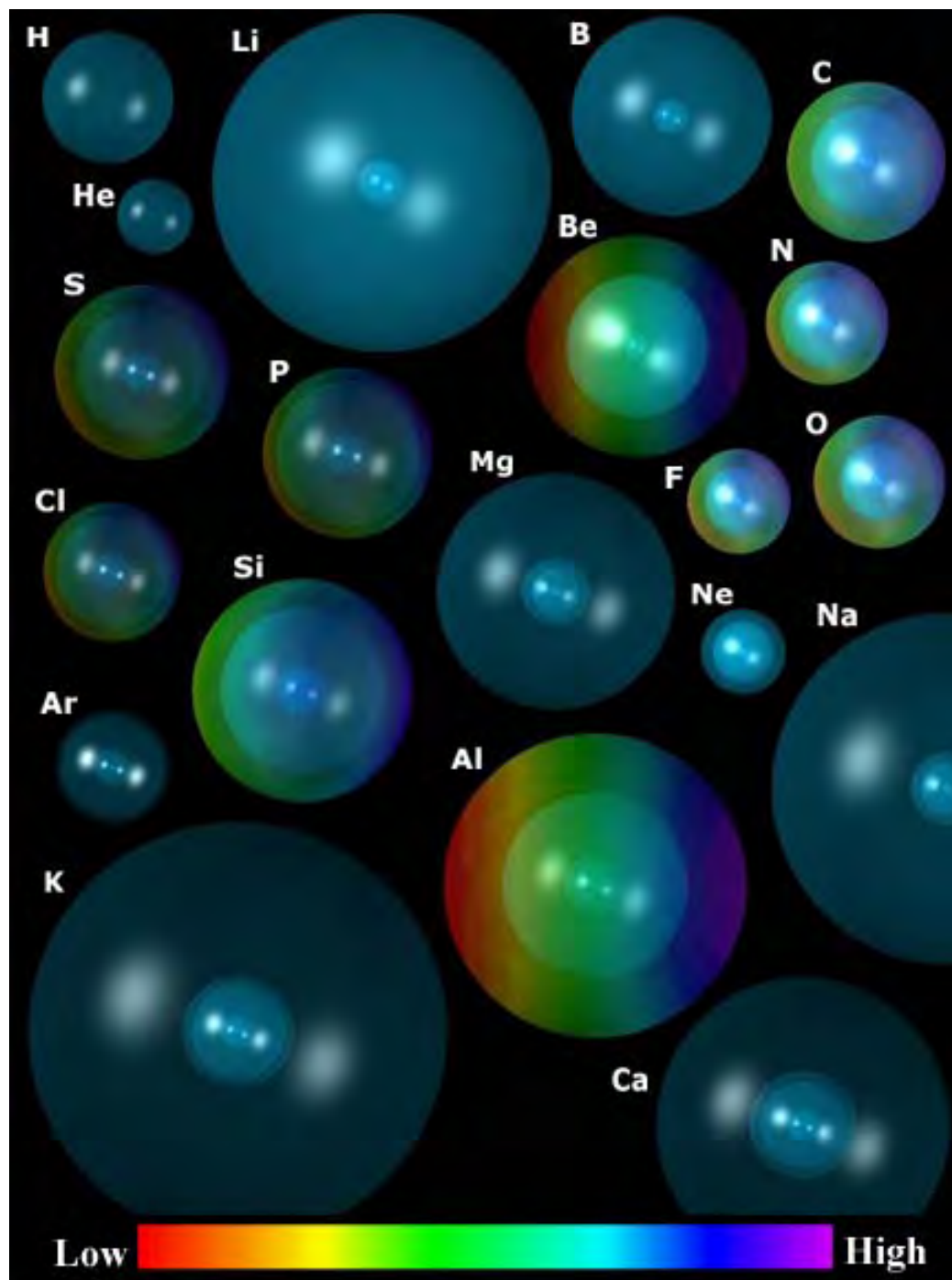
Sectional View
of the
Potassium (K)
Atom

(Electrons
shown at
relative size
scale, but
nucleus not to
scale.)



Visualization of
the One-Through-
Twenty Electron
Atoms.

Color-Scaled
Charge-Densities
shown with
relative-size-scale.



One- Through Twenty-Electron Atoms cont'd

In each case, the corresponding force balance of the central Coulombic, paramagnetic, and diamagnetic forces was derived for each n-electron atom that was solved for the radius of each electron.

The central Coulombic force was that of a point charge at the origin since the electron charge-density functions are spherically symmetrical with a time dependence that was nonradiative.

This feature eliminated the electron-electron repulsion terms and the intractable infinities of quantum mechanics and permitted general solutions.

The ionization energies were obtained using the calculated radii in the determination of the Coulombic and any magnetic energies.

The radii and ionization energies for all cases are given by equations having fundamental constants and each nuclear charge, Z , only.

The predicted ionization energies and electron configurations are in remarkable agreement with the experimental values known for 400 atoms and ions.

General Equation for the Ionization Energies of Five Through Ten-Electron Atoms

For example, for each n-electron atom having a central charge of Z times that of the proton and an electron configuration $1s^2 2s^2 2p^{n-4}$, there are two indistinguishable spin-paired electrons in an orbitalsphere with radii r_1 and r_2 both given by:

$$r_1 = r_2 = a_o \left[\frac{1}{Z-1} - \frac{\sqrt{\frac{3}{4}}}{Z(Z-1)} \right]$$

two indistinguishable spin-paired electrons in an orbitalsphere with radii r_3 and r_4 both given by:

$$r_4 = r_3 = \frac{a_o \left(1 - \frac{\sqrt{\frac{3}{4}}}{Z} \right) \pm a_o \sqrt{\frac{\left(1 - \frac{\sqrt{\frac{3}{4}}}{Z} \right)^2}{\left((Z-3) - \left(\frac{1}{4} - \frac{1}{Z} \right) \frac{\sqrt{\frac{3}{4}}}{r_1} \right)^2} + 4 \frac{\left[\frac{Z-3}{Z-2} \right] r_1^{10} \sqrt{\frac{3}{4}}}{\left((Z-3) - \left(\frac{1}{4} - \frac{1}{Z} \right) \frac{\sqrt{\frac{3}{4}}}{r_1} \right)^2}}}{2}}{2}$$

r_1 in units of a_o

Equation for the Ionization Energies of Five through Ten-Electron Atoms cont'd

and $n - 4$ electrons in an orbitsphere with radius r_n given by

$$r_n = \frac{a_0 \left((Z - (n-1)) - \left(\frac{A}{8} - \frac{B}{2Z} \right) \frac{\sqrt{3}}{r_3} \right) \pm a_0 \sqrt{ \frac{1}{ \left((Z - (n-1)) - \left(\frac{A}{8} - \frac{B}{2Z} \right) \frac{\sqrt{3}}{r_3} \right)^2 } + \frac{20\sqrt{3} \left[\frac{Z-n}{Z-(n-1)} \right] \left(1 - \frac{\sqrt{2}}{2} \right) r_3}{ \left((Z - (n-1)) - \left(\frac{A}{8} - \frac{B}{2Z} \right) \frac{\sqrt{3}}{r_3} \right) } }{2}$$

r_3 in units of a_0

1s² 2s² 2pⁿ⁻⁴-Atom Ionization Energies cont'd

The parameter A corresponds to the diamagnetic force, $\mathbf{F}_{diamagnetic}$:

$$\mathbf{F}_{diamagnetic} = -\sum_m \frac{(\ell + |m|)!}{(2\ell + 1)(\ell - |m|)!} \frac{\hbar^2}{4m_e r_n^2 r_3} \sqrt{s(s+1)} \mathbf{i}_r$$

The parameter B corresponds to the paramagnetic force, \mathbf{F}_{mag2} :

$$\mathbf{F}_{mag2} = \frac{1}{Z} \frac{\hbar^2}{m_e r_n^2 r_3} \sqrt{s(s+1)} \mathbf{i}_r$$

or

$$\mathbf{F}_{mag2} = \frac{1}{Z} \frac{4\hbar^2}{m_e r_n^2 r_3} \sqrt{s(s+1)} \mathbf{i}_r$$

depending on the positive or negative superposition of spin and orbital angular momentum.

The ionization energies for the n-electron atoms are given by the negative of the electric energy, $E(electric)$:

$$E(ionization) = -Electric\ Energy = \frac{(Z - (n - 1))e^2}{8\pi\epsilon_o r_n}$$

Summary of the Parameters of Five through Ten- Electron Atoms

Atom Type	Electron Configuration	Ground State Term	Orbital Arrangement of 2p Electrons (2p state)			Diamagnetic Force Factor A	Paramagnetic Force Factor B
Neutral 5 e Atom <i>B</i>	$1s^2 2s^2 2p^1$	$^2P_{1/2}^0$	\uparrow 1	--- 0	--- -1	1	0
Neutral 6 e Atom <i>C</i>	$1s^2 2s^2 2p^2$	3P_0	\uparrow 1	\uparrow 0	--- -1	$\frac{2}{3}$	0
Neutral 7 e Atom <i>N</i>	$1s^2 2s^2 2p^3$	$^4S_{3/2}^0$	\uparrow 1	\uparrow 0	\uparrow -1	$\frac{1}{3}$	1
Neutral 8 e Atom <i>O</i>	$1s^2 2s^2 2p^4$	3P_2	$\uparrow\downarrow$ 1	\uparrow 0	\uparrow -1	1	2
Neutral 9 e Atom <i>F</i>	$1s^2 2s^2 2p^5$	$^2P_{3/2}^0$	$\uparrow\downarrow$ 1	$\uparrow\downarrow$ 0	\uparrow -1	$\frac{2}{3}$	3
Neutral 10 e Atom <i>Ne</i>	$1s^2 2s^2 2p^6$	1S_0	$\uparrow\downarrow$ 1	$\uparrow\downarrow$ 0	$\uparrow\downarrow$ -1	0	3
5 e Ion	$1s^2 2s^2 2p^1$	$^2P_{1/2}^0$	\uparrow 1	--- 0	--- -1	$\frac{5}{3}$	1
6 e Ion	$1s^2 2s^2 2p^2$	3P_0	\uparrow 1	\uparrow 0	--- -1	$\frac{5}{3}$	4
7 e Ion	$1s^2 2s^2 2p^3$	$^4S_{3/2}^0$	\uparrow 1	\uparrow 0	\uparrow -1	$\frac{5}{3}$	6
8 e Ion	$1s^2 2s^2 2p^4$	3P_2	$\uparrow\downarrow$ 1	\uparrow 0	\uparrow -1	$\frac{5}{3}$	6
9 e Ion	$1s^2 2s^2 2p^5$	$^2P_{3/2}^0$	$\uparrow\downarrow$ 1	$\uparrow\downarrow$ 0	\uparrow -1	$\frac{5}{3}$	9
10 e Ion	$1s^2 2s^2 2p^6$	1S_0	$\uparrow\downarrow$ 1	$\uparrow\downarrow$ 0	$\uparrow\downarrow$ -1	$\frac{5}{3}$	12

Ionization Energies for Some Five-Electron Atoms

5 e Atom	Z	r_1 (a_0)	r_3 (a_0)	r_5 (a_0)	Theoretical Ionization Energies (eV)	Experimental Ionization Energies (eV)	Relative Error
<i>B</i>	5	0.20670	1.07930	1.67000	8.30266	8.29803	-0.00056
<i>C</i> ⁺	6	0.17113	0.84317	1.12092	24.2762	24.38332	0.0044
<i>N</i> ²⁺	7	0.14605	0.69385	0.87858	46.4585	47.44924	0.0209
<i>O</i> ³⁺	8	0.12739	0.59020	0.71784	75.8154	77.41353	0.0206
<i>F</i> ⁴⁺	9	0.11297	0.51382	0.60636	112.1922	114.2428	0.0179
<i>Ne</i> ⁵⁺	10	0.10149	0.45511	0.52486	155.5373	157.93	0.0152
<i>Na</i> ⁶⁺	11	0.09213	0.40853	0.46272	205.8266	208.5	0.0128
<i>Mg</i> ⁷⁺	12	0.08435	0.37065	0.41379	263.0469	265.96	0.0110
<i>Al</i> ⁸⁺	13	0.07778	0.33923	0.37425	327.1901	330.13	0.0089
<i>Si</i> ⁹⁺	14	0.07216	0.31274	0.34164	398.2509	401.37	0.0078
<i>P</i> ¹⁰⁺	15	0.06730	0.29010	0.31427	476.2258	479.46	0.0067
<i>S</i> ¹¹⁺	16	0.06306	0.27053	0.29097	561.1123	564.44	0.0059
<i>Cl</i> ¹²⁺	17	0.05932	0.25344	0.27090	652.9086	656.71	0.0058
<i>Ar</i> ¹³⁺	18	0.05599	0.23839	0.25343	751.6132	755.74	0.0055
<i>K</i> ¹⁴⁺	19	0.05302	0.22503	0.23808	857.2251	861.1	0.0045
<i>Ca</i> ¹⁵⁺	20	0.05035	0.21308	0.22448	969.7435	974	0.0044
<i>Sc</i> ¹⁶⁺	21	0.04794	0.20235	0.21236	1089.1678	1094	0.0044
<i>Ti</i> ¹⁷⁺	22	0.04574	0.19264	0.20148	1215.4975	1221	0.0045
<i>V</i> ¹⁸⁺	23	0.04374	0.18383	0.19167	1348.7321	1355	0.0046
<i>Cr</i> ¹⁹⁺	24	0.04191	0.17579	0.18277	1488.8713	1496	0.0048
<i>Mn</i> ²⁰⁺	25	0.04022	0.16842	0.17466	1635.9148	1644	0.0049
<i>Fe</i> ²¹⁺	26	0.03867	0.16165	0.16724	1789.8624	1799	0.0051
<i>Co</i> ²²⁺	27	0.03723	0.15540	0.16042	1950.7139	1962	0.0058
<i>Ni</i> ²³⁺	28	0.03589	0.14961	0.15414	2118.4690	2131	0.0059
<i>Cu</i> ²⁴⁺	29	0.03465	0.14424	0.14833	2293.1278	2308	0.0064

Ionization Energies for Some Six-Electron Atoms

6 e Atom	Z	r_1 (a_0)	r_3 (a_0)	r_6 (a_0)	Theoretical Ionization Energies (eV)	Experimental Ionization Energies (eV)	Relative Error
C	6	0.17113	0.84317	1.20654	11.27671	11.2603	-0.0015
N^+	7	0.14605	0.69385	0.90119	30.1950	29.6013	-0.0201
O^{2+}	8	0.12739	0.59020	0.74776	54.5863	54.9355	0.0064
F^{3+}	9	0.11297	0.51382	0.63032	86.3423	87.1398	0.0092
Ne^{4+}	10	0.10149	0.45511	0.54337	125.1986	126.21	0.0080
Na^{5+}	11	0.09213	0.40853	0.47720	171.0695	172.18	0.0064
Mg^{6+}	12	0.08435	0.37065	0.42534	223.9147	225.02	0.0049
Al^{7+}	13	0.07778	0.33923	0.38365	283.7121	284.66	0.0033
Si^{8+}	14	0.07216	0.31274	0.34942	350.4480	351.12	0.0019
P^{9+}	15	0.06730	0.29010	0.32081	424.1135	424.4	0.0007
S^{10+}	16	0.06306	0.27053	0.29654	504.7024	504.8	0.0002
Cl^{11+}	17	0.05932	0.25344	0.27570	592.2103	591.99	-0.0004
Ar^{12+}	18	0.05599	0.23839	0.25760	686.6340	686.1	-0.0008
K^{13+}	19	0.05302	0.22503	0.24174	787.9710	786.6	-0.0017
Ca^{14+}	20	0.05035	0.21308	0.22772	896.2196	894.5	-0.0019
Sc^{15+}	21	0.04794	0.20235	0.21524	1011.3782	1009	-0.0024
Ti^{16+}	22	0.04574	0.19264	0.20407	1133.4456	1131	-0.0022
V^{17+}	23	0.04374	0.18383	0.19400	1262.4210	1260	-0.0019
Cr^{18+}	24	0.04191	0.17579	0.18487	1398.3036	1396	-0.0017
Mn^{19+}	25	0.04022	0.16842	0.17657	1541.0927	1539	-0.0014
Fe^{20+}	26	0.03867	0.16165	0.16899	1690.7878	1689	-0.0011
Co^{21+}	27	0.03723	0.15540	0.16203	1847.3885	1846	-0.0008
Ni^{22+}	28	0.03589	0.14961	0.15562	2010.8944	2011	0.0001
Cu^{23+}	29	0.03465	0.14424	0.14970	2181.3053	2182	0.0003

Ionization Energies for Some Seven-Electron Atoms

7 e Atom	Z	r_1 (a_0)	r_3 (a_0)	r_7 (a_0)	Theoretical Ionization Energies (eV)	Experimental Ionization Energies (eV)	Relative Error
<i>N</i>	7	0.14605	0.69385	0.93084	14.61664	14.53414	-0.0057
<i>O</i> ⁺	8	0.12739	0.59020	0.78489	34.6694	35.1173	0.0128
<i>F</i> ²⁺	9	0.11297	0.51382	0.67084	60.8448	62.7084	0.0297
<i>Ne</i> ³⁺	10	0.10149	0.45511	0.57574	94.5279	97.12	0.0267
<i>Na</i> ⁴⁺	11	0.09213	0.40853	0.50250	135.3798	138.4	0.0218
<i>Mg</i> ⁵⁺	12	0.08435	0.37065	0.44539	183.2888	186.76	0.0186
<i>Al</i> ⁶⁺	13	0.07778	0.33923	0.39983	238.2017	241.76	0.0147
<i>Si</i> ⁷⁺	14	0.07216	0.31274	0.36271	300.0883	303.54	0.0114
<i>P</i> ⁸⁺	15	0.06730	0.29010	0.33191	368.9298	372.13	0.0086
<i>S</i> ⁹⁺	16	0.06306	0.27053	0.30595	444.7137	447.5	0.0062
<i>Cl</i> ¹⁰⁺	17	0.05932	0.25344	0.28376	527.4312	529.28	0.0035
<i>Ar</i> ¹¹⁺	18	0.05599	0.23839	0.26459	617.0761	618.26	0.0019
<i>K</i> ¹²⁺	19	0.05302	0.22503	0.24785	713.6436	714.6	0.0013
<i>Ca</i> ¹³⁺	20	0.05035	0.21308	0.23311	817.1303	817.6	0.0006
<i>Sc</i> ¹⁴⁺	21	0.04794	0.20235	0.22003	927.5333	927.5	0.0000
<i>Ti</i> ¹⁵⁺	22	0.04574	0.19264	0.20835	1044.8504	1044	-0.0008
<i>V</i> ¹⁶⁺	23	0.04374	0.18383	0.19785	1169.0800	1168	-0.0009
<i>Cr</i> ¹⁷⁺	24	0.04191	0.17579	0.18836	1300.2206	1299	-0.0009
<i>Mn</i> ¹⁸⁺	25	0.04022	0.16842	0.17974	1438.2710	1437	-0.0009
<i>Fe</i> ¹⁹⁺	26	0.03867	0.16165	0.17187	1583.2303	1582	-0.0008
<i>Co</i> ²⁰⁺	27	0.03723	0.15540	0.16467	1735.0978	1735	-0.0001
<i>Ni</i> ²¹⁺	28	0.03589	0.14961	0.15805	1893.8726	1894	0.0001
<i>Cu</i> ²²⁺	29	0.03465	0.14424	0.15194	2059.5543	2060	0.0002

Ionization Energies for Some Eight-Electron Atoms

8 e Atom	Z	r_1 (a_0)	r_3 (a_0)	r_8 (a_0)	Theoretical Ionization Energies (eV)	Experimental Ionization Energies (eV)	Relative Error
<i>O</i>	8	0.12739	0.59020	1.00000	13.60580	13.6181	0.0009
<i>F</i> ⁺	9	0.11297	0.51382	0.7649	35.5773	34.9708	-0.0173
<i>Ne</i> ²⁺	10	0.10149	0.45511	0.6514	62.6611	63.45	0.0124
<i>Na</i> ³⁺	11	0.09213	0.40853	0.5592	97.3147	98.91	0.0161
<i>Mg</i> ⁴⁺	12	0.08435	0.37065	0.4887	139.1911	141.27	0.0147
<i>Al</i> ⁵⁺	13	0.07778	0.33923	0.4338	188.1652	190.49	0.0122
<i>Si</i> ⁶⁺	14	0.07216	0.31274	0.3901	244.1735	246.5	0.0094
<i>P</i> ⁷⁺	15	0.06730	0.29010	0.3543	307.1791	309.6	0.0078
<i>S</i> ⁸⁺	16	0.06306	0.27053	0.3247	377.1579	379.55	0.0063
<i>Cl</i> ⁹⁺	17	0.05932	0.25344	0.2996	454.0940	455.63	0.0034
<i>Ar</i> ¹⁰⁺	18	0.05599	0.23839	0.2782	537.9756	538.96	0.0018
<i>K</i> ¹¹⁺	19	0.05302	0.22503	0.2597	628.7944	629.4	0.0010
<i>Ca</i> ¹²⁺	20	0.05035	0.21308	0.2434	726.5442	726.6	0.0001
<i>Sc</i> ¹³⁺	21	0.04794	0.20235	0.2292	831.2199	830.8	-0.0005
<i>Ti</i> ¹⁴⁺	22	0.04574	0.19264	0.2165	942.8179	941.9	-0.0010
<i>V</i> ¹⁵⁺	23	0.04374	0.18383	0.2051	1061.3351	1060	-0.0013
<i>Cr</i> ¹⁶⁺	24	0.04191	0.17579	0.1949	1186.7691	1185	-0.0015
<i>Mn</i> ¹⁷⁺	25	0.04022	0.16842	0.1857	1319.1179	1317	-0.0016
<i>Fe</i> ¹⁸⁺	26	0.03867	0.16165	0.1773	1458.3799	1456	-0.0016
<i>Co</i> ¹⁹⁺	27	0.03723	0.15540	0.1696	1604.5538	1603	-0.0010
<i>Ni</i> ²⁰⁺	28	0.03589	0.14961	0.1626	1757.6383	1756	-0.0009
<i>Cu</i> ²¹⁺	29	0.03465	0.14424	0.1561	1917.6326	1916	-0.0009

Ionization Energies for Some Nine-Electron Atoms

9 e Atom	Z	r_1 (a_0)	r_3 (a_0)	r_9 (a_0)	Theoretical Ionization Energies (eV)	Experimental Ionization Energies (eV)	Relative Error
<i>F</i>	9	0.11297	0.51382	0.78069	17.42782	17.42282	-0.0003
<i>Ne</i> ⁺	10	0.10149	0.45511	0.64771	42.0121	40.96328	-0.0256
<i>Na</i> ²⁺	11	0.09213	0.40853	0.57282	71.2573	71.62	0.0051
<i>Mg</i> ³⁺	12	0.08435	0.37065	0.50274	108.2522	109.2655	0.0093
<i>Al</i> ⁴⁺	13	0.07778	0.33923	0.44595	152.5469	153.825	0.0083
<i>Si</i> ⁵⁺	14	0.07216	0.31274	0.40020	203.9865	205.27	0.0063
<i>P</i> ⁶⁺	15	0.06730	0.29010	0.36283	262.4940	263.57	0.0041
<i>S</i> ⁷⁺	16	0.06306	0.27053	0.33182	328.0238	328.75	0.0022
<i>Cl</i> ⁸⁺	17	0.05932	0.25344	0.30571	400.5466	400.06	-0.0012
<i>Ar</i> ⁹⁺	18	0.05599	0.23839	0.28343	480.0424	478.69	-0.0028
<i>K</i> ¹⁰⁺	19	0.05302	0.22503	0.26419	566.4968	564.7	-0.0032
<i>Ca</i> ¹¹⁺	20	0.05035	0.21308	0.24742	659.8992	657.2	-0.0041
<i>Sc</i> ¹²⁺	21	0.04794	0.20235	0.23266	760.2415	756.7	-0.0047
<i>Ti</i> ¹³⁺	22	0.04574	0.19264	0.21957	867.5176	863.1	-0.0051
<i>V</i> ¹⁴⁺	23	0.04374	0.18383	0.20789	981.7224	976	-0.0059
<i>Cr</i> ¹⁵⁺	24	0.04191	0.17579	0.19739	1102.8523	1097	-0.0053
<i>Mn</i> ¹⁶⁺	25	0.04022	0.16842	0.18791	1230.9038	1224	-0.0056
<i>Fe</i> ¹⁷⁺	26	0.03867	0.16165	0.17930	1365.8746	1358	-0.0058
<i>Co</i> ¹⁸⁺	27	0.03723	0.15540	0.17145	1507.7624	1504.6	-0.0021
<i>Ni</i> ¹⁹⁺	28	0.03589	0.14961	0.16427	1656.5654	1648	-0.0052
<i>Cu</i> ²⁰⁺	29	0.03465	0.14424	0.15766	1812.2821	1804	-0.0046

Ionization Energies for Some Ten-Electron Atoms

10 e Atom	Z	r_1 (a_0)	r_3 (a_0)	r_{10} (a_0)	Theoretical Ionization Energies (eV)	Experimental Ionization Energies (eV)	Relative Error
<i>Ne</i>	10	0.10149	0.45511	0.63659	21.37296	21.56454	0.00888
<i>Na</i> ⁺	11	0.09213	0.40853	0.560945	48.5103	47.2864	-0.0259
<i>Mg</i> ²⁺	12	0.08435	0.37065	0.510568	79.9451	80.1437	0.0025
<i>Al</i> ³⁺	13	0.07778	0.33923	0.456203	119.2960	119.992	0.0058
<i>Si</i> ⁴⁺	14	0.07216	0.31274	0.409776	166.0150	166.767	0.0045
<i>P</i> ⁵⁺	15	0.06730	0.29010	0.371201	219.9211	220.421	0.0023
<i>S</i> ⁶⁺	16	0.06306	0.27053	0.339025	280.9252	280.948	0.0001
<i>Cl</i> ⁷⁺	17	0.05932	0.25344	0.311903	348.9750	348.28	-0.0020
<i>Ar</i> ⁸⁺	18	0.05599	0.23839	0.288778	424.0365	422.45	-0.0038
<i>K</i> ⁹⁺	19	0.05302	0.22503	0.268844	506.0861	503.8	-0.0045
<i>Ca</i> ¹⁰⁺	20	0.05035	0.21308	0.251491	595.1070	591.9	-0.0054
<i>Sc</i> ¹¹⁺	21	0.04794	0.20235	0.236251	691.0866	687.36	-0.0054
<i>Ti</i> ¹²⁺	22	0.04574	0.19264	0.222761	794.0151	787.84	-0.0078
<i>V</i> ¹³⁺	23	0.04374	0.18383	0.210736	903.8853	896	-0.0088
<i>Cr</i> ¹⁴⁺	24	0.04191	0.17579	0.19995	1020.6910	1010.6	-0.0100
<i>Mn</i> ¹⁵⁺	25	0.04022	0.16842	0.19022	1144.4276	1134.7	-0.0086
<i>Fe</i> ¹⁶⁺	26	0.03867	0.16165	0.181398	1275.0911	1266	-0.0072
<i>Co</i> ¹⁷⁺	27	0.03723	0.15540	0.173362	1412.6783	1397.2	-0.0111
<i>Ni</i> ¹⁸⁺	28	0.03589	0.14961	0.166011	1557.1867	1541	-0.0105
<i>Cu</i> ¹⁹⁺	29	0.03465	0.14424	0.159261	1708.6139	1697	-0.0068
<i>Zn</i> ²⁰⁺	30	0.03349	0.13925	0.153041	1866.9581	1856	-0.0059

The Nature of the Chemical Bond of Hydrogen

The Laplacian in ellipsoidal coordinates is solved with the constraint of nonradiation

$$(\eta - \zeta)R_\xi \frac{\delta}{\delta \xi} \left(R_\xi \frac{\delta \phi}{\delta \xi} \right) + (\zeta - \xi)R_\eta \frac{\delta}{\delta \eta} \left(R_\eta \frac{\delta \phi}{\delta \eta} \right) + (\xi - \eta)R_\zeta \frac{\delta}{\delta \zeta} \left(R_\zeta \frac{\delta \phi}{\delta \zeta} \right) = 0$$

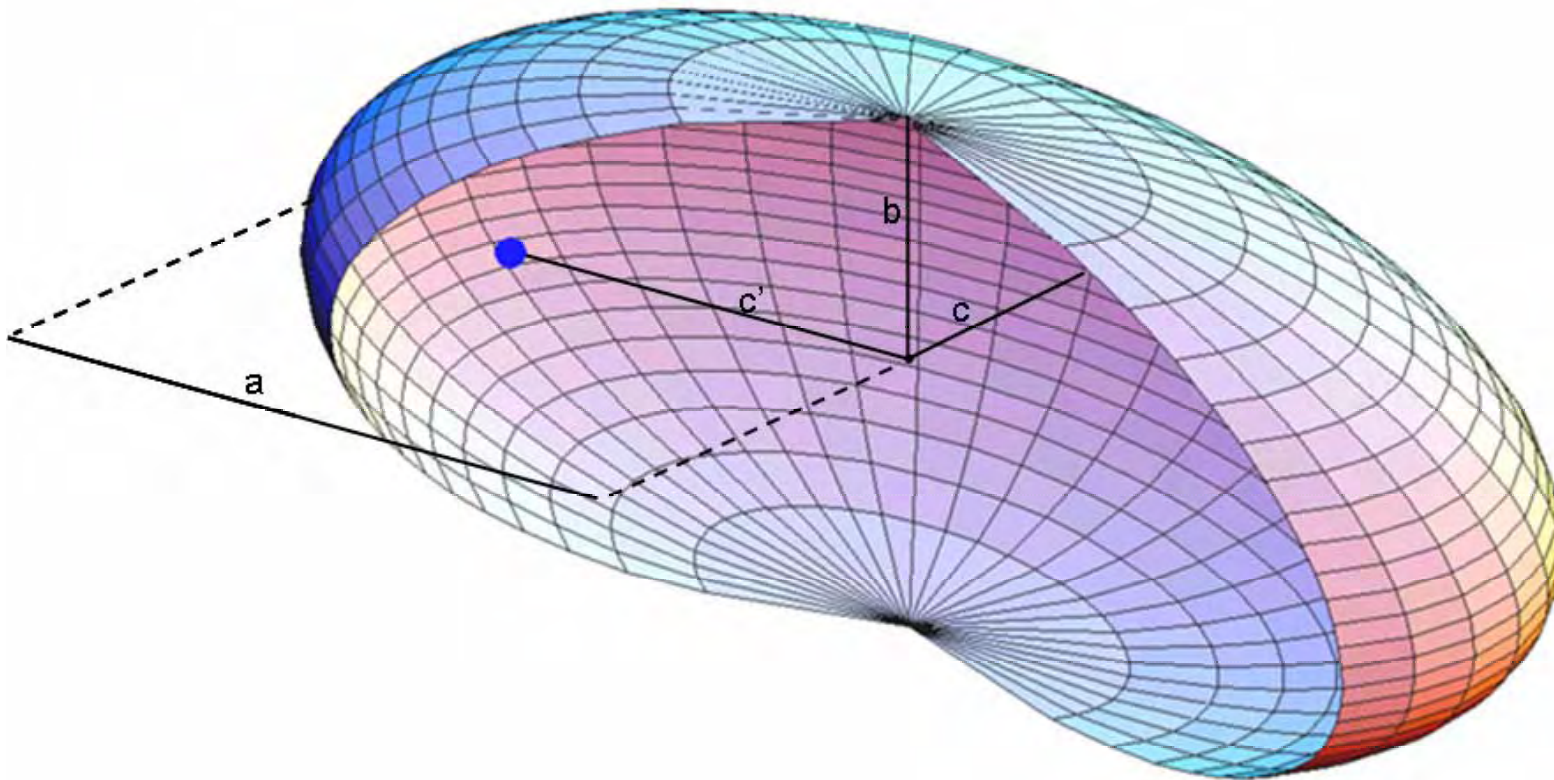
The Force Balance Equation for the Hydrogen Molecule

$$\frac{\hbar^2}{m_e a^2 b^2} D = \frac{e^2}{8\pi \epsilon_0 a b^2} D + \frac{\hbar^2}{2m_e a^2 b^2} D \quad \text{where } D = r(t) \text{ is the distance from the origin to the ellipsoid}$$

$r(t)$ has the parametric solution $r(t) = \mathbf{i}a \cos \omega t + \mathbf{j}b \sin \omega t$

When the **Semimajor Axis**, a , is $a = a_o$.

The Nature of the Chemical Bond of Hydrogen cont'd



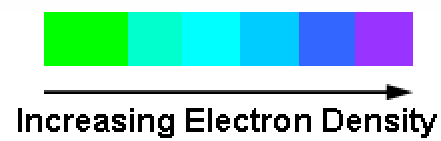
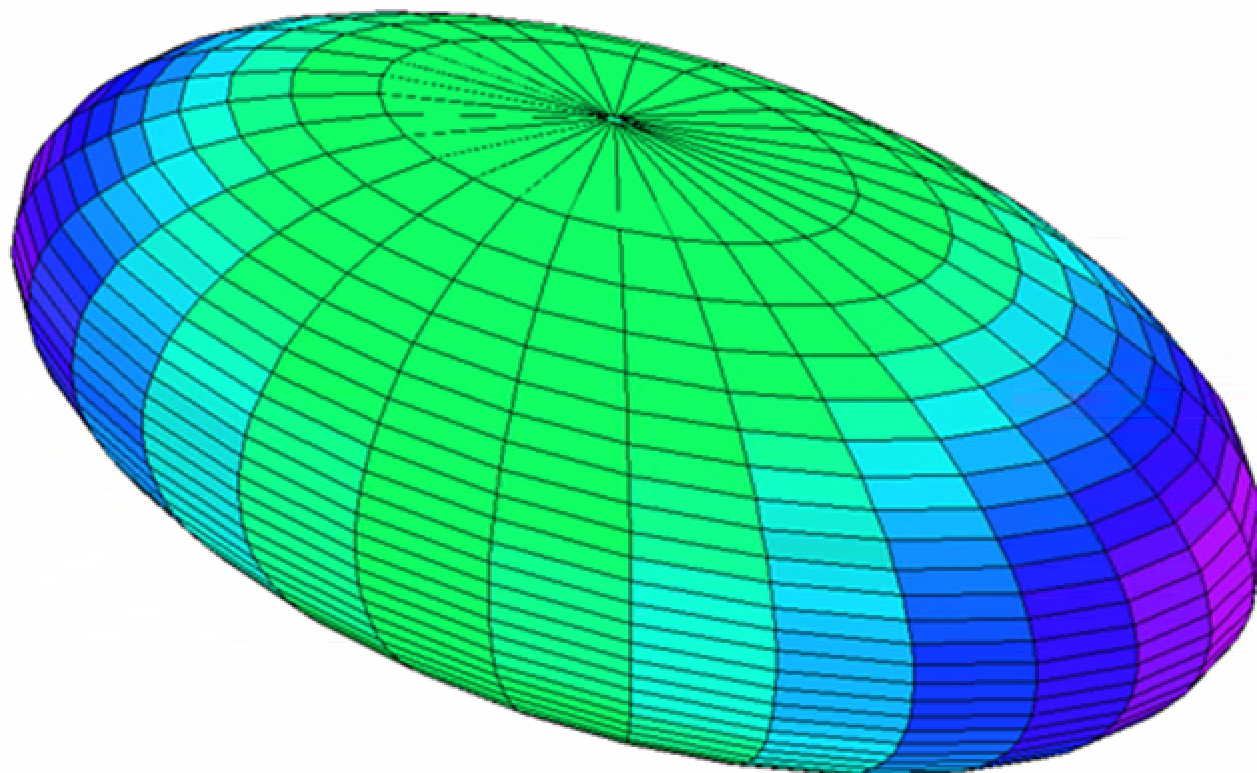
The Internuclear Distance, $2c'$, which is the distance between the foci is $2c' = \sqrt{2}a_o$.

The experimental internuclear distance is $\sqrt{2}a_o$.

The Semiminor Axis, b , is $b = \frac{1}{\sqrt{2}} a_o$

The Eccentricity, e , is $e = \frac{1}{\sqrt{2}}$

Charge-Density Function



The Energies of the Hydrogen Molecule

The Potential Energy of the Two Electrons in the Central Field of the Protons at the Foci

$$V_e = \frac{-2e^2}{8\pi\epsilon_0\sqrt{a^2-b^2}} \ln \frac{a+\sqrt{a^2-b^2}}{a-\sqrt{a^2-b^2}} = -67.8358 \text{ eV}$$

The Potential Energy of the Two Protons

$$V_p = \frac{e^2}{8\pi\epsilon_0\sqrt{a^2-b^2}} = 19.2415 \text{ eV}$$

The Kinetic Energy of the Electrons

$$T = \frac{\hbar^2}{2m_e a \sqrt{a^2-b^2}} \ln \frac{a+\sqrt{a^2-b^2}}{a-\sqrt{a^2-b^2}} = 33.9179 \text{ eV}$$

The Energy, V_m , of the Magnetic Force Between the Electrons

$$V_m = \frac{-\hbar^2}{4m_e a \sqrt{a^2-b^2}} \ln \frac{a+\sqrt{a^2-b^2}}{a-\sqrt{a^2-b^2}} = -16.9589 \text{ eV}$$

The Energies of the Hydrogen Molecule cont'd

During bond formation, the electrons undergo a reentrant oscillatory orbit with vibration of the protons. The corresponding energy \bar{E}_{osc} is the difference between the Doppler and average vibrational kinetic energies.

$$\bar{E}_{osc} = \bar{E}_D + \bar{E}_{Kvib} = (V_e + T + V_m + V_p) \sqrt{\frac{2\bar{E}_K}{Mc^2}} + \frac{1}{2} \hbar \sqrt{\frac{k}{\mu}}$$

The Total Energy of the Hydrogen Molecule

$$E_T = V_e + T + V_m + V_p + \bar{E}_{osc}$$

$$E_T = -13.60 \text{ eV} \left[\left(2\sqrt{2} - \sqrt{2} + \frac{\sqrt{2}}{2} \right) \ln \frac{\sqrt{2} + 1}{\sqrt{2} - 1} - \sqrt{2} \right] \left[1 + \sqrt{\frac{2\hbar \sqrt{\frac{e^2}{4\pi\epsilon_0 a_0^3}}}{m_e c^2}} \right] + \frac{1}{2} \hbar \sqrt{\frac{k}{\mu}} = -31.689 \text{ eV}$$

The calculated and experimental parameters of H_2 , D_2 , H_2^+ and D_2^+ .

Parameter	Calculated	Experimental	Eqs. ^a
H_2 Bond Energy	4.478 eV	4.478 eV	12.251
D_2 Bond Energy	4.556 eV	4.556 eV	12.253
H_2^+ Bond Energy	2.654 eV	2.651 eV	12.220
D_2^+ Bond Energy	2.696 eV	2.691 eV	12.222
H_2 Total Energy	31.677 eV	31.675 eV	12.247
D_2 Total Energy	31.760 eV	31.760 eV	12.248
H_2 Ionization Energy	15.425 eV	15.426 eV	12.249
D_2 Ionization Energy	15.463 eV	15.466 eV	12.250
H_2^+ Ionization Energy	16.253 eV	16.250 eV	12.218
D_2^+ Ionization Energy	16.299 eV	16.294 eV	12.219
H_2^+ Magnetic Moment	$9.274 \times 10^{-24} \text{ JT}^{-1}$	$9.274 \times 10^{-24} \text{ JT}^{-1}$	14.1-14.7
	μ_B	μ_B	
Absolute H_2 Gas-Phase NMR Shift	-28.0 ppm	-28.0 ppm	12.362
H_2 Internuclear Distance ^b	0.748 Å	0.741 Å	12.238
	$\sqrt{2}a_0$		
D_2 Internuclear Distance ^b	0.748 Å	0.741 Å	12.238
	$\sqrt{2}a_0$		
H_2^+ Internuclear Distance ^c	1.058 Å	1.06 Å	12.207
	$2a_0$		
D_2^+ Internuclear Distance ^b	1.058 Å	1.0559 Å	12.207
	$2a_0$		
H_2 Vibrational Energy	0.517 eV	0.516 eV	12.259
D_2 Vibrational Energy	0.371 eV	0.371 eV	12.264
H_2 $\omega_e x_e$	120.4 cm^{-1}	121.33 cm^{-1}	12.261
D_2 $\omega_e x_e$	60.93 cm^{-1}	61.82 cm^{-1}	12.265
H_2^+ Vibrational Energy	0.270 eV	0.271 eV	12.228
D_2^+ Vibrational Energy	0.193 eV	0.196 eV	12.232
H_2 J=1 to J=0 Rotational Energy ^b	0.0148 eV	0.01509 eV	14.45
D_2 J=1 to J=0 Rotational Energy ^b	0.00741 eV	0.00755 eV	14.37-14.45
H_2^+ J=1 to J=0 Rotational Energy ^c	0.00740 eV	0.00739 eV	14.49
D_2^+ J=1 to J=0 Rotational Energy ^b	0.00370 eV	0.003723 eV	14.37-14.43, 14.49

^a R. Mills, *The Grand Unified Theory of Classical Quantum Mechanics*, September 2001 Edition, BlackLight Power, Inc., Cranbury, New Jersey, Distributed by Amazon.com; January (2003) Edition posted at www.blacklightpower.com.

^b The internuclear distances are not corrected for the reduction due to \bar{E}_{osc} .

^c The internuclear distances are not corrected for the increase due to \bar{E}_{osc} .

Proton and Neutron

The proton and neutron each comprise three charged fundamental particles called quarks and three massive photons called gluons.

Proton Parameters

$$\lambda_{C,p} = \hat{\lambda}_{c,q} = \frac{2\pi a_o m_e}{\alpha^{-1} m_p} = 1.3 \times 10^{-15} m = r_p = r_q$$

m_p proton rest mass

$$m_p = m_q + m_g'' = m_q''$$

$\lambda_{C,p}$ is the Compton wavelength of the proton

$$m_q = \frac{m_p}{2\pi}$$

$\hat{\lambda}_{c,q}$ is the Compton wavelength bar of the quarks

$$m_q'' = 2\pi m_q = 2\pi \times \frac{m_p}{2\pi} = m_p$$

r_p is the radius of the proton

r_q is the radius of the quarks

$$m_g'' = m_p - m_q = m_p \left[1 - \frac{1}{2\pi} \right]$$

m_q is the rest mass of the quarks

m_g'' is the relativistic mass of the gluons

$$E = m_q c^2 + m_g c^2 = \frac{m_p}{2\pi} c^2 + m_p \left[1 - \frac{1}{2\pi} \right] c^2 = m_p c^2$$

m_q'' is the relativistic mass of the quarks

Proton and Neutron cont'd

Neutron Parameters

$$\lambda_{C,n} = \hat{\lambda}_{c,q} = \frac{2\pi a_0 m_e}{\alpha^{-1} m_N} = 1.3214 \times 10^{-15} m = r_n = r_q$$

$$m_N = m_q + m_g'' = m_q''$$

$$m_q = \frac{m_N}{2\pi}$$

$$m_q'' = 2\pi m_q = 2\pi \times \frac{m_N}{2\pi} = m_N$$

$$m_g'' = m_N - m_q = m_N \left[1 - \frac{1}{2\pi} \right]$$

$$E = m_q c^2 + m_g c^2 = \frac{m_N}{2\pi} c^2 + m_N \left[1 - \frac{1}{2\pi} \right] c^2 = m_N c^2$$

m_N neutron rest mass

$\hat{\lambda}_{c,p}$ is the Compton wavelength of the neutron

$\hat{\lambda}_{c,q}$ is the Compton wavelength bar of the quarks

r_n is the radius of the neutron

r_q is the radius of the quarks

m_q is the rest mass of the quarks

m_g'' is the relativistic mass of the gluons

m_q'' is the relativistic mass of the quarks

Quark and Gluon Functions of the Proton

The proton functions can be viewed as a linear combination of three fundamental particles, three quarks, of charge $+\frac{2}{3}e$, $+\frac{2}{3}e$, and $-\frac{1}{3}e$. Each quark is associated with its gluon where the quark mass/charge function has the same angular dependence as the gluon mass/charge function.

The quark mass function of a proton is

$$\frac{m_P}{2\pi} \left[\frac{1}{3}(1 + \sin \theta \sin \phi) + \frac{1}{3}(1 + \sin \theta \cos \phi) + \frac{1}{3}(1 + \cos \theta) \right] \delta(r - \lambda_{C,p})$$

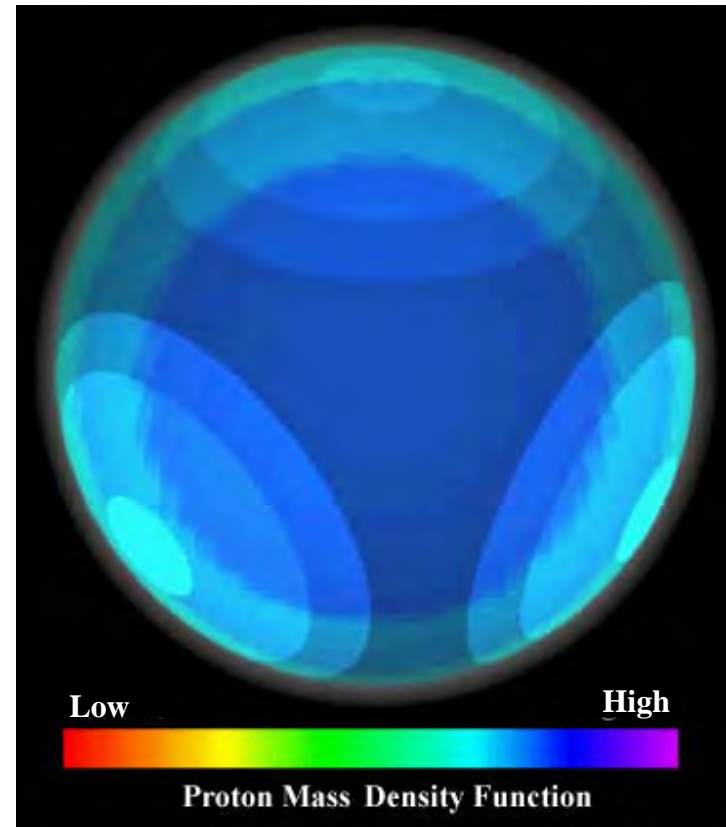
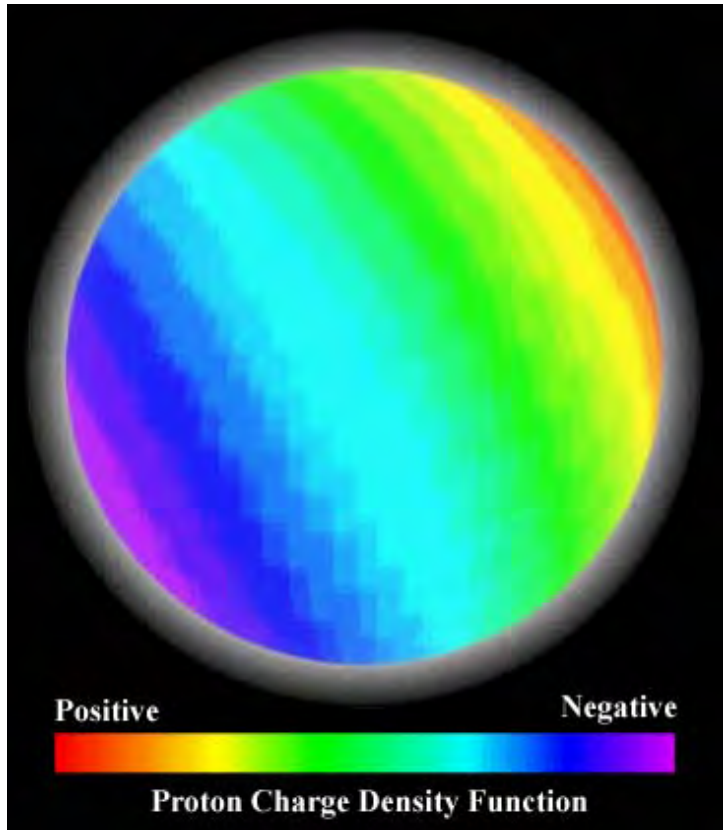
The charge function of the quarks of a proton is

$$e \left[\frac{2}{3}(1 + \sin \theta \sin \phi) + \frac{2}{3}(1 + \sin \theta \cos \phi) - \frac{1}{3}(1 + \cos \theta) \right] \delta(r - \lambda_{C,p})$$

The radial electric field of a proton is

$$E_r = \frac{-\alpha^{-1}e}{4\pi\epsilon_0 r^3} \frac{2\pi a_0}{\frac{m_N}{m_e} \alpha^{-1}} \left[\frac{3}{2}(1 + \sin \theta \sin \phi) + \frac{3}{2}(1 + \sin \theta \cos \phi) - 3(1 + \cos \theta) \right] \delta(r - \lambda_{C,p})$$

Quark and Gluon Functions of the Proton Cont...



Quark and Gluon Functions of the Neutron

The neutron functions can be viewed as a linear combination of three fundamental particles, three quarks, of charge $+\frac{2}{3}e$, $-\frac{1}{3}e$, and $-\frac{1}{3}e$. Each quark is associated with its gluon where the quark mass/charge function has the same angular dependence as the gluon mass/charge function.

The quark mass function of a neutron is

$$\frac{m_N}{2\pi} \left[\frac{1}{3}(1 + \sin \theta \sin \phi) + \frac{1}{3}(1 + \sin \theta \cos \phi) + \frac{1}{3}(1 + \cos \theta) \right] \delta(r - \lambda_{C,n})$$

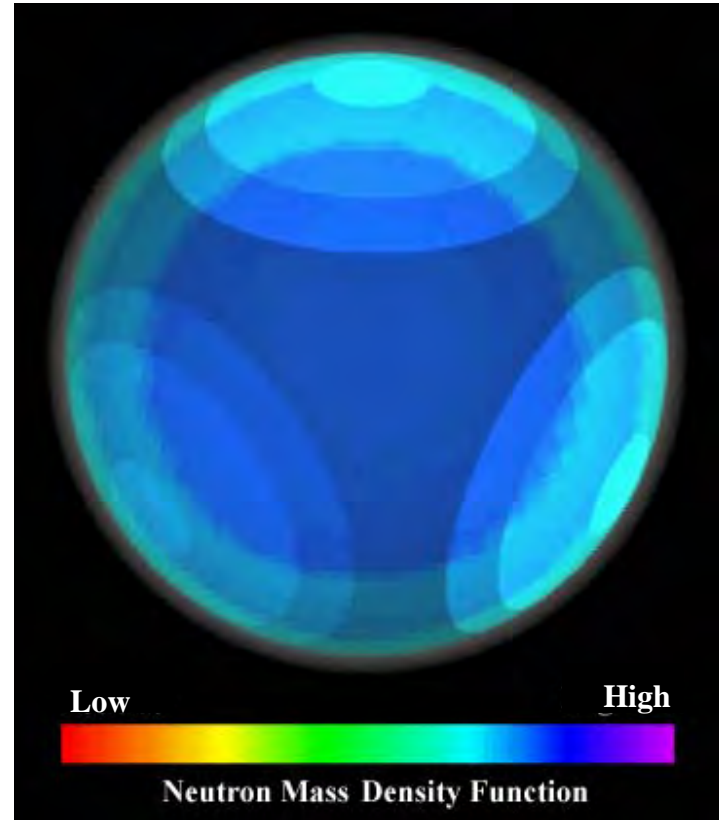
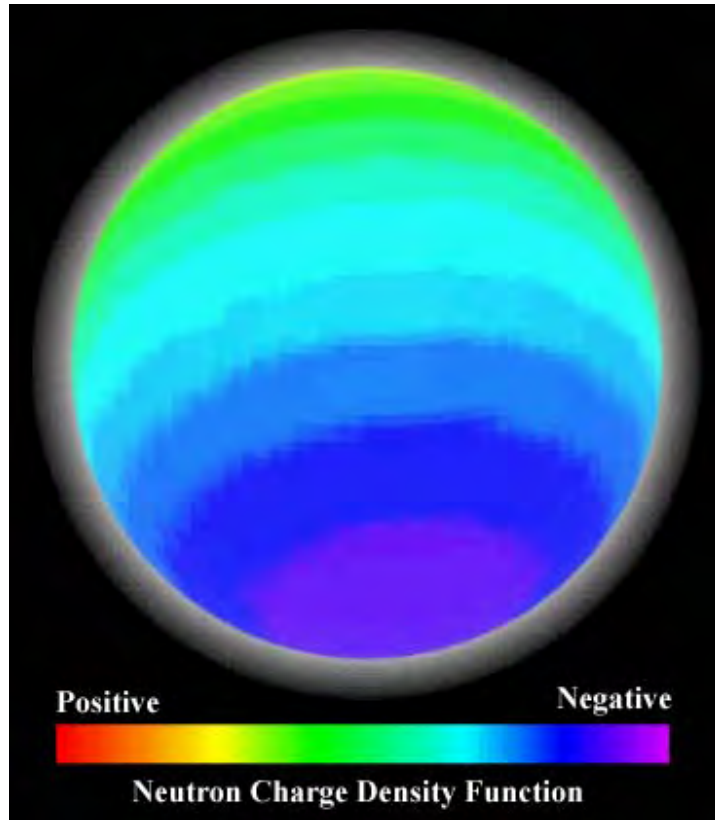
The charge function of the quarks of a neutron is

$$e \left[\frac{2}{3}(1 + \sin \theta \sin \phi) - \frac{1}{3}(1 + \sin \theta \cos \phi) - \frac{1}{3}(1 + \cos \theta) \right] \delta(r - \lambda_{C,n})$$

The radial electric field of a neutron is

$$E_r = \frac{-\alpha^{-1}e}{4\pi\epsilon_0 r^3} \frac{2\pi a_0}{\frac{m_N}{m_e} \alpha^{-1}} \left[\frac{3}{2}(1 + \sin \theta \sin \phi) - 3(1 + \sin \theta \cos \phi) - 3(1 + \cos \theta) \right] \delta(r - \lambda_{C,n})$$

Quark and Gluon Functions of the Neutron Cont...



Magnetic Moments

Proton Magnetic Moment

$$\mu = \frac{\text{charge} \times \text{angular momentum}}{2 \times \text{mass}}$$

$$\mu_{\text{proton}} = \frac{\frac{2}{3} e \frac{2}{3} \hbar}{2 \frac{m_p}{2\pi}} = \frac{4}{9} 2\pi \frac{e\hbar}{2m_p} = 2.79253 \mu_N$$

where μ_N is the nuclear magneton $\frac{e\hbar}{2m_p}$

The experimental magnetic moment of the proton is $2.79268 \mu_N$

Neutron Magnetic Moment

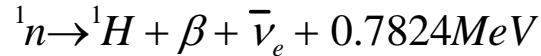
The magnetic moment of the neutron, μ_n , is

$$\mu_n = \left[1 - \frac{4}{9} 2\pi - \frac{3}{25} \right] \mu_N = -1.91253 \mu_N$$

The experimental magnetic moment of the neutron is $-1.91315 \mu_n$

The Weak Nuclear Force: Beta Decay of the Neutron

The nuclear reaction for the beta decay of a neutron is



where $\bar{\nu}_e$ is the electron antineutrino. The energy terms of the beta decay are

$$E_{mag} = m_p c^2 \frac{\alpha}{2\pi} = 1.089727 \times 10^6 \text{ eV} \quad E_{mag}(\text{gluon}) = \left[\frac{3}{25} \right]^2 E_{mag} = 1.569207 \times 10^4 \text{ eV}$$

$$E_{ele} = \frac{e^2}{8\pi\epsilon_o \lambda_{C,n}} = 5.456145 \times 10^5 \text{ eV} \quad E_\nu(\lambda_{C,n}, \lambda_{C,p}) = \frac{e^2}{4\pi\epsilon_o} \left(\frac{1}{\lambda_{C,n}} - \frac{1}{\lambda_{C,p}} \right) = 1502.2 \text{ eV}$$

$$T = \frac{1}{2} m v^2 = \frac{1}{2} \frac{m_e \hbar^2}{\left[\frac{m_N}{2\pi} \right]^2 \left(\frac{2\pi\alpha_o m_e}{\alpha^{-1} m_N} \right)^2} = \frac{1}{2} m_e \left(\frac{\hbar}{m_e \lambda_C} \right)^2$$

$$= \frac{1}{2} m_e c^2 = 2.555017 \times 10^5 \text{ eV}$$

The beta decay energy is

$$E_\beta = E_{mag} - E_{mag}(\text{gluon}) - E_{ele} - E_\nu(\lambda_{C,n}, \lambda_{C,p}) + T$$

$$E_\beta = 0.7824 \text{ MeV}$$